Effect of Heat Treatment on the Flow Induced Corrosion of Aluminum-SiC(p) Composites at Elevated Temperatures

by

Aleem Aman Khokhar

A Thesis Presented to the

FACULTY OF THE COLLEGE OF GRADUATE STUDIES

KING FAHD UNIVERSITY OF PETROLEUM & MINERALS

DHAHRAN, SAUDI ARABIA

In Partial Fulfillment of the
Requirements for the Degree of

MASTER OF SCIENCE

In

MECHANICAL ENGINEERING

July, 1995

INFORMATION TO USERS

This manuscript has been reproduced from the microfilm master. UMI films the text directly from the original or copy submitted. Thus, some thesis and dissertation copies are in typewriter face, while others may be from any type of computer printer.

The quality of this reproduction is dependent upon the quality of the copy submitted. Broken or indistinct print, colored or poor quality illustrations and photographs, print bleedthrough, substandard margins, and improper alignment can adversely affect reproduction.

In the unlikely event that the author did not send UMI a complete manuscript and there are missing pages, these will be noted. Also, if unauthorized copyright material had to be removed, a note will indicate the deletion.

Oversize materials (e.g., maps, drawings, charts) are reproduced by sectioning the original, beginning at the upper left-hand corner and continuing from left to right in equal sections with small overlaps. Each original is also photographed in one exposure and is included in reduced form at the back of the book.

Photographs included in the original manuscript have been reproduced xerographically in this copy. Higher quality 6" x 9" black and white photographic prints are available for any photographs or illustrations appearing in this copy for an additional charge. Contact UMI directly to order.

UMI

A Bell & Howell Information Company
300 North Zeeb Road, Ann Arbor MI 48106-1346 USA
313/761-4700 800/521-0600

Effect of Heat Treatment on the Flow Induced Corrosion of Aluminum-SiC(p) Composites at Elevated Temperatures

BY

Aleem Aman Khokhar

A Thesis Presented to the

FACULTY OF THE COLLEGE OF GRADUATE STUDIES

KING FAHD UNIVERSITY OF PETROLEUM & MINERALS

DHAHRAN, SAUDI ARABIA

In Partial Fulfillment of the
Requirements for the Degree of

MASTER OF SCIENCE
In
MECHANICAL ENGINEERING

July, 1995

KING FAHD UNIVERSITY OF PETROLEUM AND MINERALS
DHAHRAN, SAUDI ARABIA
COLLEGE OF GRADUATE STUDIES

This thesis, written by

Aleem Aman Khokhar

under the direction of his Thesis Advisor, and approved by his Thesis committee, has been presented to and accepted by the Dean, College of Graduate Studies, in partial fulfillment of the requirements for the degree of

MASTER OF SCIENCE IN MECHANICAL ENGINEERING

Thesis Committee :

Dr. Zaki Ahmed (Chairman)

Dr. H. Saricimen (Member)

Dr. Zafarullah Khan (Member)

Dr. O.A. Ashiru (Member)

Mr. Abdul Aleem (Member)

Department Chairman (Mech. Engg.)

Dean, College of Graduate Studies

Date: 13-9-95

COLLEGE OF GRADUATE STUDIES

Dedicated to

my *Wife, Brother, Sister*

&

our *Parents*

Acknowledgment

In the name of Allah, Most Gracious, Most Merciful. Read in the name of thy Lord and Cherisher, Who created. Created man from a {*leech-like* } clot. Read and thy Lord is Most Bountiful. He Who taught {the use of} the pen. Taught man that which he knew not. Nay, but man doth transgress all bounds. In that he looketh upon himself as self-sufficient. Verily, to thy Lord is the return {of all}.

(The Holy Quran, Surah 96)

First and foremost, all praise to Allah, *subhanahu-wa-ta'ala*, the Almighty, Who gave me an opportunity, courage and patience to carry out this work. I feel privileged to glorify His name in the sincerest way through this small accomplishment. I seek His mercy, favor, and forgiveness. And I ask Him to accept my little effort. May He, *subhanahu-wa-ta-Aaala*, guide us and the whole humanity to the right path *(Aameen)*.

Acknowledgement is due to King Fahd University of Petroleum & Minerals for providing support to this research work.

I am indebted to my thesis chairman, Dr. Zaki Ahmad for his help and advice. I acknowledge him for his valuable time, encouragement and guidance especially during the early stages of this work and my M.S studies. Working with him was indeed a learning experience.

I am grateful to all of my thesis committee members, Dr. H. Saricimen, Dr. Zafarullah Khan, Dr. O.A. Ashiru, and Mr. Abdul Aleem for their deep interest, constructive criticism and stimulating discussions during the course of this work. Thanks are also due to Mr. Abdul Quddus from R.I, Mr. Younas from Central Research Workshop, and Mr. Fakri from Corrosion Lab.

I am thankful to the department chairman, Dr. Mohammad O. Budair and other faculty members for their cooperation.

I am thankful to my fellow graduate students and all my friends on the campus especially Amir Mahmood, Ikram and Zaka who provided a wonderful company. Last but not the least, thanks are due to the members of my family for their emotional and moral support throughout my academic career. No personal development could ever take place without the proper guidance of parents. They taught me the fundamental concept of life, "Tough times never last, tough people do". My elder brother Saleem, deserve special mention for his help, constant inspiration and guid-

ance. I am grateful to my Father for his support and motivation during the final stages of the work. I acknowledge with gratitude, the affection and encouragement of my sister (Samina) and sisters in law (Zareen, Farheen and Aysha) that helped me overcome homesickness and concentrate on my work.

Contents

List of Tables

List of Figures

Abstract

Name: Aleem Aman Khokhar

Title: Effect of Heat Treatment on the Flow Induced Corrosion of Aluminum-SiC(P) Composites Elevated Temperatures

Major Field: Mechanical Engineering

Date of Degree: July, 1995

Experimental studies such as electrochemical polarization measurements, weight loss, open circuit potential and elevated temperature closed loop techniques were used to investigate the effect of heat treatment on the corrosion resistance of Aluminum metal matrix composite Al6013-20SiC(P) in 3.5 wt% NaCl solution and Arabian Gulf water, at temperatures ranging from 30°C to 130°C under controlled variable velocities.

It was shown that alloy Al6013-20SiC(P) in T4-temper (age hardened) showed maximum resistance to corrosion. Studies on the variation of open circuit-potential of alloy Al6013-20SiC(P) in T4-temper with time, showed that the potential of the alloy shifted to more noble values compared to alloy in O-temper and F-form. A strong tendency for an oxide film formation on alloy in T4-temper was therefore suggested. Pitting was the most predominant form of localized corrosion attack, observed on the alloy. It occurred at metal matrix/SiC interface, and there was no evidence of attack on SiC particles. The pitting resistance of the alloy in general decreased on increasing the temperature from 30°C to 130°C. The alloy in T4-temper also showed a maximum resistance to pitting at elevated temperatures, compared to O-temper and F-form.

Master of Science Degree
Department of Mechanical Engineering
King Fahd University of Petroleum and Minerals
Dhahran, Saudi Arabia
July, 1995

خلاصة الرسالة

الإسم : عليم أمان كوكر

عنوان الرسالة : تأثير المعاملات الحرارية على التآكل فى الإسياب الحثى للسبائك المركبة من الألمنيوم والسليكون كاربيير (موسنور) عند درجات الحرارة المرتفعة ٠

التخصص : الهندسة الميكانيكية

تاريخ الشهادة : يوليو ١٩٩٥م

لقد أجريت عملية مثل قياسات الإستقطاب الكهروكيميائى ، فقدان الوزن ، دائرة الجهد المفتوح وتغيير درجات الحرارة فى دائرة مغلقة كأساليب لدراسة تأثير المعاملات الحرارية على مقاومة التآكل للسبائك المركبة من (AL 6013 - 20SiC (P)) فى مسائل تركيبه ٠ر٣٪ وزن من كلوريد الصوديوم أ ومياه الخليج العربى عند درجات حرارة تتراوح بين ٣٣٠ إلى ١٣٠ م وسرعات متميزة منتظمة ٠

وأوضحت الدراسة أن السبائك المركبة من (AL6013 - 20SiC (P)) من نوع T4 لها أعلى مقاومة لعملية التآكل ، كما أن الدراسات التى أجريت على التغيير فى دائرة الجهد المفتوح مع الوقت للسبائك المركبة (AL6013 - 20SiC (P))من نوع T4 بينت أن قيم الجهد لتلك السبائك ذات أهمية مغيرة مقارنة بقيم الجهد الناتجة من السبائك من نوع O أ و F ٠ولذا فإن يرجح بنشر أو تكون طبقة رقيقة من الأوكسجين على السبائك من نوع T4 ٠ وقد شوهد أن التآكل كان بشكل عام على هيئة نقر بسيطة على السبائك ٠ كما وجدت هذه النقر عند السطح الفاصل بين المعدن والسليكون كربيد بينما لم يستدل على مثل هذه النقر على جزئيات السليكون كربيد وبشكل عام فإن مقاومة السبائك لنقر التآكل تقل بزيادة درجة الحرارة من ٢٠ م إلى ١٣٠ م ٠ ولقد أظهرت السبائك من نوع T 4 أعلى مقاومة لنقر الصدأ عند درجات الحرارة العالية مقارنة بتلك السبائك من نوع O أو F ٠

درجة الماجستير فى العلوم

قسم الهندسة الميكانيكية

جامعة الملك فهد للبترول والمعادن

الظهران - المملكة العربية السعودية

يوليو ١٩٩٥م ٠

NOMENCLATURE

A	Surface area of specimen (cm^2)
E_{corr}	Corrosion potential (mV_{SCE})
E_P	Pitting Potential (mV_{SCE})
E_{PP}	Protection Potential (mV_{SCE})
ΔE	Width of the hysterisis loop or Pitting resistance (mV_{SCE})
F	Faradays constant (96500 cb/mole)
I_L	Limiting Current (mA/cm^2)
m/s	Meters per second
n	Number of electrons (Charge of metallic ion)
OCP	Open circuit potential
Re.	Reynolds number
SCE	Standard calomel electrode
t	Time of exposure (Hours)
τ	(1/t) Induction time
V	Velocity of flow (m/sec)
W	Weight Loss (grams)
ρ	Density of aluminum alloy (g/cm^2)

Chapter 1

INTRODUCTION

1.1 General

The properties of aluminum that make this metal and its alloys the most economical and attractive for a wide variety of uses are appearance, lightweight, fabricability, optimum combination of physical properties, mechanical properties and superior corrosion resistance. The development of aluminum alloys has been governed largely by the quest for better mechanical properties which contributed in the application of high strength alloys in aerospace industry [1]. In addition to the mechanical properties considerable development work has been directed in the last three decades to improve corrosion resistance of aluminum alloys. Aluminum alloys of 7XXX series were made to meet the desired weight reduction requirement of aircraft industries but suffered corrosion problems. This led the researchers to turned to highly corrosion resistant 6XXX series alloys [2]. The 6XXX series alloys are known for their excellent formability and corrosion resistance but generally lack the strength needed for primary structural applications. In mid 80's aluminum alloy 6013 was developed and successfully replaced alloy 2024 in the aircraft industry because of its yield strength which was 25 % greater than 6061-T6 and 12% greater than 2024-T3 in sheet gauges [3].

In recent years the focus on materials has shifted to composites and the development of metal matrix composites (MMCs) has been one of the major innovations. The unmatched properties of MMCs are important to spacecraft and aircraft industries because of the potentially large reductions (25-50 percent) in weight. Their high temperature strength retention is important, thus making them suitable for diesel and aircraft engines. In aircraft applications, the lower weight reduction means lower engine power and, therefore, less fuel consumption, and hence lower total weight. Aluminum matrix composites represent high performance tailor-made substitute materials for a variety of applications. Interest in the application of MMCs in marine environments is rapidly expanding for naval and defense applications. Although the initial research and development work was stimulated by needs of aerospace industry, economically light weight composites with less than the highest-strength performance are finding more and more application in transportation and military vehicles. A large amount of research is currently directed towards defining a relationship between the mechanical properties, microstructure and processing route.

Aluminum matrix composites find extensive applications because of their high strength to weight ratio, high specific modulus and a combination of desired properties. Extensive investigations on the production, mechanical properties

and corrosion behavior of aluminum metal matrix composites reinforced with Boron, graphite and SiC have been carried out [4].

1.2 Reinforcement of Aluminum Alloys by Silicon Carbide

The addition of silicon carbide particles to aluminum alloys results in an increased elastic modulus, due to the higher elastic modulus of the silicon carbide (SiC), which may also be accompanied by an increased flow stress, depending on the matrix alloy chosen, heat treatment and manufacturing method used. Other significant advantages of discontinuously reinforced aluminum alloy metal matrix composites are enhanced resistance to wear, corrosion and fatigue crack initiation resistance when compared to the matrix material [5]. Discontinuous reinforcements are usually defined in three different termenologies.

1.2.1 *Particles*

A reinforcement is considered to be a "*particle*" if all of its dimensions are roughly equal. Thus particles reinforced composites include those reinforced by spheres, rods, flakes and other shapes roughly equal axes.

Particles have low aspect ratios and are usually less expensive than whiskers and fibers. The strengthening mechanism of particles is similar to that of

dispersion strengthened alloys, because particles in the matrix prevent the motion of dislocations [6].

1.2.2 *Whiskers*

A reinforcement is considered to be a "*whiskers*" if a short single crystal fiber or filament is used as a reinforcement in a matrix.

Whiskers are very thin single crystals that have large length to diameter ratio. As a consequence of their small size, they have a high degree of crystalline perfection and are virtually flaw free, which accounts for their exceptionally high strength. Whiskers reinforcements offers a variety of physical characteristics or morphologies and they also exhibit different chemical reactivity with aluminum [6,7].

1.2.3 *Short Fibers*

A composite is considered to be a discontinuous fiber or "*short fiber*" composite if its properties vary with fiber length.

Even though reinforcements efficiency is lower for short fibers than for continuous fibers, they are extensively used in commercial applications. Short fibers composites are preferred in most of the cases because of their inherent isotropy, which allow the material to demonstrate maximum strength in more than one direction [6,7].

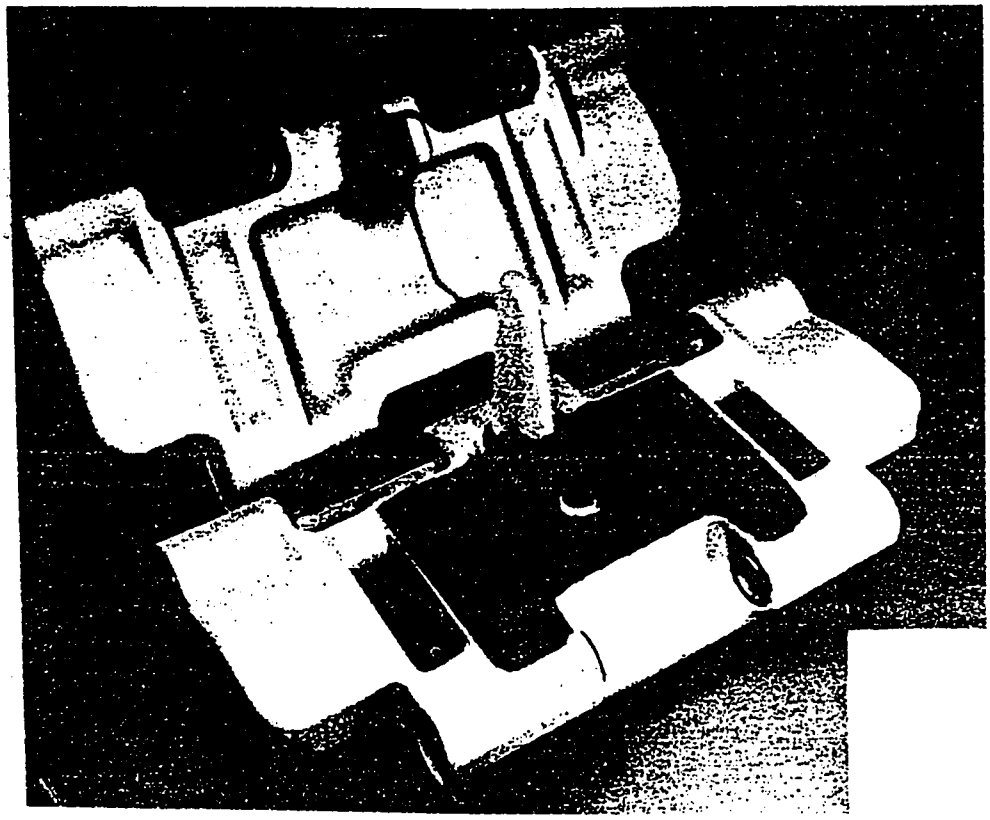

Fig 1.1: A forged track shoe for an armored vehicle. [8]

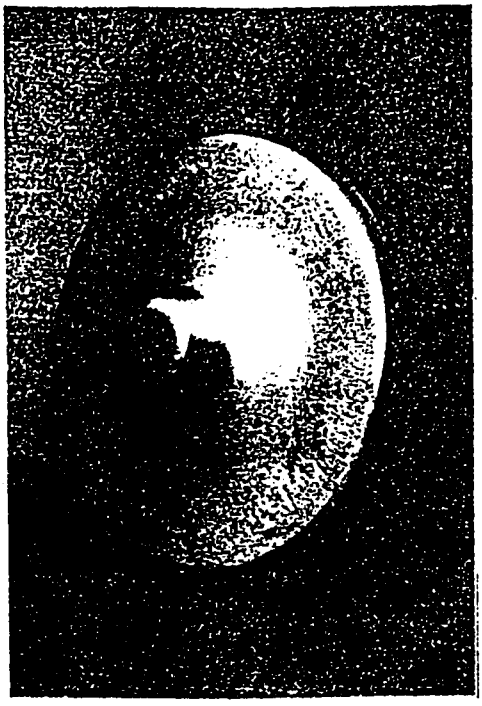

Fig 1.2: A turbine disc made by high energy rate forging. [8]

Fig 1.3: Missile wings made by high energy rate forging. [8]

1.3 Applications

Metal matrix composites found their first applications in aerospace structure, sports and leisure equipment, fields which require high specific strength and specific rigidity. The applications being developed today range from artificial joints and organs to reinforced building materials, and from ship hulls to precision audio equipment [7].

1.3.1 *Defense Applications*

SiC whisker and particulate reinforced MMC have been under development by different chemical companies since the late 1970s. The materials designated SXA-24 and SXA-61, have greater stiffness and densities approaching that of aluminum. Products already made from these materials include: a forged tract shoe for an armored vehicle, a turbine disc made by high energy rate forging, and missile wings (Fig 1.1 to 1.3) [8]. Because of the heavy military involvement in MMC research and development, information exchange is restricted. In particular, details concerning processing techniques and test data are not commonly available. Another driving force in the development of MMCs is the shortcomings of polymer-matrix composites. Maximum operating temperature of these materials is seen as limited, and some are sensitive to moisture.

1.3.2 *Missile Applications*

A large number of solid-propellant missiles use composites for major structural elements, including the rocket motor case. This element of the structure greatly influences missile performance in terms of range and weight of payload. The solid-propellant-type motor burns its fuel inside the case, generating moderately high pressure, which are contained by the large case wall. High tensile strength, together with the low weight of composites, is the most important advantage [8].

1.3.3 *Automotive Applications*

The alumina fiber FP is now being used in a number of experimental MMC components such as an automotive connecting rod. The composite used in the rod is made by molten aluminum infusion of the fiber. The resulting material is about 50% fiber by volume, has a maximum tensile strength of 80 Kpsi and a thermal expansion coefficient parallel to the reinforcing fibers (Fig1.4) [8].

1.3.4 *Aircraft Applications*

Silicon carbide reinforced aluminum alloys are finding increasing applications in aerospace industry. For instance aluminum alloy 6013-T6 has been selected for the fuselage skin and other applications on the U.S. Navy's P-7A

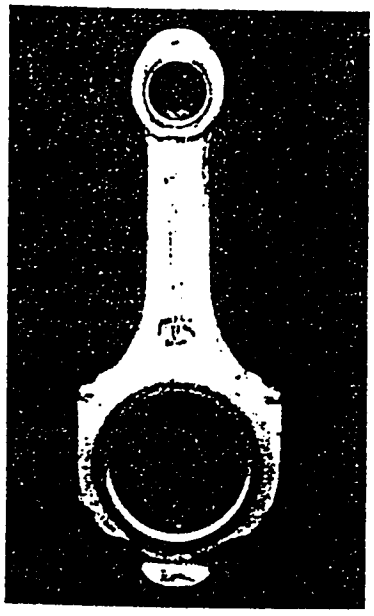

Fig 1.4: Automotive connecting rod made by molten aluminum infusion of the fiber.[8]

airplane, in place of the traditional 2024-T3 clad sheet. Testing at Lockheed and Alcoa laboratories has shown that uncoated 6013-T6 sheet could replace clad 2024-T3, T4 or T6, providing improved corrosion resistance with equal or better mechanical properties and formability. Lockheed has selected 6013-T6 as a primary structural aluminum alloy on the P-7A, where the alloy permits a one-to-one size substitution for traditional 2024 [9].

Although sufficient information on the mechanical and physical properties of MMCs is available in the literature, the corrosion data on light-weight aluminum matrix composites such as 2024, 7075 and 6061 is sparse because of the pre-occupation of the workers with more pressing problems related to fabrication processing of MMCs for defense applications. In particular the corrosion data on Al 6013-20SiC(P) which has been developed in recent years and looks a highly promising material is far from being sufficient. Work on the development and application potentials of MMCs has been restricted by lack of published data on corrosion. Therefore, a great need exists for systematic investigations of the corrosion behavior of aluminum metal matrix composites and their application potentials in corrosive environments.

Systematic investigations on the corrosion behaviour of Al6013-20SiC(p) using weight loss and electrochemical techinique have been represented. The effect of heat treatments on the corrosion behaviour of the above alloy is also

not known. Alloy 6013 is an aluminum magnesium-silicon-copper alloy finding increasing applications as structural materials. The above alloy reinforced with 20SiC(P) was designed to obtain a higher mechanical strength and more improved corrosion resistance than alloy 2024-SiC(P), 2124-SiC(P) and 6061-SiC(P), the later being the focus of current attention.

Because of absence of reliable corrosion data, the corrosion resistance of alloy 6013-20SiC(P) in 3.5 wt% NaCl and Arabian Gulf sea water was extensively investigated at room temperature and elevated temperature upto 130°C. To obtain a relationship between a microstructure and corrosion resistance, three tempers of the alloy in F (as fabricated), O (annealed) and T4 (aged hardened) were investigated. Based on the results obtain some suggestions for the potential application of the alloy in the Gulf region are being made.

Chapter 2

LITERATURE REVIEW

2.1 Mechanical Properties and Heat Treatment

Aluminum matrix composites have been the subject of intensive interest because of their remarkable improvement in strength, stiffness, wear, fatigue strength and high temperature resistance. Several difficulties, such as prohibitive cost of reinforcement fibers and problems related to processing have restricted their wider use. Aluminum, magnesium and titanium have been widely used as matrix materials, whereas boron, graphite, silicon, silicon carbide and fiberglass have been the most important reinforcement materials. Aluminum matrix composites are reinforced with either continuous or discontinuous fibers such as boron, silicon, whiskers or particulate of silicon carbide and boron carbide. Typical matrix materials used are shown in Table 2.1, [11] and properties of common reinforcement fibers are shown in Table 2.2 [12].

Aluminum alloys 2024, 6001 and 7075 have been widely used as matrix materials for aerospace and structural applications and are extensively studied. In earlier attempts, graphite powder was used to reinforce aluminum alloys. Graphite powder provided favorable effects on wear resistance, hardness and compressive strength.

TABLE 2.1: Different materials used as matrix in composites [11]

METALLICS	PLASTICS	CERAMICS
Aluminum	Epoxies	Aluminum Oxide
Magnesium	Polyamides	Porcelain
Titanium	Polysulfones	Plaster
Copper	Polystyrenes	Carbon
Nickel	Diallylphathhalate	Silicon Nitride
Lead	Phenolics	
Silver	Armides	
Zinc	Polyesters	
Bronze	Polycarbonates	
Cobalt		
Iron		
All alloys of above		

TABLE 2.2: Properties of fibers [12]

Material	Tensile Modulus (E) (GN/m^2)	Tensile Strength (σy) (GN/m^2)	Density (ρ) (g/cm^3)	Specific Modulus (E/ρ)	Specific Strength ($\sigma u/\rho$)
Fibers					
E-Glass	72.4	3.5[a]	2.54	28.5	1.38
S-Glass	85.5	4.6[a]	2.48	34.5	1.85
Graphite (High modulus)	390.0	2.1	1.90	205.0	1.1
Graphite (High tensile strength)	240.0	2.5	1.90	126.0	1.3
Boron	385.0	2.8	2.63	146.0	1.1
Silica	72.4	5.8	2.19	33.0	2.65
Tungsten	414.0	4.2	19.30	21.0	0.22
Beryllium	240.0	1.3	1.83	131.0	0.71
Kevlar-49 (aramid polymer)	130.0	2.8	1.50	87.0	1.87

a= Virgin strength value. Actual strength value prior to incorporation into composite are approximately 2.1 GN/m^2

However a weak dispersive bonding between planes results in a low shear modulus, which is a detrimental property of a fiber. Improvements in fibers of carbon, boron, graphite, aluminum and silicon carbide have increased the tensile strength, and the use of short fibers for reinforcement improved the stiffness. SiC fibers are preferred for aluminum matrix composites, because of their low cost and high temperature stability and compatibility with aluminum. Sufficient information is available on the mechanical and physical properties of Al-SiC composites. Based on a through review of the published literature of the Al-SiC composites, a summary of some important mechanical and corrosion characteristics is provided below. The schematic representation of the literature survey is given in Fig 2.1.

Tanaka *et al.*[13] in 1982, worked on the mechanical properties of 1100-SiC, 5052-SiC and 6061-SiC composites and found that in 5052-SiC, aluminum was not well permeated among the SiC fibers, but in both 1100-SiC and 6061-SiC, aluminum was well permeated among the fibers and exhibited excellent compatibility between the SiC fibers and 1100 and 6061 matrix. The fracture behavior of 1100-SiC was ductile and that of 6061-SiC was brittle. The bonding between SiC and the 6061 matrix was excellent in comparison with 1100-SiC. However, the tensile strengths of both composites obeyed the rule of mixtures predictions.

Another study in 1988 by Arone *et al.* [14], microstructural parameters such as SiC particle size, distribution and matrix/SiC(P) bonding were studied. It was found that the Al6061-40 vol% of SiC(P) had relatively poor bonding, and thus had lowest plasticity

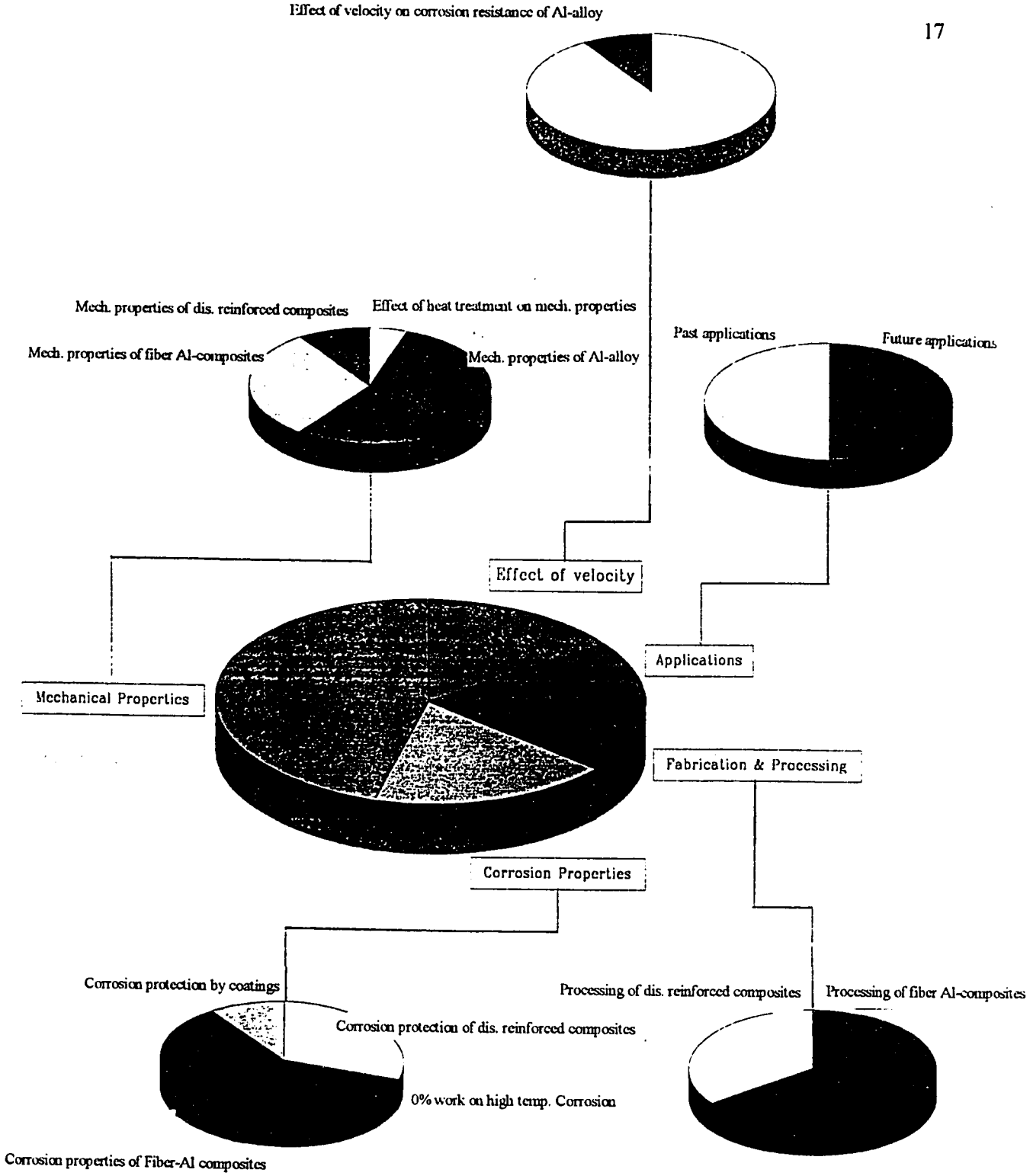

Fig. 2.1: Schematic representation of the literature survey

while the Al 2014-40vol% of SiC(P) sustained substantial plastic deformation. It was concluded that metal matrix areas were the main factors of fatigue crack growth resistance. The presence of large clusters of particles in Al 6061-40vol% of SiC(P) and Al 2014-40vol% of SiC(P) promoted crack propagation, while uniformly distributed particles retard the crack advance.

In early 90's Kaneko *et al.* [15] worked on Aluminum alloy 6013 sheet for new U.S. Navy Aircraft (P7A). In the study it was concluded that the toughness of 6013-T6 bare (uncoated) sheet was significantly higher than the 2024-T3 clad and bare sheet.

In 1992, Aidun, Martin and Sun [16] studied the effects of heat treatment on the mechanical properties of Al6061-SiC(P) composite. They found that the strength of 6061-SiC(P) was greatly dependent on the heat treatment. The trend was same as that of the matrix alloy. However to obtain the optimal matrix properties, the effect of the presence of SiC particles must be encountered by varying, heat treatment parameters. It was concluded that both particle clusters and iron-rich inclusions act as fracture initiation sites in 6061-SiC(P) aluminum.

In more recent work Wei and Huang [17] studied the influence of heat treatment and hot working on fracture toughness of cast aluminum base composites. The study showed that the fracture energy tends to decrease markedly with increasing aging time, from the under-aged to the over-aged condition. The decrease in total fracture energy was found to be mainly caused by the drastic reduction of propagation energy. The initiation energy did not

seem to be affected by artificial aging. Wei *et al.* also concluded that hot extrusion or rolling can lead to (i) elimination of residual pores and defects formed during casting. (ii) Much more uniform distribution of the reinforcing particles. (iii) Stronger bonding between the matrix and particles. (iv) A more ductile matrix resulting from the homogenization and refinement of grains during working.

It is to be observed that the existing data on the effect of heat treatment on Al-SiC MMCs is far from being sufficient.

2.2 Corrosion Resistance

Trzaskoma Mc. Cafferty and Crowe [18], conducted anodic polarization studies of Aluminum MMCs with 20 vol% SiC in 0.1M NaCl solution. The polarization procedure involved immersing of composites in corrosive solution for 2 hours until a steady E_{corr} (Corrosion potential) was recorded and then stepping the potential in 10mV increments and recording the steady current (after every 10 minutes). The results for 2024 and 6061 alloys with their corresponding MMCs are shown in Table 2.3. In deaerated solutions the presence of SiC reinforcement was found to cause a shift in the corrosion potential to more noble values. The pitting potential (E_{corr}) of alloys 6061 and 5456 showed little effect of SiC but for alloy 2024 the pitting potential was lowered by about ~ 100mV. It was also demonstrated

TABLE 2.3: Results of 2024 and 6061 alloys with their corresponding MMCs [19]

	E_{corr} (V SCE)	E_{pit}
Al 2024	- 1.065	- 0.540
SiC_w/Al 2024	- 0.899	- 0.640
Al 2024 HC	(- 0.728 to - 0.822)	- 0.530
SiC_w/Al 2024 HC	(- 0.585 to - 0.638)	- 0.450
Al 6061	- 1.272	- 0.640
SiC_w/Al 6061	- 1.108	- 0.665
Al 6061 HC	(- 0.568 to - 0.945)	- 0.550
SiC_w/Al 6061 HC	(- 0.686 to - 0.899)	- 0.530
Al 6061 (N)	(- 0.806V)	- 0.625
SiC_w/Al 6061 (N)	(- 0.893 to - 1.068)	- 0.650

that this decrease was due specifically to the SiC and not to any effect of processing on matrix microstructure. It was also noted that pits in the Al6061/SiC MMC were small, shallow and rounded whereas the pits in the alloy Al6061 (unreinforced) were larger and irregularly shaped. There was no corrosion of pits initiation sites in MMCs with SiC whiskers but their presence was considered to affect the morphology and growth.

Comparison of corrosion-fatigue properties of 6013 bare, Alcad 2024, and 2024 bare aluminum alloy sheet was done by Chaudhuri *et al.* [19]. In their study it was shown that the Alcad (cathodically protected from corrosion) 2024-T3 alloy had a better corrosion-fatigue resistance compared to the 2024-T3 bare (unprotected) and 6013-T3 bare alloys. The 2024-T3 bare showed a slightly better corrosion-fatigue resistance than 6013-T6. Longer corrosion-fatigue life of Alcad 2024-T3 was attributed to the corrosion protection provided by the Alcad layer to the base metal. Lower fatigue life of the 6013-T6 bare was attributed to the observed intergranular corrosion. Fractrographic examination showed that Alcad 2024 had a smooth fracture surface with the crack originating from the notch. On the other hand, both the 2024 and 6013 bare had a rough fracture surface, resulting from multiple crack initiations at the notch and at the surface of the specimen indicating multiple crack propagation's before coalescence to large cracks.

Trzaskoma [18] in her recent work on pit morphology showed that pit initiation occurred at micro-particles in the metal matrix which in the case of Al 5456 and its composites were intermetallic phases containing Mg, Cr, Mn, Al and Fe as impurity. More

pits were initiated and propagated in the composites than on the wrought and powder compacted alloys because the composite had a greater number of detrimental intermetallic phases, precipitation of which was apparently enhanced by the presence of SiC whiskers. The diameter of pits formed in the composite were about an order of magnitude smaller than for the parent alloy (though more in number) and were shallower though specific depths were not given .

Aylor and Moran [21] used cyclic anodic potentiodynamic polarization to characterize the pitting propensity of PM (Powder metallurgy) Al6061-SiC (whiskers), wrought Al6061-T6 alloy and PM6061 Al. The volume fraction of SiC was 25% and the whiskers were 0.1 to several microns in diameter and 1 to 50μm in length. Potentiodynamic tests, at a scan rate of 0.1 mV/s and potentiostatic tests were carried out in ASTM simulated sea water. Additionally, panels were exposed for periods of 1 to 12 months in filtered sea water at a temperature of 30°C and in a marine atmosphere. All panels suffered pitting with the 6061 and the MMC being most severely attacked although the relative behavior of these two materials was not indicated. SEM analysis of the MMC revealed that pitting corrosion was concentrated round the SiC whiskers, which the authors associated with crevices formed at SiC-Al interfaces.

In another work by Pacceij and Agarwal [22], the susceptibility of AA7091 alloy 20 vol% SiC(p) was attributed to the dispersed noble phase of SiC. Alloy (PM) AA 7091-20 vol% SiC showed enhanced attack at the regions where SiC particles were

clustered. The corrosion resistance was enhanced by solution heat treatment because of an increase in the void content. The local attack associated with SiC and Gr reinforcement has been attributed to the formation of aluminum carbide ($Al_4 C_3$), which on hydrolysis liberates methane gas according to the following chemical equation.

$$Al_4C_3 + 12H_2O\ (l) \Longrightarrow 4Al(OH)_3 + 3CH_4\ (g)$$

However the role of SiC in relation to pit initiation is not clearly established and further work in the direction is needed. It is also clear that, no work has been reported on high temperature corrosion of metal matrix composites.

2.3 Effect of Velocity on Corrosion

When a metal is exposed to a flowing environment, the rate of metal loss is greater than it would be if exposed to the same environment under stagnant conditions. The removal of metal or erosion, takes place partly due to mechanical process and partly due to electromechanical or chemical process. The relative velocity between a metal surface and its environment plus the geometry of the flow are major factors in determining corrosion rate of the metal [23].

Flow induced corrosion, generally involve the following types of reactions.

(a) Cathodic and anodic chemical reactions. (b) Transport of cations reacting species to the metal solution interface. (c) Transport of metallic anions away from the metal

solution interface. (d) Transport of cathodic product away from the interface. (e) Transport of secondary reactant to either anode or cathode or both, for reactions with the anodic or cathodic products. (f) Transport of secondary product away from the reacting zone.

Cathodic and anodic reactions are controlled by rate of charge transfer and factor (f) is controlled by mass transfer. Hence for all the above reactions a relationship based on mass transport phenomenon may be applied. Such relationships include geometry of the flow, velocity of the fluid, type of liquid (environment) interface and physiochemical properties of the system such as temperature, pressure and the concentration of the liquid. Thus mass transfer phenomenon can be an alternative procedure for the measurement of corrosion rate in hydrodynamic conditions [24].

2.3.1 *Flow Dependent Corrosion*

The surface layer on the metal experiencing flow breaks usually by the mechanical and electromechanical factors. Once the surface layer disappears entirely, the reactant is transported to the surface. If the flow rate is increased further, an extreme stage is reached, depending upon the velocity and phase boundary reaction. The effect of velocity is largely dependent on formation of passive film on the materials. As in the case of copper-nickel alloys the corrosion resistance at low velocities depends on the formation of a protective layer consisting mainly of CuO. Copper and copper alloys show a gradual rise

in the corrosion rate with increase in the flow rate until a critical flow rate is reached, above which the rate of metal removal increases sharply, due to anodic dissolution.

A characteristic curve showing the relation of erosion corrosion rate with velocity is shown in Fig 2.2. The curve has five zones, labeled A through E [25]. Although Figure 2.3 is specific for Cu-Ni alloys, it provides a good understanding of the mechanism of flow induced corrosion.

Zone A has limited oxygen supply but protective oxide layer. Because of the limited oxygen available, the cathodic reaction is dominant and the metal surface is well protected. Since flow is laminar, shear forces are not sufficient enough to destroy the oxide film.

Zone B has turbulent flow having low oxygen content. The oxide film is beginning to break in patches but still provides adequate protection to the material.

Zone C has a higher degree of turbulence and shear forces, thus breaking the oxide layer. The exposed area is severely attacked, the attack is accelerated by galvanic currents flowing between the metal and the oxide layer. Still some chances of repassivation remains.

Zone D is characterized by more oxide film removal than zone C, both anodic and cathodic reactions proceed rapidly. Repassivation of the material is not possible.

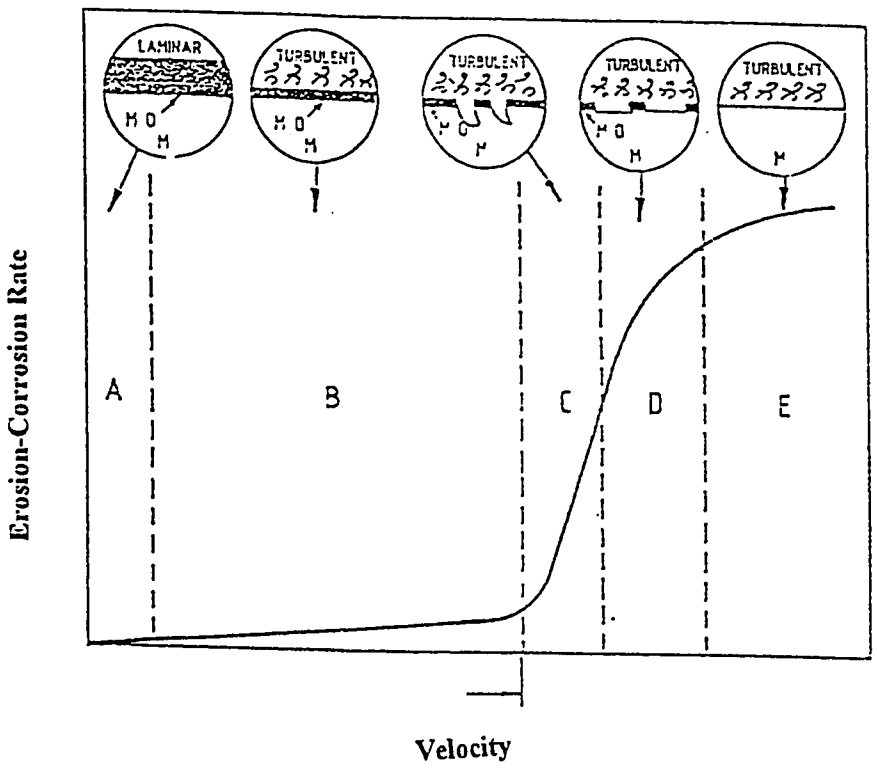

Fig. 2.2: Schematic representation of erosion-corrosion rate with velocity [26]

Zone E has completely removed oxide film. Both anodic and cathodic reactions proceeds very rapidly as the velocity is increased due to increase in oxygen supply. Repassivation in this zone is impossible. Zone E is very rarely observed except in low pH environments.

2.4 Electrochemical Studies in Recirculating Loops

Electrochemical methods have been widely used in the study of corrosion phenomenon. One of the widely used electrochemical methods is the potentiodynamic method. In this method the specimen potential is scanned slowly in both anodic and cathodic direction, and a complete current potential plot of the specimen is obtained. Another method is the potentiostatic method which involves polarizing a specimen at constant potential with reference to a reference electrode and measuring the current flowing between the specimen and the counter electrode. The data obtained is plotted as potential vs logarithm of current to get a polarization curve. Another most used technique for instantaneously measuring corrosion rate is linear polarization technique. This method involves measuring the slope of polarization curve at the origin. The result obtained is the polarization resistance. which is the inverse of the slope of the polarization curve.

Sufficient information on the effect of velocity on electrochemical parameters e.g. corrosion current, pitting potential, protection potential and limiting current density has not been reported in literature. Flow dependent corrosion has been studied extensively and a number of methods such as rotating disk, rotating cylinder, coaxial cylinder and tubular flow have been employed.

Ross *et al.* [26] studied the behavior of iron as a flat plate under anodic control in flowing acids. They found that the corrosion potential and anodic polarization curves shifted in the positive direction with increase in velocity.

Markides *et al.* [27] showed that the potential and dissolution rate of rotating specimen increased with velocity in air and in saturated hydrochloric acid, but had no significant effect in deaerated acid solutions.

Studies involving the effect on corrosion potential (E_{corr}) of 0.2% carbon steel in turbulent flowing hydrochloric acid at temperature upto 80°C have been reported by South and Jones [28]. It was observed that the value of E_{corr} moved anodically (positive direction) as flow rate was increased, which is consistent with the findings of Ross *et al.* [27]. The test loop arrangement used for this analysis is shown in Fig. 2.3. The arrangement included rotameters, expansion tubes, hydrodynamic entrance tubes, a corrosion cell (See Fig.2.4) and a return pipe assembly. A constant potential was maintained on the specimen by impressing the desired voltage from the potentiostat.

The potential was varied by a motorized potentiometer and a plot of potential vs. current was recorded by X-Y plotter.

In another study conducted by Bohlmann *et al.* [29], the corrosion rate of two aluminum alloys 5454 and 6061 by electrochemical methods, was investigated using a high temperature recirculating titanium loop. The loop used for these studies was constructed entirely from titanium as shown in Fig. 2.5. It was equipped with a heater and a pump capable of circulating 650 ml volume of solution past the electrode surfaces at linear velocities ranging from 8 to 24 ft/sec, depending upon the electrode diameter. Provisions were provided for continuous addition and with drawl of fresh solution. The other components used in the loop included, a sampling valve, a metering pump for injection of acid or base for control of pH, and provision for deaerating, aerating, or oxygenating the solutions to be circulated.

In comparative study at 150°C in 1M NaCl, pH 6-10.5, it was found that alloy 6061 was most resistant to corrosion attack among the two alloys investigated.

The specimens used were hollow cylindrical electrodes, through which the solution flows. The assembly contained two specimen electrodes in tandem separated by the polarizing electrodes. The electrodes were insulated from each other by silicon rubber.

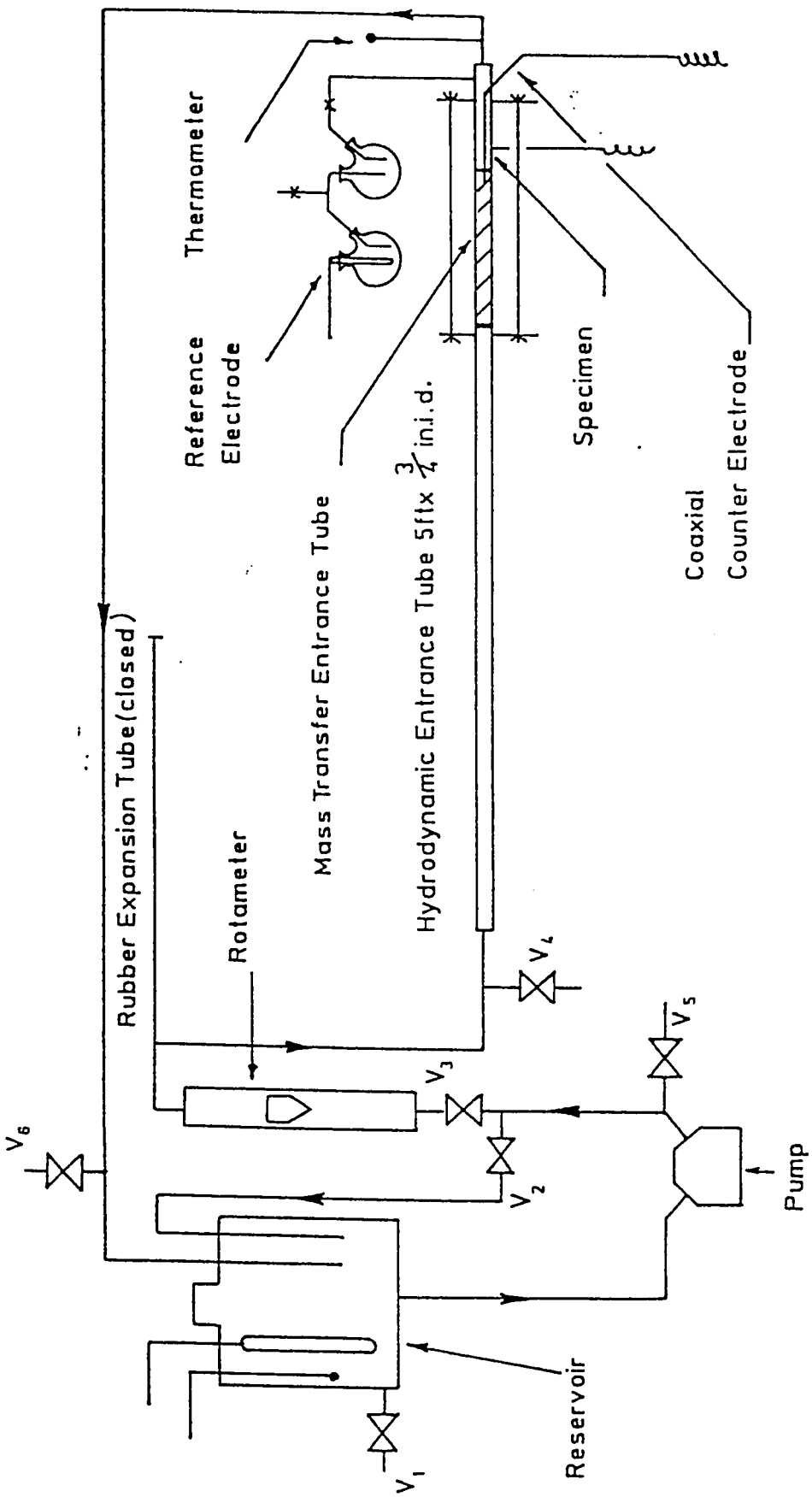

Fig. 2.3: Test Loop arrangement [28]

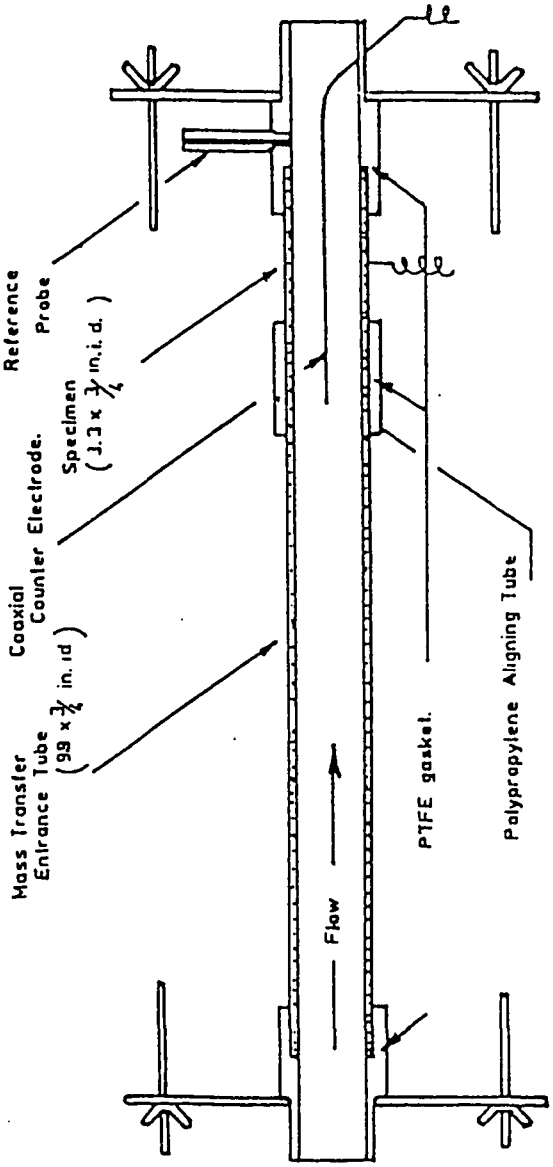

Fig. 2.4: Tubular Electrode Corrosion Cell [28]

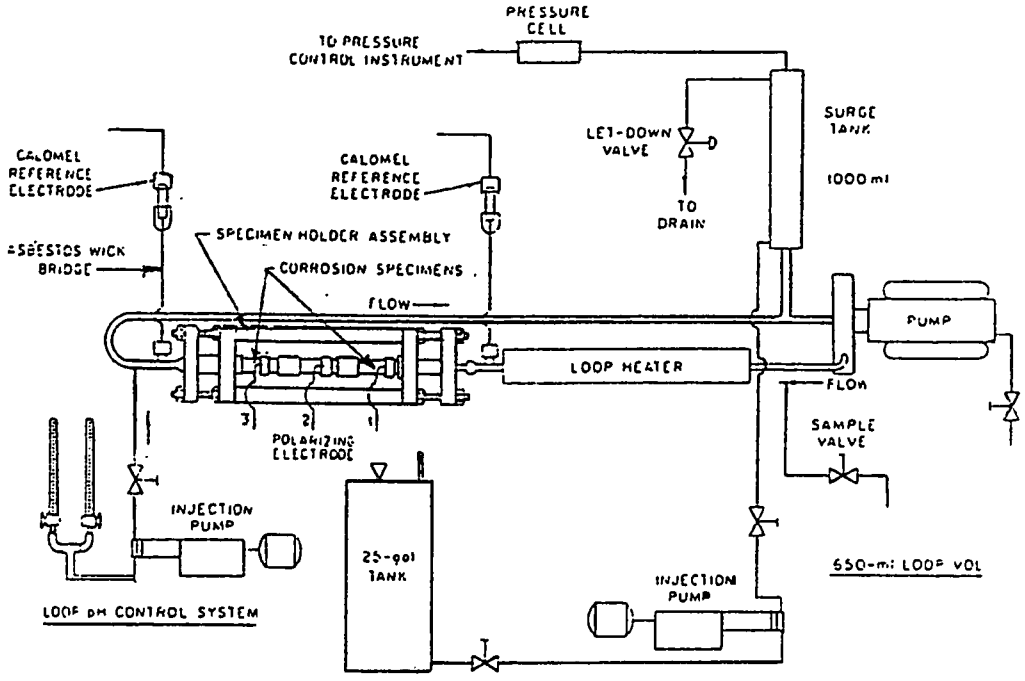

Fig. 2.5: High Temperature Recirculating Titanium Loop [29]

It can observed from the above literature review that the research conducted so far has been focused more on the mechanical properties of aluminum metal matrix composites, whereas the studies on the corrosion behavior are far from being adequate. The published data on corrosion behavior of the aluminum MMCs under elevated temperature and pressure conditions is virtually non-existent. Corrosion data even upto 150°C is scarce.

In view of the lack of information on the corrosion behavior of aluminum MMCs particularly at elevated and high temperature, and the promising applications potential of the alloys, there is an ample justification for the work conducted on Al6013-20SiC(P) metal matrix composite.

Chapter 3

MATERIALS AND TESTING ENVIRONMENT

3.1 Material

Al6013-20SiC(P) metal matrix composite in the sheet form having a thickness of 2.5 mm was used as an experimental material.. The composition of aluminum matrix alloy (6013) is shown in Table 3.1. The grain size of the composite was less than 10 micron and was partially recrystallized.

3.2 Heat Treatment

The temper designation indicates the treatment that alloy has received in arriving at its present condition and associated properties. Alloy 6013-20SiC(P) was used in as fabricated condition (F), annealed (O) and age hardened (T4).

Temper designation "O" applies to wrought products which are annealed to obtain the lowest strength temper, and to cast products, which are annealed to improve ductility and dimensional stability.

TABLE 3.1: Chemical composition of aluminum alloy 6013 (wt%)

si	Fe	Cu	Mn	Mg	Cr	zn	Ti	Al
0.6-1	0.5	0.6-1.1	0.2-0.8	0.8-1.2	0.1	0.25	0.1	Remainder

Annealing of Al6013-20SiC(P) was accomplished by heating the sheet to 415°C and cooling at a rate of about 30°C/hour from the annealing temp to 260°C, to remove the effect of cold work, or to partly remove the effect of heat treatment.

Temper designation "T4" applies to products which are not cold worked after solution heat treatment, or in which the effect of cold work in flattening or straightening may not be recognized in mechanical properties limits. T4-temper was achieved by heating the sheet to 546°C for one hour and quenching it in water at room temperature and was left for natural aging for about one day.

3.3 Testing Environment

Four type of testing environments were used.

a) 3.5% NaCl solution, Areated condition.

b) 3.5% NaCl solution, Deaerated condition.

c) Arabian Gulf water, Areated condition.

d) Arabian Gulf water, Deaerated condition.

The composition of Arabian Gulf water is given in Table 3.2. Deaeration was carried out by passing nitrogen (N_2) through the solution, till the solution became saturated with 99.5 % N_2.. Arabian Gulf water was obtained from the King Fahad University of Petroleum and Minerals beach, located 20 kms East of Dhahran. The water samples were

TABLE 3.2: Analysis of Arabian Gulf water (milligrams/liter)

Ions	Na^{+}	Ca^{+2}	Mg^{+2}	SO_4^{-2}	Cl^{-}	CO_3^{-}	HCO_3^{-2}	Total
Arabian Gulf water	19186	704	2400	4894	34080	18	189	61471

Metal Traces	Milligrams/liter
Na	18800.00
K	677.00
Sr	15.00
Ba	<0.50
Cu	0.01
Mn	<0.01
Zn	0.01
Pb	<0.01
Si	<2.00
B	<10.00
Li	0.29
Rb	0.13
Al	<1.00
Fe	<0.10

taken from a point about 0.1 Km away from the shore and stored at room temperature in plastic containers.

3.4 Surface Topography

In order to see the effect of heat treatments on microstructure and the type of corrosion taking place on Al6013-20SiC(P), surface topography was performed, using a light microscope and Jeol JSM 300 scanning electron microscope (SEM).

3.5 Sample Dimensions

For the weight loss analysis, square samples of 25 mm by 25 mm were used. The exposed area was 625 mm^2. Open circuit vs time analysis was done on circular samples of 15 mm diameter. The exposed area of the sample was 78.55 mm^2. Rectangular samples of 25 mm by 10 mm were used in electrochemical analysis. The exposed area of the sample was 500 mm^2.

Chapter 4

WEIGHT LOSS STUDIES IN STATIC AND DYNAMIC CONDITIONS

4.1 Introduction

Weight loss experiments were conducted to determine the rate of corrosion of alloy 6013-20SiC(P). The specimens were subjected to corrosion for some known time, the metal lost due to corrosion was identified and rate of corrosion was calculated. The experiments were carried out according to the ASTM standard G31-72 [31].

4.2 Determination of Corrosion Rate by Weight Loss Technique in static conditions

4.2.1 *Experimental Procedure*

a) *Apparatus*

The specimens were suspended in a 60 liters glass tank containing 3.5 wt% NaCl solution at room temperature by using fluorocarbon plastic strings. The tank was covered with a plastic cover to avoid contamination and to minimize evaporation.

b) *Test Specimen*

Duplicate samples, measuring 25 mm by 25 mm were used. The exposed surface area of the specimen was calculated with an accuracy of ±1%. The chemical composition of the specimen used has already been given in Table 3.1.

c) *Specimen Preparation*

Before exposure, the samples were treated with a hot commercial detergent solution for five minutes at 70°C to 80°C and then rinsed with distilled water. The samples were then exposed to a solution containing Potassium dichromate, 28 ml of phosphoric acid and deminralized water to make 1 liter of solution and then degreased, cleaning was done in an ultrasonic cleaner in distilled water.

After cleaning the samples were dried in desiccator for 24 hours. The dried samples were weighted in an analytical balance with an accuracy of ± 0.5 mg. After each test period, the corroded samples were treated with a same solution of potassium dichromate and phosphoric acid to remove corrosion products without damaging the surface in accordance with ASTM standard G5-72 [32]. An ultrasonic cleaning was also done in distilled water. The samples were dried in a desiccator for 24 hours and the dried samples were weighed in an analytical balance.

d) *Test Conditions*

The samples were tested in both aereated and deaerated conditions at room temperature in a 3.5% NaCl solution under stationary conditions. The samples were not stamped for identification in order to avoid unnecessary stresses. Weight loss was determined after every 100 hours of exposure, and once taken out, the samples were not re-exposed.

4.3 Determination of Corrosion rate by Weight Loss Technique in Dynamic Conditions

4.3.1 *Experimental Procedure*

a) *Apparatus (PVC Loop)*

For the experiments under dynamic conditions a polyvinyl chloride (PVC) loop was used. A continuos circulation of corrosive media was maintained under controlled velocities. The loop used is capable of producing a flow rate of $20m^3/h$ which allows a variety of velocities ranging upto 5 m/s. The loop also has a provision for a titanium heater, for conducting experiments at elevated temperatures. The details of loop are given in Figs. 4.1 and 4.2 [25]. Tests were conducted at 1.15 m/s, 1.68 m/s, 2.45 m/s and 3.53 m/s.

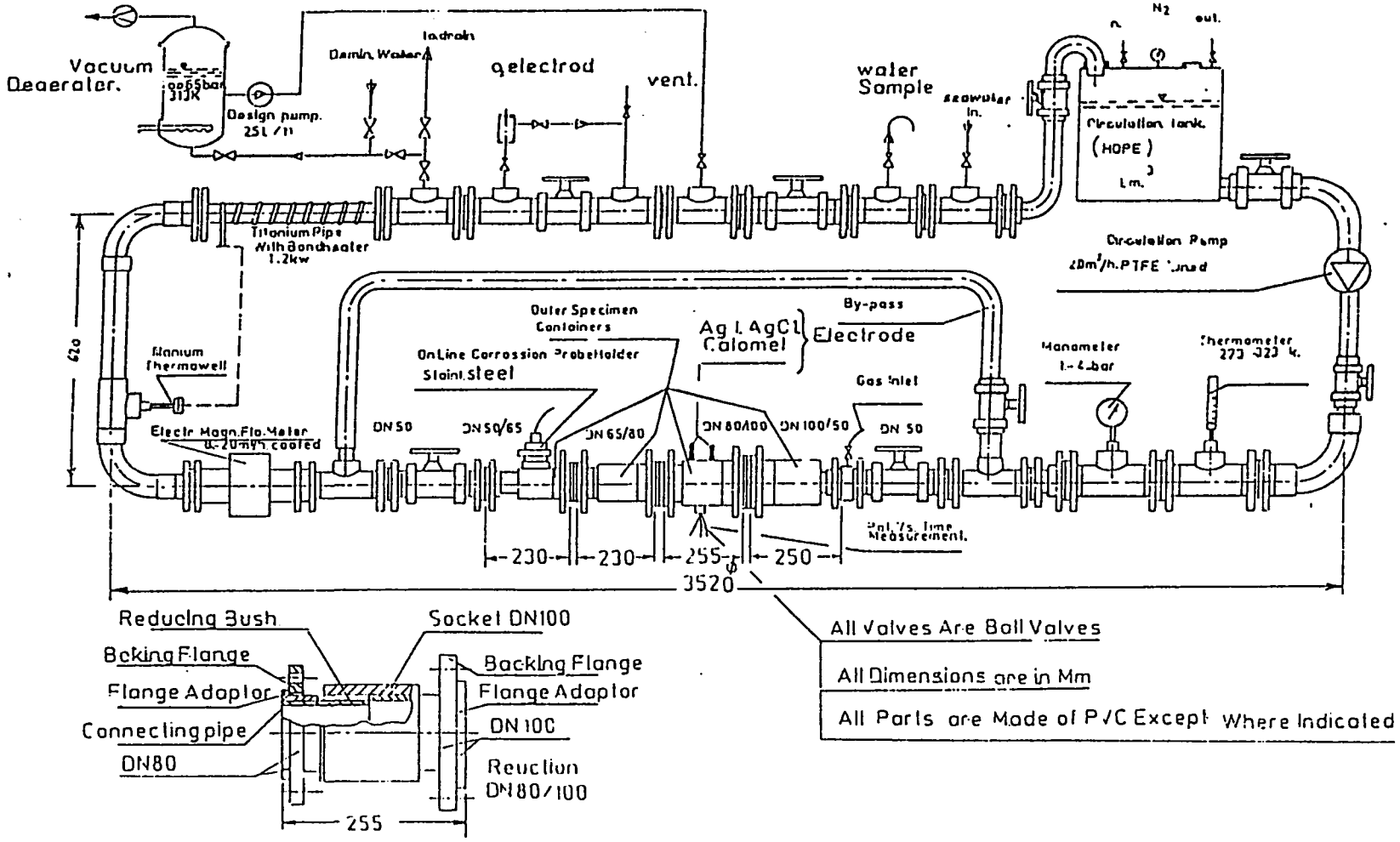

Fig. 4.1: PVC loop for material testing in marine environment

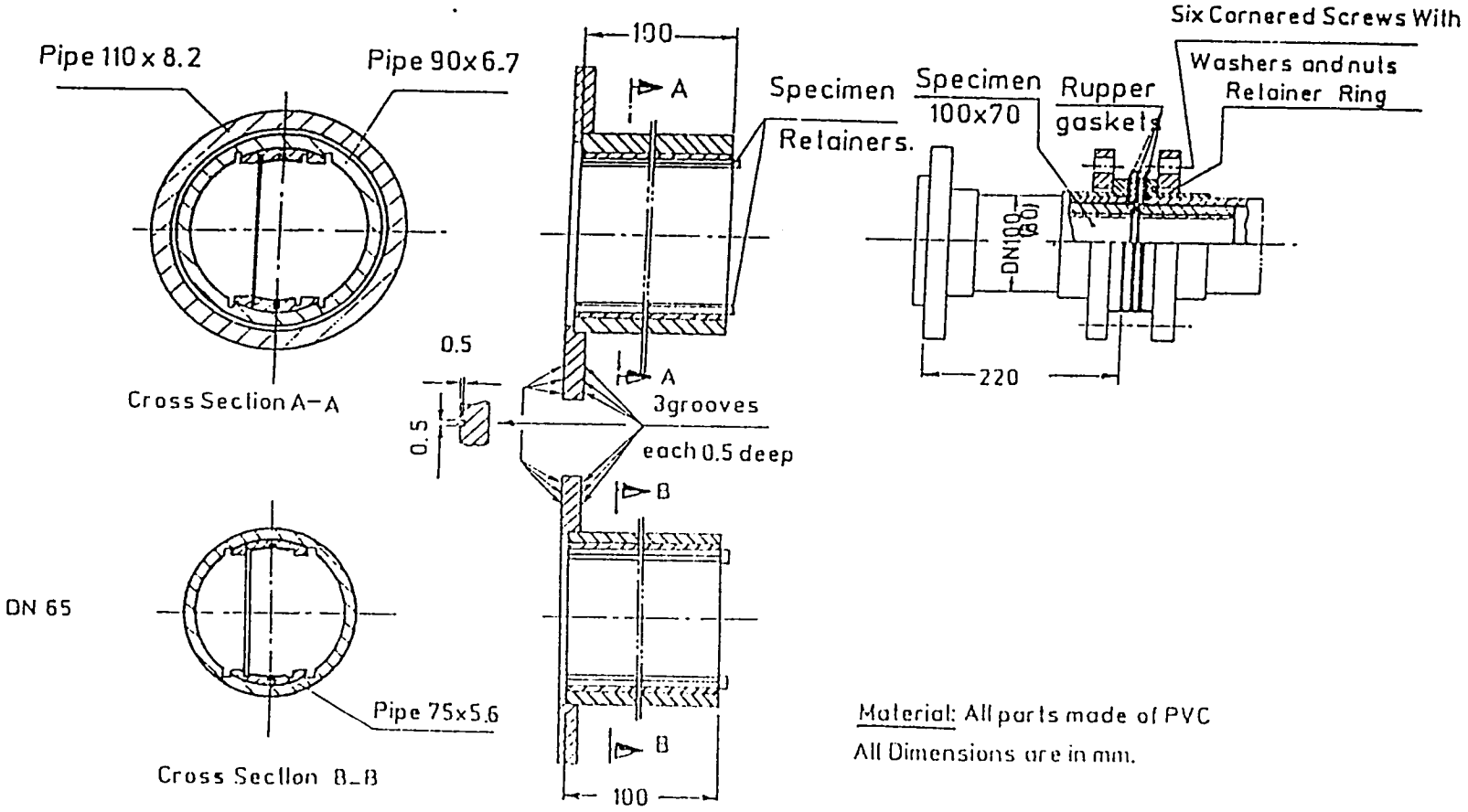

Fig. 4.2: Details of specimen containers

b) *Test Specimens*

For the experiments under dynamic conditions, flat plate type specimens of the following dimensions were used in four velocities sections, respectively.

i) 70 by 100 mm^2

ii) 58 by 100 mm^2

iii) 48 by 100 mm^2

iv) 40 by 100 mm^2

Specimen preparation procedure before and after exposure was the same as was done with samples tested in static conditions.

c) *Test Conditions*

The tests were conducted in two different conditions. 3.5 wt% NaCl solution was used at room temperature in aereated conditions and in deaerated conditions. Weight loss of the samples were determined after 200 hours of exposure.

4.4 Corrosion Rate Calculation

The corrosion rate (CR) was calculated by the following equation [25].

$$\textbf{Corrosion Rate} = (K*W) / (A*t)$$

Where:

K = Constant, and its value varies with the unit used for calculating corrosion rate.

Different values of K, are given in Table 4.1.

W = Weight loss in grams

A = Exposed surface area of the specimen in cm^2

t = Time of exposure in hours

4.5 Results and Discussions

The variation of corrosion rates of Al-6013-20SiC(p) for O, F and T4 tempers, as a function of exposure time in both aerated and deaerated conditions in 3.5% NaCl solution are shown in Fig.'s 4.3 to 4.5. The details of corrosion rates after every 100 hours for F, O and T4 tempers are given in Tables 4.2 to 4.4. All curves indicate an initial decrease in corrosion rate, which is followed by a periodic rise and fall in corrosion rate. This rise and fall in corrosion rate can be attributed to the removal or damaging and reformation of protective film of $Al(OH)_3$. The fluctuation in corrosion rate becomes steady after about 1800 hours. However it is clear that out of three tempers O, T4 and F, T4-temper has the lowest corrosion rate in aerated solution (5.67 mpy) followed by F-temper (6.03 mpy) and O-temper (7.02 mpy) respectively. The weight loss analysis in deaerated condition has shown the same behavior, with T4-temper having the minimum corrosion rate (2.55 mpy) , followed by F-temper (3.42 mpy), and O-temper (2.84 mpy).

TABLE 4.1: Different values of constant 'K'

Corrosion Rate Unit	*Constant 'K' in the Corrosion rate Equation*
Mils per year (mpy)	3.45×10^6
Inches per year (ipy)	3.45×10^3
Millimeters per year (mm/y)	8.76×10^4
Micrometers per year (μm/year)	8.76×10^7
Grams per square meter per hour (g/m^2h)	$1.0 \times 10^4 \times \rho$
Milligrams per square decimeter per day (mdd)	$2.40 \times 10^6 \times \rho$

The variation of corrosion rates of Al6013-20SiC(p) for O, F and T4-tempers, as a function of velocity in both aereated and deaerated conditions in 3.5 wt% NaCl solution are shown in Figs. 4.6 and 4.7. The details of variation of corrosion rate with velocity is given in Table 4.4a and 4.5b. It is evident from the graphs, that the corrosion rate of Al 6013-20SiC(P) in all three tempers increases with velocity. However T4-temper showed relatively lower corrosion rate of 109 mpy, 124.01 mpy, 149 mpy, and 162.193 mpy in aerated condition and 81.99 mpy, 85.96 mpy, 87.76 mpy and 96.36 mpy in deaerated condition at velocities 1.15 m/s, 1.68 m/s, 2.45 m/s and 3.53 m/s, respectively. The trend was therefore similar.

On analyzing the microstructure of unexposed alloy 6013-20SiC(P) O, F and T4 tempers (Fig 4.8 to 4.10), it is evident that in F-temper, SiC particles are randomly placed and are not uniformly distributed. It is also clear, that most of the particles have sharp edges (Fig. 4.8). The micrographs of O-temper shows some uniformity in the distribution of SiC particles, however the grain boundaries are not well defined (Fig. 4.9)

The micrograph of T4-temper shows that age hardening not only made the SiC particles more uniform, but the grain boundaries are also well defined. The edges of SiC particles are not as sharp as in the case of F-temper (Fig. 4.10.).

Micrograph of exposed T4-temper sample is shown in Fig. 4.11. Small cracks between the grains indicate that intergranular corrosion is the most dominant type of corrosion taking place during immersion tests in static condition,. It is shown in Fig.

4.12 that corrosion of T4-temper in dynamic condition occurs by dislodging of the SiC particles.

TABLE 4.2: Variation of corrosion rate of Al6013-20SiC(P)-O with time in aerated and deaerated 3.5 wt% NaCl solution

Time (Hrs)	Corrosion rate Aereated condition (mpy)	(mdd)	Corrosion rate Deaerated condition (mpy)	(mdd)
100	25.06	46.98	19.57	36.21
200	13.52	25.36	8.03	14.87
300	9.62	18.03	4.13	7.65
400	9.37	17.57	3.88	7.19
500	12.43	23.31	6.94	12.85
600	14.12	26.46	8.63	15.96
700	7.82	14.58	4.5	8.43
800	9.34	17.88	5.07	9.51
900	9.34	17.51	9	16.87
1000	9.09	17.03	4.62	8.66
1200	7.2	13.5	2.73	5.13
1400	7.2	13.5	2.73	5.13
1600	7.02	13.15	2.55	4.78
2000	7.02	13.15	2.55	4.78

TABLE 4.3: Variation of corrosion rate of Al6013-20SiC(P)-F with time in aerated and deaerated 3.5 wt% NaCl solution

Time (Hrs)	Corrosion rate Aereated condition (mpy)	(mdd)	Corrosion rate Deaerated condition (mpy)	(mdd)
100	14.76	27.73	10.73	20.21
200	10.73	20.12	8.73	16.29
300	7.12	13.32	4.23	7.92
400	8.19	15.3	4.32	8.19
500	10.6	19.8	6.41	11.97
600	11.39	21.33	7.93	14.85
700	6.37	11.94	7.11	13.32
800	9.18	17.19	5.19	9.72
900	9.4	17.63	6.51	12.24
1000	9.91	18.59	7.11	13.32
1200	6.3	11.8	2.47	4.693
1400	6.21	11.63	3.42	6.4
1600	6.03	11.3	3.42	6.4
2000	6.03	11.3	3.42	6.4

TABLE 4.4: Variation of corrosion rate of Al6013-20SiC(P)-T4 with time in aerated and deaerated 3.5 wt% NaCl solution

Time (Hrs)	Corrosion rate Aereated condition (mpy)	(mdd)	Corrosion rate Deaerated condition (mpy)	(mdd)
100	9.72	18.22	6.3	11.79
200	7.9	14.85	5.4	10.12
300	6.21	11.65	3.6	6.75
400	6.29	11.79	3.26	6.15
500	7.2	13.5	3.26	6.21
600	9.72	18.32	6.88	12.9
700	6.9	12.94	4.5	8.43
800	8.56	16.06	4.77	8.95
900	7.47	14	3.68	6.89
1000	8.1	15.18	1.89	3.56
1200	5.4	10.12	2.51	4.7
1400	5.4	10.12	1.61	2.99
1600	5.4	10.12	1.88	3.51
2000	5.4	10.12	1.88	3.51

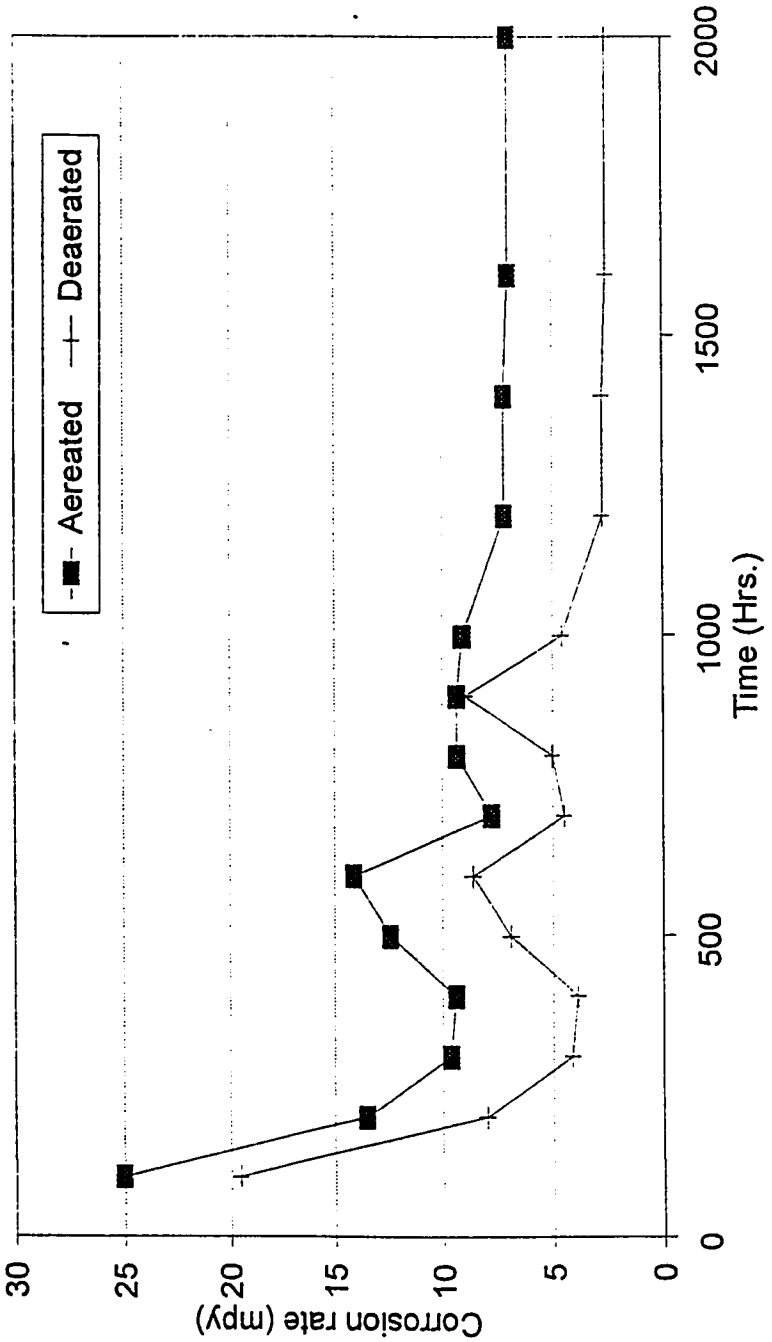

Fig 4.3: Variation of corrosion rate of Al6013-20SiC(P)-O with time

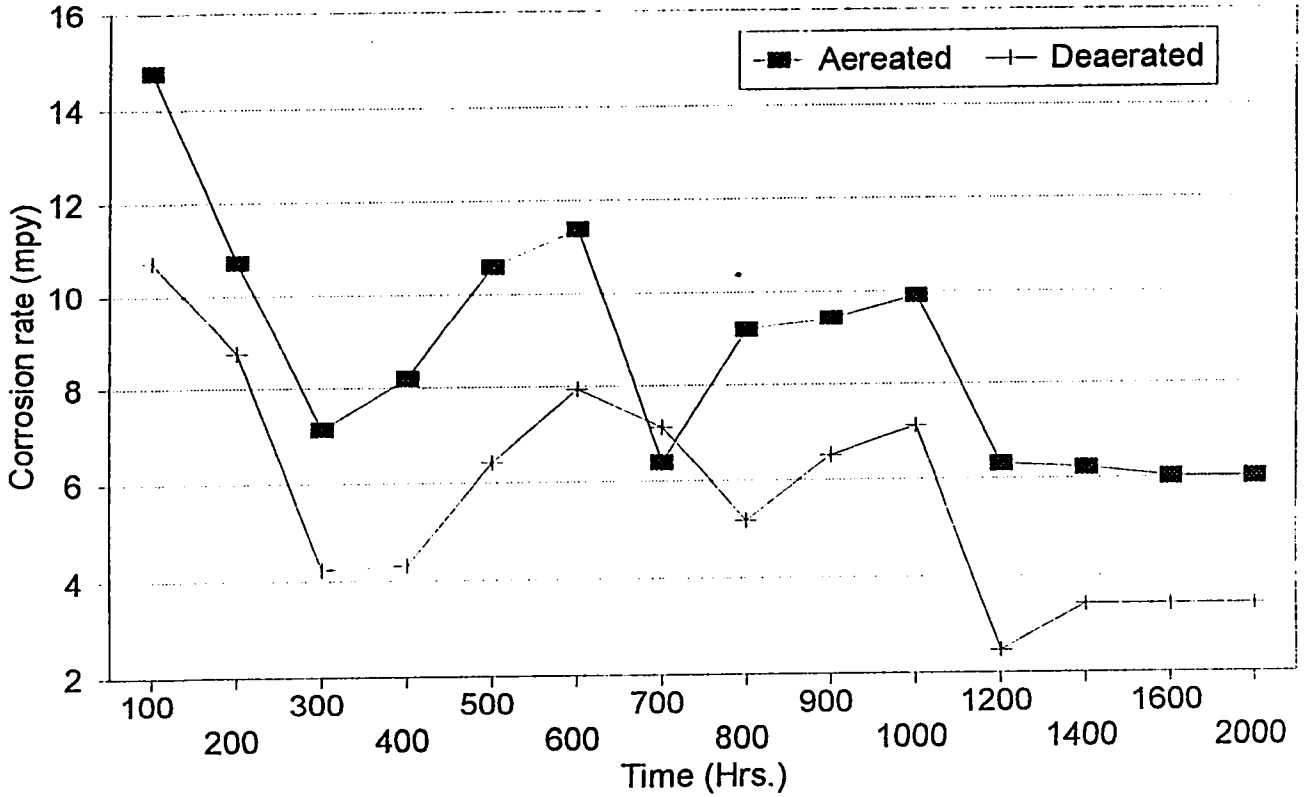

Fig 4.4: Variation of corrosion rate of Al6013-20SiC(P)-F with time

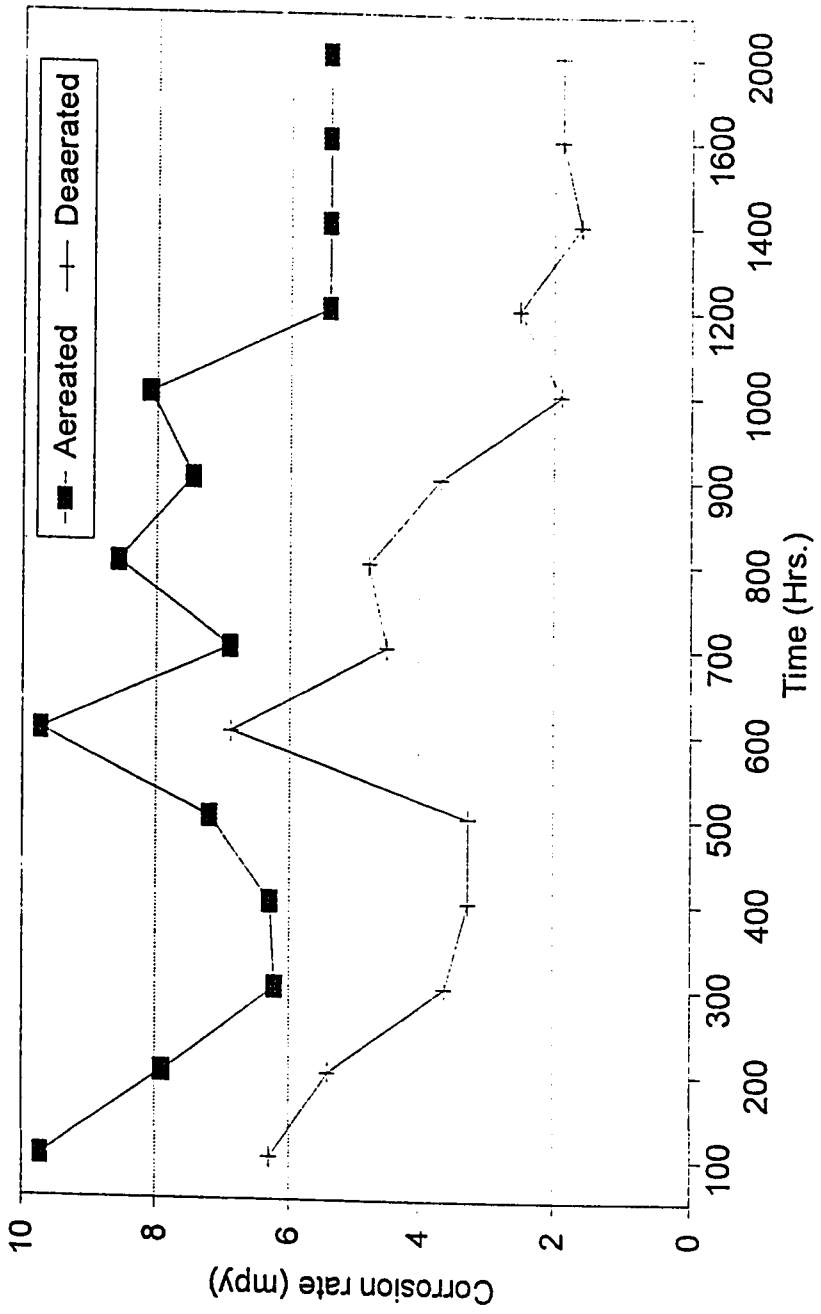

Fig 4.5: Variation of corrosion rate of Al6013-20SiC(P)-T4 with time

TABLE 4.5: Variation of corrosion rate with velocity in (a) aerated condition (b) deaerated condition

(a)

Re No.	Velocity (m/s)	O-Temper (mpy)	O-Temper (mdd)	F-Temper (mpy)	F-Temper (mdd)	T4-Temper (mpy)	T4-Temper (mdd)
37600	1.15	120.6	222.3	109.81	203.13	109.4	193.14
59300	1.68	144.03	266.46	126.49	234.01	124.01	229.43
69700	2.45	171.95	318.11	146.07	270.23	149.81	268.04
81800	3.53	173.97	321.9	169.2	313.02	162.19	300.04

(b)

Re No.	Velocity (m/s)	O-Temper (mpy)	O-Temper (mdd)	F-Temper (mpy)	F-Temper (mdd)	T4-Temper (mpy)	T4-Temper (mdd)
37600	1.15	90.27	166.99	87.48	161.83	81.99	151.67
59300	1.68	95.75	177.13	86.96	160.88	85.96	159.04
69700	2.45	100.71	186.33	88.1	162.99	87.87	162.57
81800	3.53	103.12	189.9	98.78	182.74	96.36	178.27

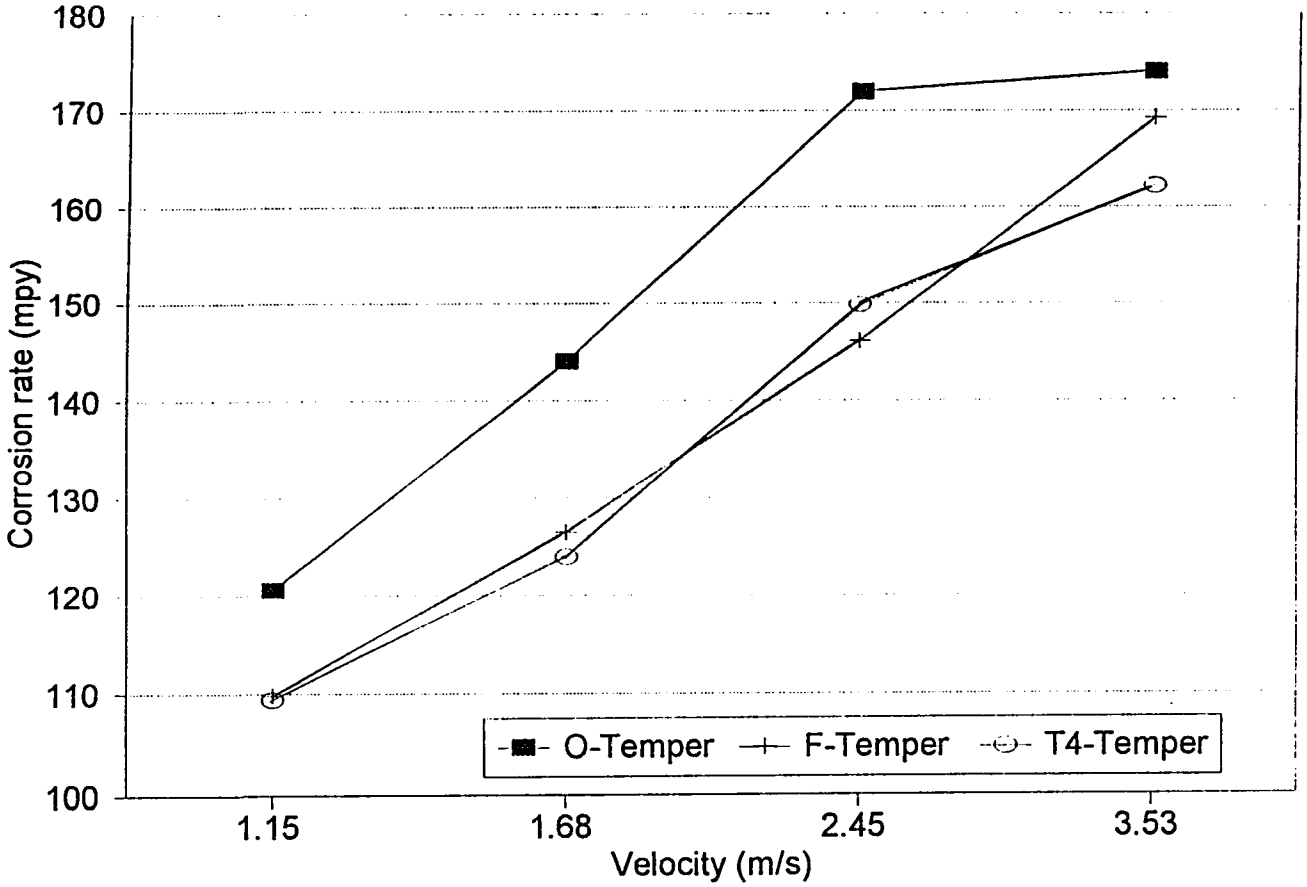

Fig 4.6: Variation of corrosion rate of Al6013-20SiC(P)-O,F and T4 with velocity, in aereated condition

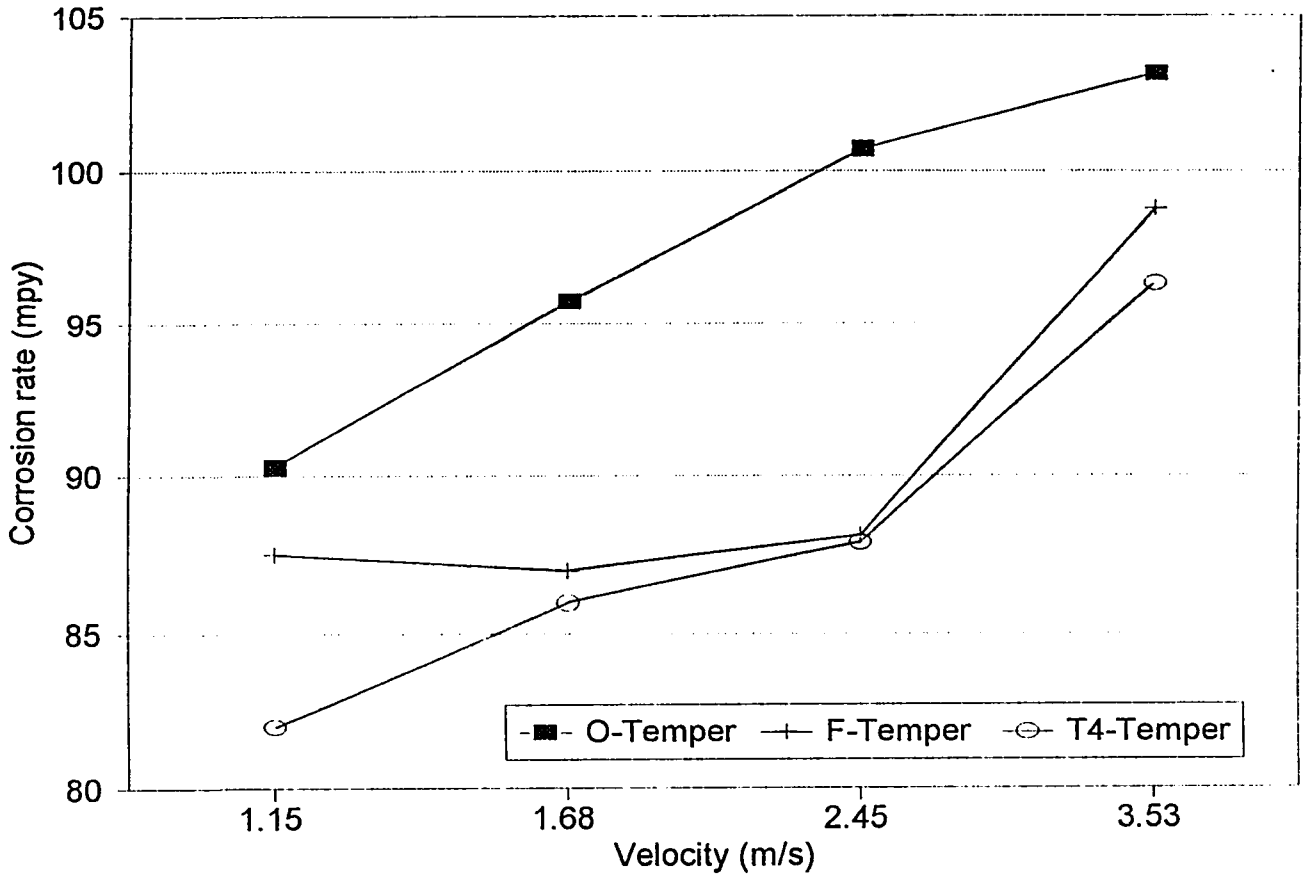

Fig 4.7: Variation of corrosion rate of Al6013-20SiC(P)-O,F and T4 with velocity, in deaereated condition

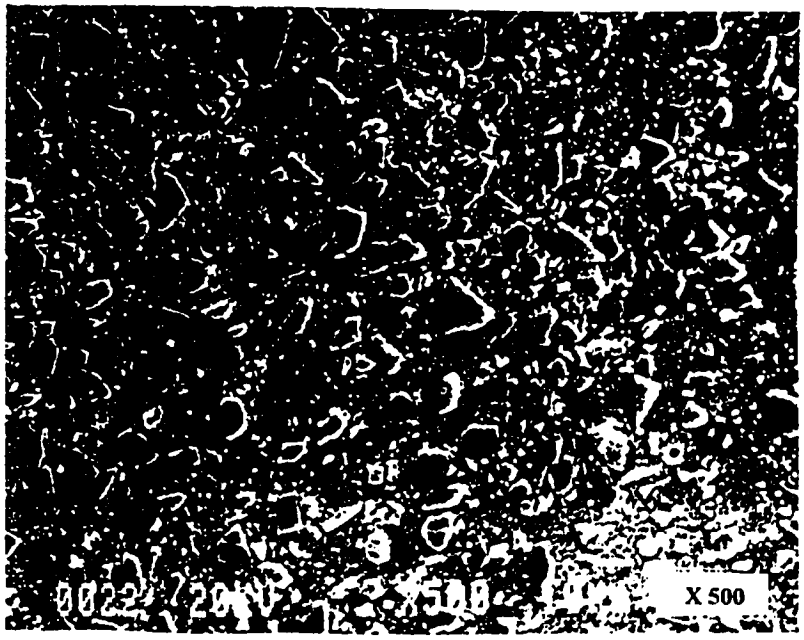

Fig 4.8: Microstructure of Al6013-20SiC(P)-F

Fig 4.9: Microstructure of Al6013-20SiC(P)-O

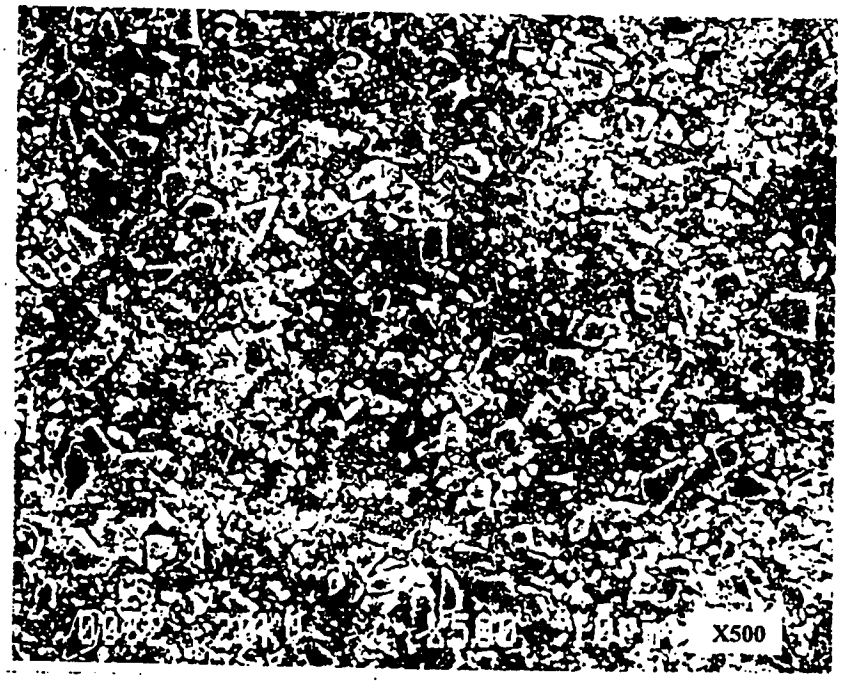

Fig 4.10: Microstructure of Al6013-20SiC(P)-T4

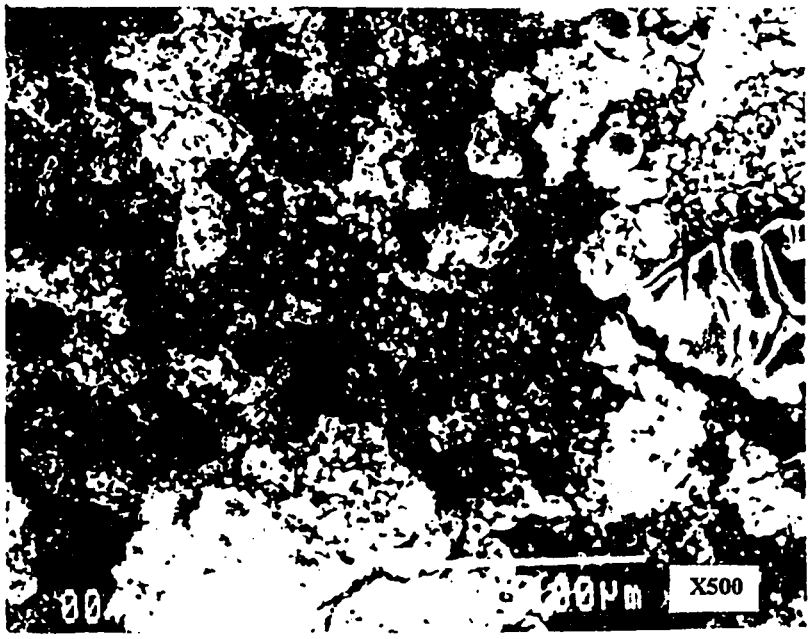

Fig 4.11: Micrograph of Al6013-20SiC(P)-T4, exposed to 3.5 wt% NaCl solution under static conditions

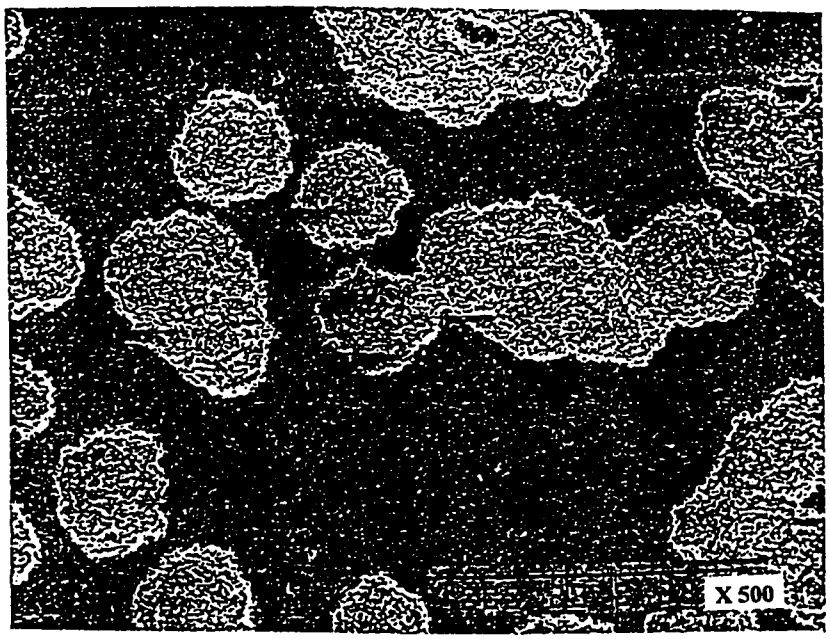

Fig 4.12: Micrograph of Al6013-20SiC(P)-T4, exposed to 3.5 wt% NaCl solution under dynamic conditions

Chapter 5

OPEN CIRCUIT POTENTIAL VS TIME STUDY

5.1 Introduction

Long term corrosion behavior of alloys in different environments is reflected well in potential time studies. It also gives a fair estimate of the dissolution kinetics of the oxide film in aluminum alloys. The fluctuations in potential time are due to the competitive process of adsorption of certain species and dissolution of metal due to the presence of reacting species. The fluctuation of potential either in positive or negative direction indicates the dissolution or film forming process on the surface of the metal. There is sufficient evidence to suggest the existence of a duplex films on aluminum alloys containing an outer porous layer and an inner compact layer [33]. The shift in potential signifies the initiation and passivation of pits and the changes in the kinetics of the oxide film. At both anodic and cathodic sites in aluminum alloys, $Al(OH)_3$ is produced and the amount formed depends on the transport characteristics of the film. At cathodic sites the main activity is cathodic reduction which results in an increase of alkalinity. The oxide film become thinner with time due to increase in the alkalinity [34].

The grain boundaries function as cathodic sites, the reaction rate being controlled by the dissolution of the oxide layer. $Al(OH)_3$ is deposited near the grain boundaries during the cathodic reaction. Increased oxygen transport takes place which

results in the onset of anodic activity, thus both reactions may occur at one site simultaneously. The transport process is impeded as the thickness of hydroxide layer is increased. The thickness of the outer layer (porous) affects the diffusion of a specie to the inner compact barrier layer. The dissolution of the outer layer would increase the diffusion path and affect the transport process for species like $(OH)^-$ [35].

The open circuit potential behavior of aluminum is represented schematically in Fig 5.1. The potential surges are very pronounced in the initial exposure period and the intensity continues to decrease until a steady state is achieved. The variation of open circuit potential with respect to time is shown within the frame work of four separate regions. Region I, corresponds to the pit initiation phase immediately after the specimen is immersed. Pits can not be detected as soon as they nucleate and considerable time is required for the pits to grow to a sufficient size to be visible under the microscope. Region II, is associated with the early phase of the pit propagation. The potential oscillates in the form of rapid surges which are predominantly in the positive direction and are caused by the evolution of H_2 bubbles. Region III, starts with the surges which are more in the negative direction and less frequent. The oscillations especially in the negative direction are typical of pure aluminum and are not always observed in the alloy metal. The region is believed to correspond to the later stage of propagation associated with reduced

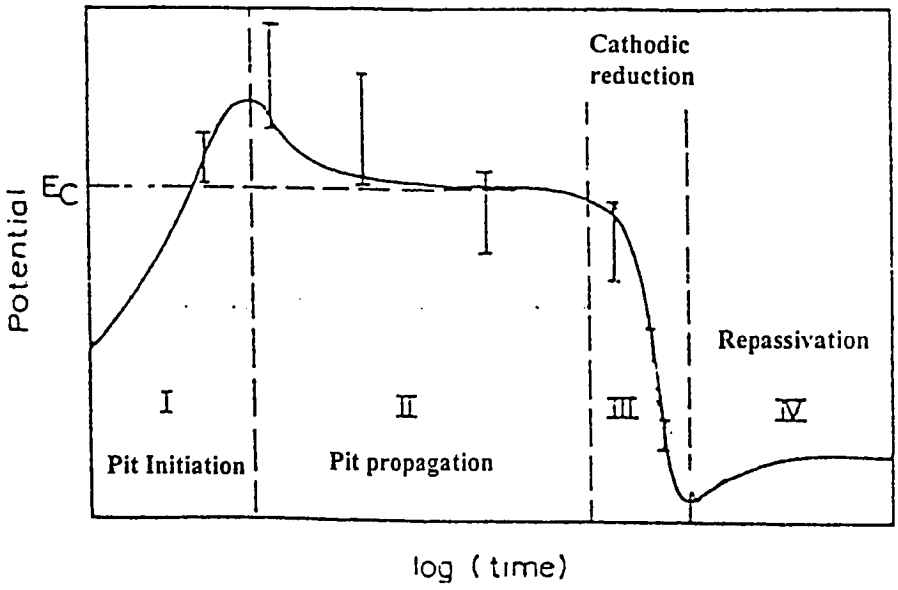

Fig 5.1: Schematic representation of open circuit potential (OCP) of Aluminum with respect to time in NaCl solution [36]

cathodic area for O_2 reduction. The decrease in the potential signals a shift in the corrosion mechanism from anodic to cathodic control as a result of this decrease in the cathodic area. In region IV, rapid surges in the potential disappear. This behavior is frequently interpreted as the onset of repassivation [36]. The potential surges observed in the initial period of immersion are highly pronounced and they tend to slow down with increased exposure time.

This technique is usually employed to assess the pitting resistance of different alloys by observing the changes in potentials and the steady state potential.

5.2 Results and Discussions

The open circuit potential behavior of alloy Al6013-20SiC(P) in O-temper, T4-temper and in as fabricated form (F), in aerated and deaerated 3.5 wt% NaCl solution and sea water under static conditions is shown in Figures 5.2, 5.3 and 5.4 respectively. The variation of potential of O-temper, T4-temper and in as fabricated form (F) is given in Table 5.1 and 5.2. In all six cases the OCP shifts in the positive direction during the early period of exposure. This shift corresponds to region I of Fig 5.1, which represents pit initiation. From the figures it is also clear that in all cases, the shift of potential of T4-temper is more towards the positive or noble direction, whereas the alloy in O-temper and in as fabricated form (F) show a lesser tendency to shift in the positive direction . A detailed comparison among the three is given in Table 5.3.

The shift of potential of T4-temper towards the positive direction indicates the tendency of film formation. The OCP values of Al6013-20SiC(P) in O, T4 and F conditions reaches a steady state after 90 to 100 hours.

From Table 5.3 it is evident that after the exposure time of 200 hours the potential of T4-temper shifts from -686mV(SCE) to -680mV(SCE) in aerated 3.5 wt% NaCl solution and from -687mV(SCE) to -675mV(SCE) in deaerated 3.5 wt% NaCl solution. The open circuit potential of the alloy in T4-temper remains for a major proportion of the time in more noble (positive) range of potential, however some fluctuations in the less nobel (negative) direction are also observed. The fluctuations in less nobel direction has been attributed to the micro-segregation caused by sudden cooling during quenching in age hardening [16]. However, the high corrosion resistance of T4-temper of the alloy can be related to the uniform distribution of SiC particles and their smooth edges thereby causing a decrease in anodic areas. This decrease in anodic areas makes the SiC and matrix interface less reactive.

From the studies conducted, it is observed that the alloy in T4-temper is least reactive to potential fluctuations, particularly in the active direction and have a good resistance to corrosion as predicted by the potential time studies.

TABLE 5.1: Variation of open circuit potential of Al6013-20SiC(P) with exposure time in aerated 3.5 wt% NaCl and Arabian Gulf water

	3.5% NaCl			Sea Water		
Time	O-Temper	F-Temper	T4-Tempe	O-Temper	F-Temper	T4-Tempe
Hrs.	mVsce	mVsce	mVsce	mVsce	mVsce	mVsce
0	-0.781	-0.734	-0.686	-0.7	-0.709	-0.687
1	-0.779	-0.715	-0.669	-0.679	-0.712	-0.631
2	-0.755	-0.715	-0.676	-0.667	-0.706	-0.635
3	-0.759	-0.713	-0.67	-0.678	-0.705	-0.634
4	-0.762	-0.712	-0.677	-0.671	-0.706	-0.628
5	-0.765	-0.713	-0.677	-0.672	-0.706	-0.633
6	-0.765	-0.713	-0.674	-0.677	-0.707	-0.635
18	-0.787	-0.722	-0.674	-0.69	-0.714	-0.642
20	-0.788	-0.723	-0.674	-0.687	-0.713	-0.646
24	-0.795	-0.721	-0.676	-0.687	-0.713	-0.645
33	-0.827	-0.758	-0.691	-0.686	-0.713	-0.648
41	-0.808	-0.758	-0.682	-0.684	-0.717	-0.648
42	-0.822	-0.754	-0.678	-0.687	-0.712	-0.649
43	-0.826	-0.76	-0.684	-0.685	-0.713	-0.651
44	-0.829	-0.76	-0.691	-0.689	-0.716	-0.658
45	-0.834	-0.762	-0.684	-0.689	-0.716	-0.659
55	-0.832	-0.761	-0.678	-0.69	-0.716	-0.66
75	-0.841	-0.764	-0.687	-0.694	-0.726	-0.669
85	-0.823	-0.763	-0.692	-0.692	-0.724	-0.664
90	-0.86	-0.764	-0.693	-0.695	-0.726	-0.668
110	-0.86	-0.763	-0.688	-0.695	-0.729	-0.67
125	-0.86	-0.764	-0.686	-0.695	-0.729	-0.67
140	-0.86	-0.755	-0.68	-0.691	-0.721	-0.67
160	-0.86	-0.755	-0.68	-0.691	-0.721	-0.66
170	-0.86	-0.755	-0.68	-0.691	-0.721	-0.66
180	-0.86	-0.755	-0.68	-0.691	-0.721	-0.66
190	-0.86	-0.755	-0.68	-0.691	-0.721	-0.66
200	-0.86	-0.755	-0.68	-0.691	-0.721	-0.66

TABLE 5.2: Variation of open circuit potential of Al6013-20SiC(P) with exposure time in deaerated 3.5 wt% NaCl and Arabian Gulf water

	3.5% NaCl			Sea Water		
Time	O-Temper	F-Temper	T4-Tempe	O-Temper	F-Temper	T4-Tempe
Hrs.	mVsce	mVsce	mVsce	mVsce	mVsce	mVsce
0	-0.84	-0.73	-0.69	-0.708	-0.73	-0.826
2	-0.97	-0.76	-0.726	-1.046	-0.76	-0.982
4	-1.07	-0.789	-0.747	-1.039	-1.04	-1.026
8	-1.1	-0.811	-0.809	-1.047	-1.05	-1.042
10	-1.11	-0.815	-0.865	-0.948	-1.06	-1.067
15	-1.11	-0.855	-0.868	-0.937	-0.791	-1.098
20	-1.11	-0.878	-0.89	-0.938	-0.769	-1.11
25	-1.11	-0.899	-0.922	-0.917	-0.732	-1.089
30	-1.126	-0.92	-0.958	-0.913	-0.735	-0.787
35	-1.124	-0.93	-0.992	-0.908	-0.731	-0.786
40	-1.125	-0.935	-1	-0.912	-0.732	-0.785
45	-1.127	-0.944	-1.082	-0.901	-0.754	-0.785
50	-1.13	-0.998	-1.085	-0.893	-0.754	-0.786
55	-1.137	-0.998	-1.081	-0.884	-0.756	-0.785
60	-1.132	-0.975	-1.088	-0.861	-0.762	-0.79
65	-1.138	-0.965	-1.086	-0.82	-0.762	-0.792
70	-1.145	-0.932	-1.088	-0.823	-0.766	-0.816
75	-1.146	-0.91	-1.086	-0.826	-0.76	-0.816
80	-1.144	-0.909	-1.088	-0.822	-0.768	-0.818
85	-1.146	-0.91	-1.094	-0.825	-0.763	-0.818
90	-1.146	-0.9	-1.1	-0.821	-0.771	-0.816
95	-1.146	-0.9	-1.098	-0.816	-0.795	-0.813
100	-1.142	-0.9	-1.099	-0.819	-0.795	-0.811
105	-1.121	-0.9	-1.103	-0.817	-0.796	-0.812
120	-1.132	-0.9	-1.102	-0.82	-0.796	-0.814
130	-1.135	-0.9	-1.103	-0.818	-0.796	-0.813
150	-1.141	-0.905	-1.105	-0.82	-0.799	-0.812
170	-1.14	-0.907	-1.105	-0.817	-0.799	-0.813
185	-1.139	-0.908	-1.104	-0.817	-0.799	-0.813
200	-1.139	-0.908	-1.105	-0.817	-0.799	-0.813

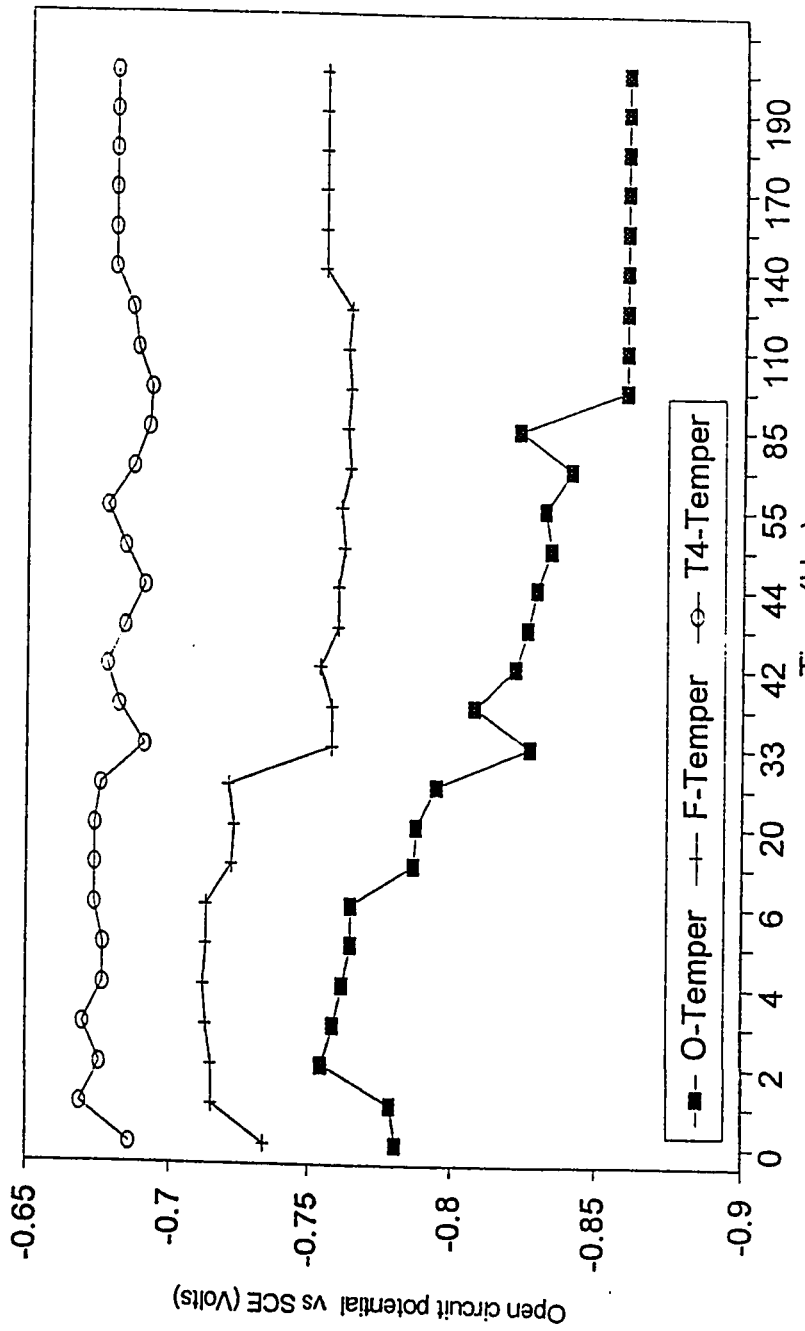

Fig 5.2: Open circuit potential of Al6013-20SiC(P) in aerated 3.5 wt% NaCl solution

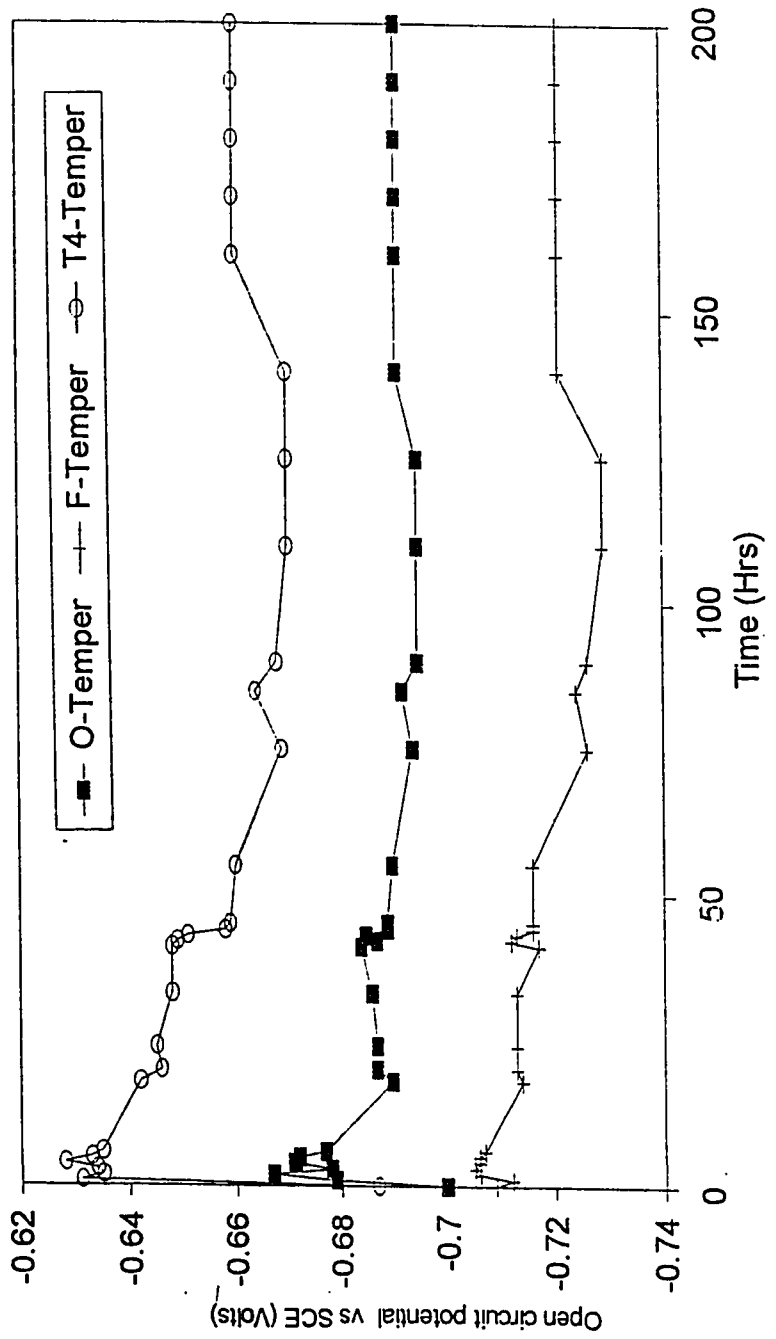

Fig 5.3: Open circuit potential of Al6013-20SiC(P) in aerated Arabian Gulf water

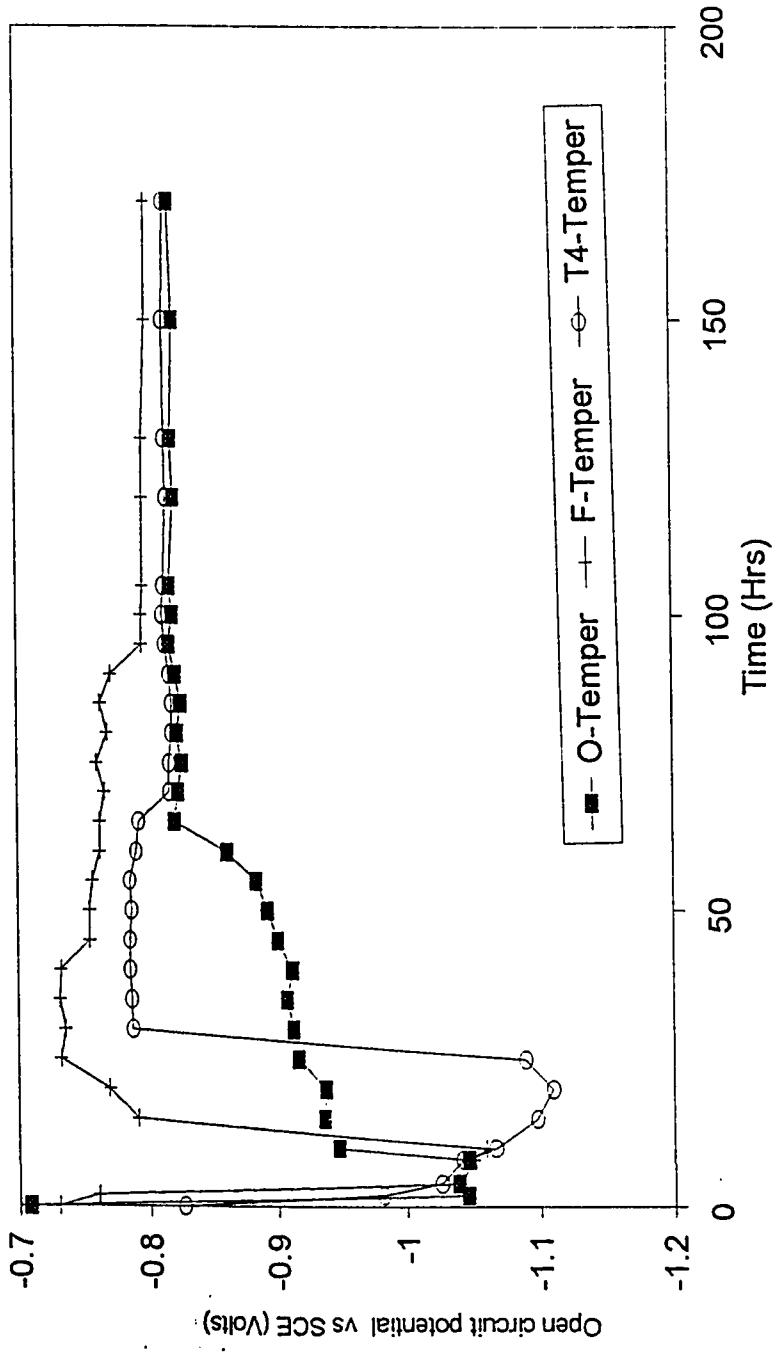

Fig 5.4: Open circuit potential of Al6013-20SiC(P) in deaerated 3.5 wt% NaCl solution

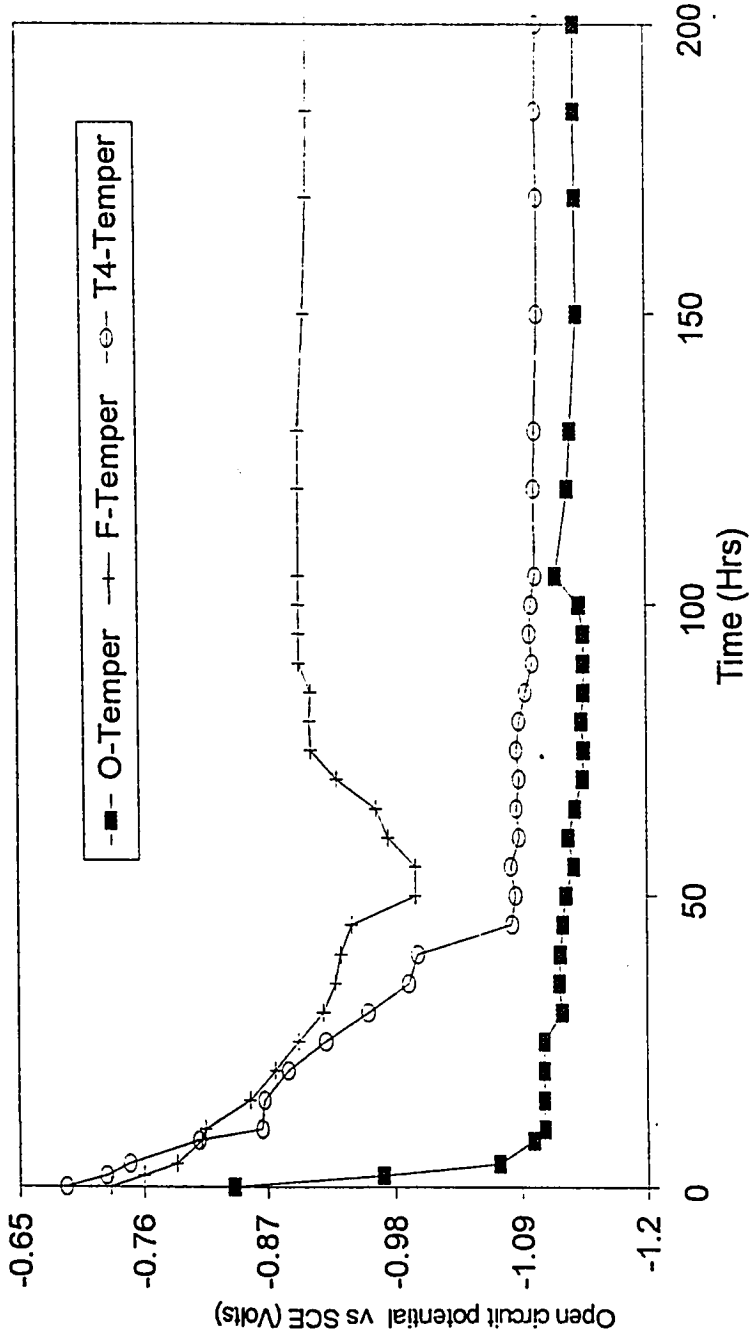

Fig 5.5: Open circuit potential of Al6013-20SiC(P) in deaerated Arabian Gulf

TABLE 5.3: Summary of open circuit potential vs time studies in (a) aerated condition (b) deaerated condition

(a)

Time (Hrs)	Solution	Potential			Condition		
		O	F	T4			
0	3.5 wt% NaCl	-0.781	-0.734	-0.686	P	P	P
200	3.5 wt% NaCl	-0.86	-0.755	-0.68	P	P	P
0	Arabian Gulf	-0.7	-0.709	-0.687	P	P	P
200	Arabian Gulf	-0.691	-0.721	-0.66	P	P	P

(b)

Time (Hrs)	Solution	Potential			Condition		
		O	F	T4			
0	3.5 wt% NaCl	-0.84	-0.73	-0.69	P	P	P
200	3.5 wt% NaCl	-1.139	-0.908	-1.105	P	P	P
0	Arabian Gulf	-0.708	-0.73	-0.826	P	P	P
200	Arabian Gulf	-0.817	-0.799	-0.813	P	P	P

Chapter 6

ELECTROCHEMICAL PITTING ANALYSIS

6.1 Introduction

6.1.1 *Pitting Corrosion*

Pitting is a special case of localized attack in which selected areas of the metal are attacked and the rest of the metal remains unaffected. Development of holes or perforations is the ultimate result of pitting. It is a serious problem for metals which show passivity. Most industrial metals and alloys are susceptible to pitting and incidentally the susceptibility decreases with increased cost of metal [37].

Pitting is the most important parameter in which the performance of an alloy in sea water and similar environment is judged. Electrochemical techniques like polarization curves and pitting scans are frequently used to evaluate and analyze pitting.

6.2 Mechanism of Pitting

Several mechanisms of pitting have been suggested, however there is no mechanism in existence which is accepted by all researchers. Some important points discussed below are however accepted by majority of researchers [11,12,21,28,34,35,36,39,47]. The process of oxidation takes place at the anode and

reduction takes place at the cathode. Pits are formed on the anodic sites. Within a pit, oxygen gets depleted because of restricted convection and metal dissolution continue to take place creating acidic conditions. The process of anodic dissolution shown in Fig 6.1 produces an excess of positive ions (metal ions). In order to neutralize charge, migration of anions (Cl^- , Br^- , I^-) take place to the pit interior, which results in the formation of metal chlorides ($M^+ Cl^-$). This is followed by the process of hydrolysis ($M^+ Cl^- H+HOH$ $\Longrightarrow MOH+H^+ +Cl^-$). The production of H^+ and Cl^- accelerates the process of dissolution. In this process the solution becomes acidic and the pit continues to grow. Inspite of the depletion of oxygen, the process of dissolution continues within the pit. The pitting process is, therefore, termed as "autocatalytic" i.e., once started it continues till the metal is perforated. In the process many new pits are inactivated because the inward migration of chloride ionizes insufficiently to offset the loss of corrosion products by diffusion and convection. The outer surfaces of the pit is protected because of the migration of electrons from the pit interior. This is one reason why the surface of the metal adjacent to the pit does not corrode.

6.3 Cyclic Polarization

One of the most common electrochemical technique used for making the pitting analysis is Hysterisis technique. A typical polarization plot is shown in Fig. 6.2. The diagram can be conveniently divided into three regions.

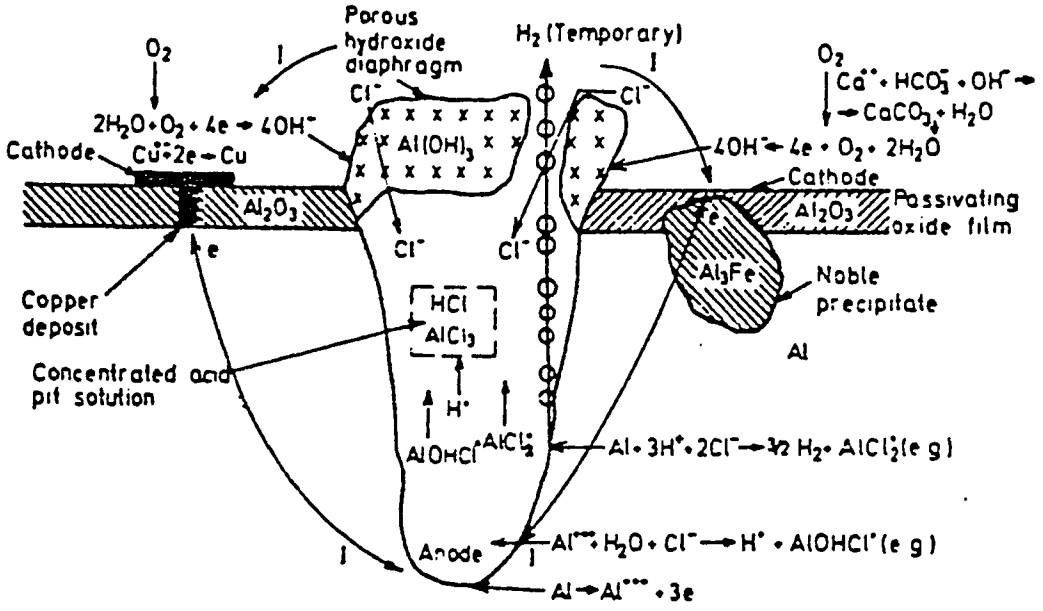

Fig 6.1: Schematic representation of pit on Aluminum showing how the rate of pitting may be facilitated by an intermetallic phase (Al_3Fe) [38].

Region {A}: This region represents immunity to pitting and potentials are more negative than Protection potential (E_{pp}). Pitting is not expected to propagate.

Region {B}: In this region new pits will not initiate, but the pits initiated in region {C} would continue to propagate. This region therefore represents the propagation of pits. Below the point designated by E_{pp} there shall be no initiation or propagation of pits. At this point the dissolution rate becomes equal to the passive current density. The potential at which the pits virtually cease to exist is called the protection potential (E_{pp}).

Region {C}: In this region pitting initiation and propagation shall take place on and above a certain potential, called breakdown potential or critical pitting potential designated as E_p. The breakdown potential and critical pitting potential have the same meaning and this potential signifies the onset of pitting.

Corrosion potential is defined as the potential at which the rate of oxidation equals the rate of reduction and it is represented by the points of intersection of anodic and cathodic curves.

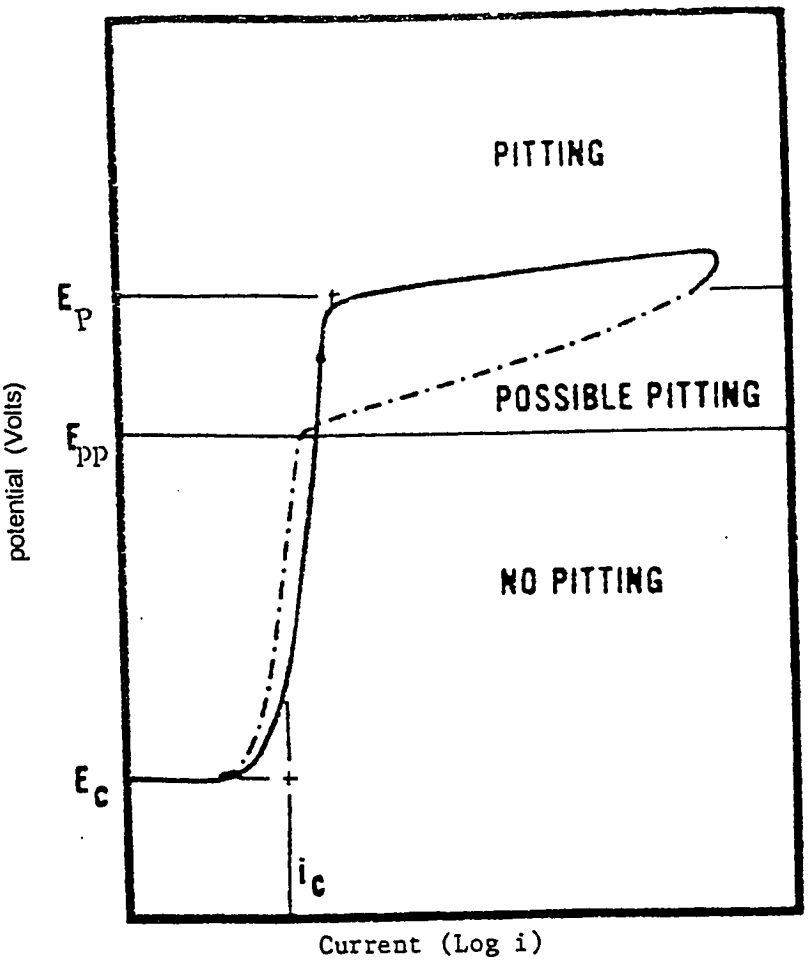

Fig 6.2: Typical anodic polarization curve showing various regions of pitting [40].

From the cyclic polarization curve, predictions of pitting susceptibility can be made. If the value of pitting potential is positive to corrosion potential, the resistance of alloy to pitting is considered high, however it is not fully established. On he other hand a value of pitting potential E_p negative to E_c, the pitting resistance is low.

6.4 Experimental Procedure

6.4.1 *Apparatus*

A potentiostat Model EG&G 273 A, interfaced with IBM PC 286 computer was used to evaluate the pitting resistance of the composites. A polarization cell consisting of a reference, auxiliary and working electrode was connected to the potentiostat (Fig 6.3). All potentials were measured with respect to a saturated calomel electrode (SCE). A high density graphite electrode was used as a counter electrode. For experiment under dynamic conditions, a newly designed and fabricated stainless steel loop was used. Again a potentiostat model 273A interfaced with IBM PC 286 was used to evaluate the pitting resistance.

6.4.2 *Specimen Preparation.*

Circular disk specimens of 1.5 cm diameter were grounded with a 600 grit silicon carbide paper to remove coarse scratches. Polishing was carried out with a 0.3 micron, silicon carbide abrasive particles and final polishing was done with 0.05 micron abrasive particles. The specimens were then treated with boiling benzene and 5% acetic

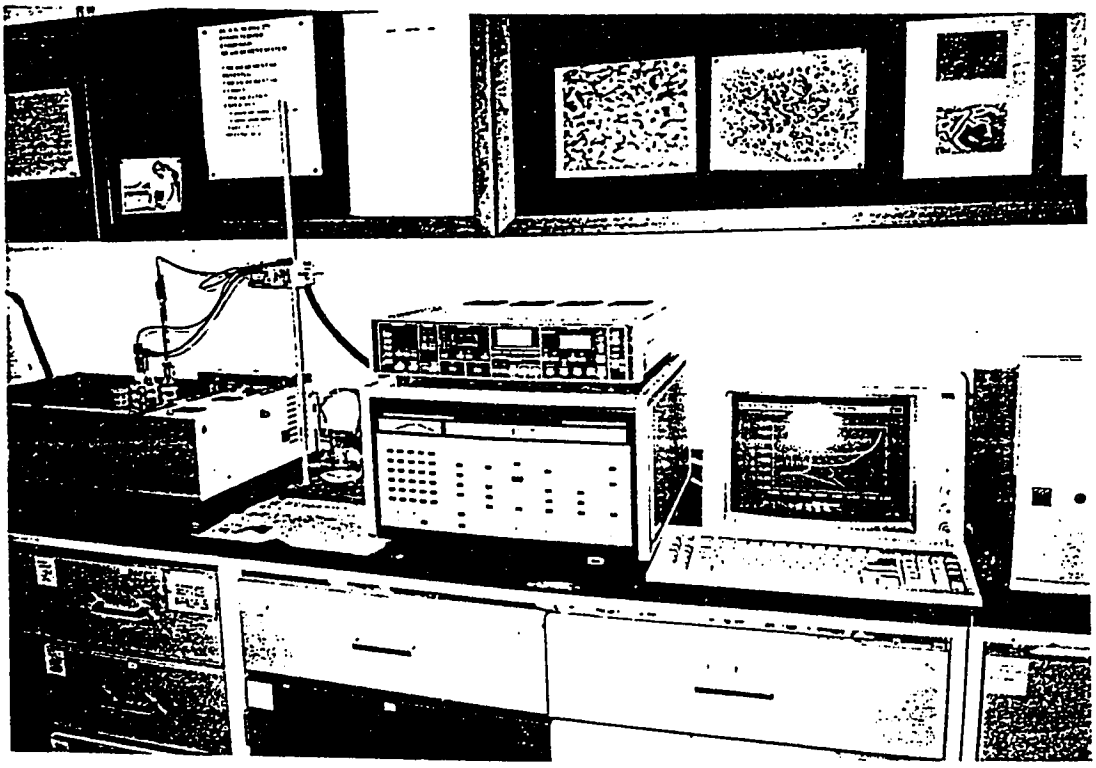

Fig 6.3: Polarization cell with potentiostat (EG&G 273A) interfaced with IBM PC.

acid for five minutes, rinsed in acetone, washed with demineralized water, air dried and stored in a desiccator for 24 hours prior to the commencement of experiment.

For the experiment under the dynamic conditions rectangular specimen of 25 mm by 10 mm were used. Sample preparation remained the same as in the case of static condition. For metallographic observations of pits, specimens were first cleaned with demieralised water, descaled in a descaling solution and finally ultrasonically cleaned in demineralised water and acetone before metallographic examination. Etching was not necessary for samples exposed to corrosive media. For scanning electron microscopy the samples were ultrasonically cleaned with acetone and dried with hot air, before mounting. The samples were gold coated at 1200V under a vacuum of 10-3 torr for 5 minutes. A film thickness of 2.0 A° was finally achieved.

6.5 Experimental Method

6.5.1 *(Potentiodynamic Analysis) E=f(t)*

The specimens were polarized for one hour at -1500 mV_{SCE} in the passive potential region. Polarization was commenced from passive state at a scan rate of 10mV/sec and continued in the noble direction until the pitting potential was reached. At pitting potential a sudden increase in the current was observed. The pitting potential (E_P) was determined by the extrapolation of polarization curve. The polarization curve was reversed at a predetermined current and the scan is continued until the current drops to

its initial value. The protection potential (E_{PP}) is represented by the intersection of the reverse polarization curve with the forward anodic polarization curve.

6.5.2 *(potentiostatic Analysis) E=Const., I=f(t)*

The value of E_p and E_{pp} were determined from I-t diagram as follows:

a) The specimen was polarized for one hour at -1500mV$_{SCE}$

b) Six values of potentials, differing by five to ten mV from each other were chosen in the vicinity of the pitting potential obtained by the potentiodynamic method. Three values of potential were chosen above E_p and three were chosen below E_p.

c) The selected potential was applied and held for 10 to 16 hours, or less if pitting corrosion was established earlier.

d) At each selected value of potential, current was measured as a function of time and I-t diagram were recorded. A new specimen was used at each potential.

e) During the entire experiment, temperature was kept constant. The electrolyte was continuously stirred and saturated with nitrogen.

f) The pitting potential E_p was determined between the most nobel potential value which gave no current increase and the most active potential which gave a current increase. The pitting potentials under these conditions were obtained with an accuracy of $E<Ep<E\pm10mV$.

The exact value of pitting potential from I-t diagram was obtained as follows:

i) The induction time (t) for pits to initiate at each potential was determined from the I-t curves

ii) The value of initiation rate (1/t) min-1 were plotted against the selected values of applied potentials, and best curve through a maximum no of points was obtained. The relationship was extrapolated to 1/t =0, (t=∞). The potential at which the curve intersects the y-axis gives the exact value of the pitting potential (E_p).

h) The pitting potential so obtained was verified by observation of initiation of pits by microscope. separate samples were used for this observation.

A similar process was adopted for determination of protection potential (E_{pp}).

6.6 Electrochemical Pitting Analysis Under Elevated Temperature and Dynamic conditions

6.6.1 *Description Of Stainless 316 High Temperature And High Pressure Recirculating Corrosion Test Loop*

For the experiments under dynamic conditions a loop as shown in Fig 6.4 was designed and fabricated for experimental investigations of pitting analysis at elevated temperature.

The loop was designed to study the effect of several variables such as oxygen, temperature, pressure, velocity and suspended solids on corrosion rates of various materials in sea water or in sodium chloride solution. It was fabricated from stainless steel 316. An electric band heater of 2.5 kW power, with two thermocouples and associated temperature controller were used for maintaining the temperature upto 130° C. A magnetically driven stainless steel 316 pump capable of maintaining velocities upto 0.95 m/s was used to recirculate the water. The corrosion cell was designed to accommodate one or two samples at a time. Details of corrosion cell are shown in Fig 6.5. A water cooled high temperature high pressure (AgCl) external reference electrode (Cortest) was used, which is designed to withstand temperatures upto 275°C and pressures upto 200 psi. The construction of reference electrode is shown in Fig. 6.6.

The working electrodes and reference electrode are positioned at an circumfrential angle of 50° to keep IR drop to a minimum.

A continuos circulating system was maintained in the loop. The corrosive media enters through the control valves and passes through the heaters. The heated media at desired temperature and pressure is then passed through the corrosion cell. The pH, oxygen and pressure level are controlled in the pressure tank.

6.6.2 *Test Specimens*

For pitting analysis under dynamic conditions, flat plate type specimens of 25 mm by 10 mm were used.

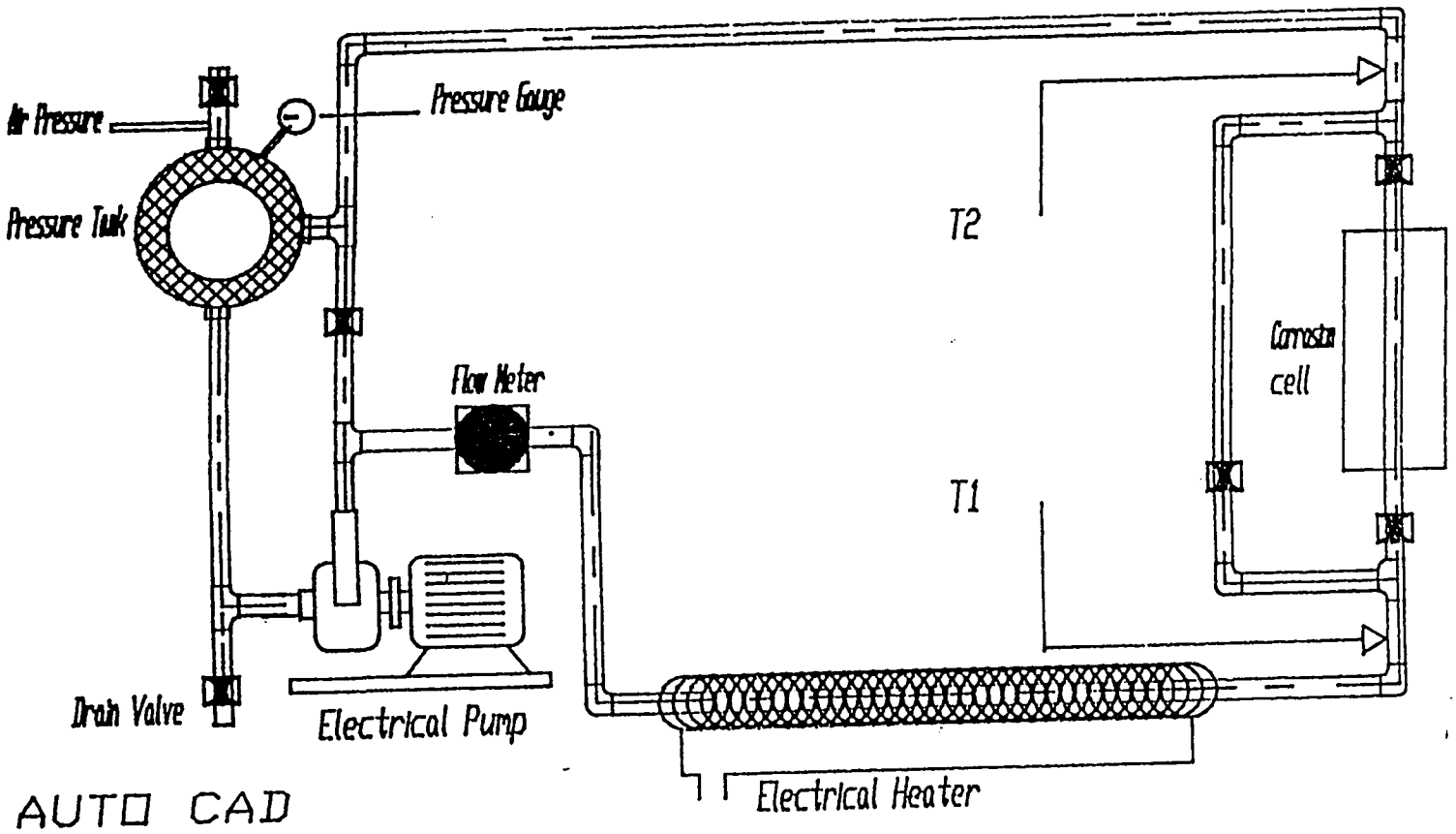

Fig 6.4: Stainless steel 316 loop, designed and fabricated for elevated temperature and pressure corrosion investigations

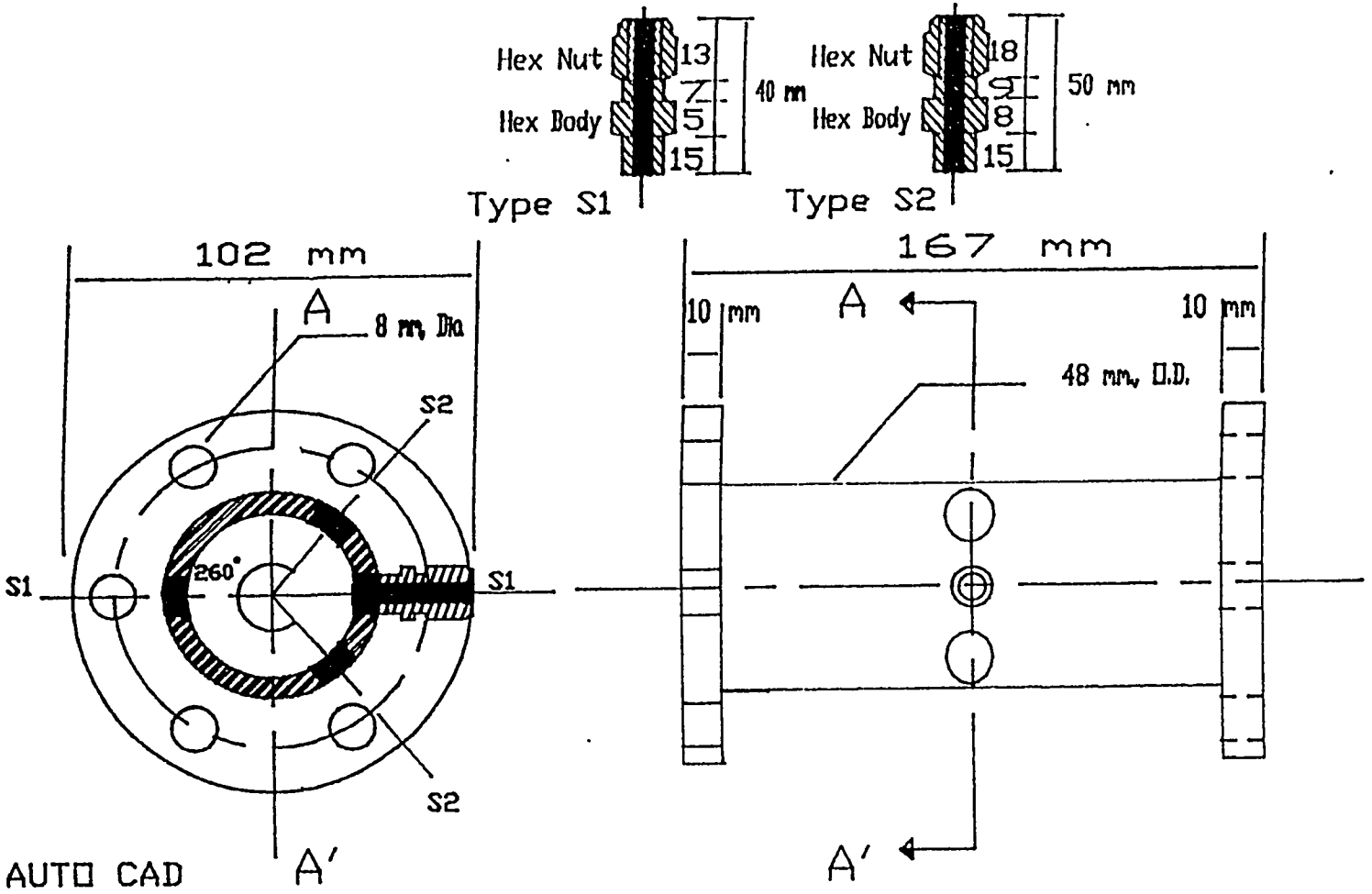

Fig 6.5: Stainless steel 316 corrosion cell for elevated temperature and pressure electrchemical analysis

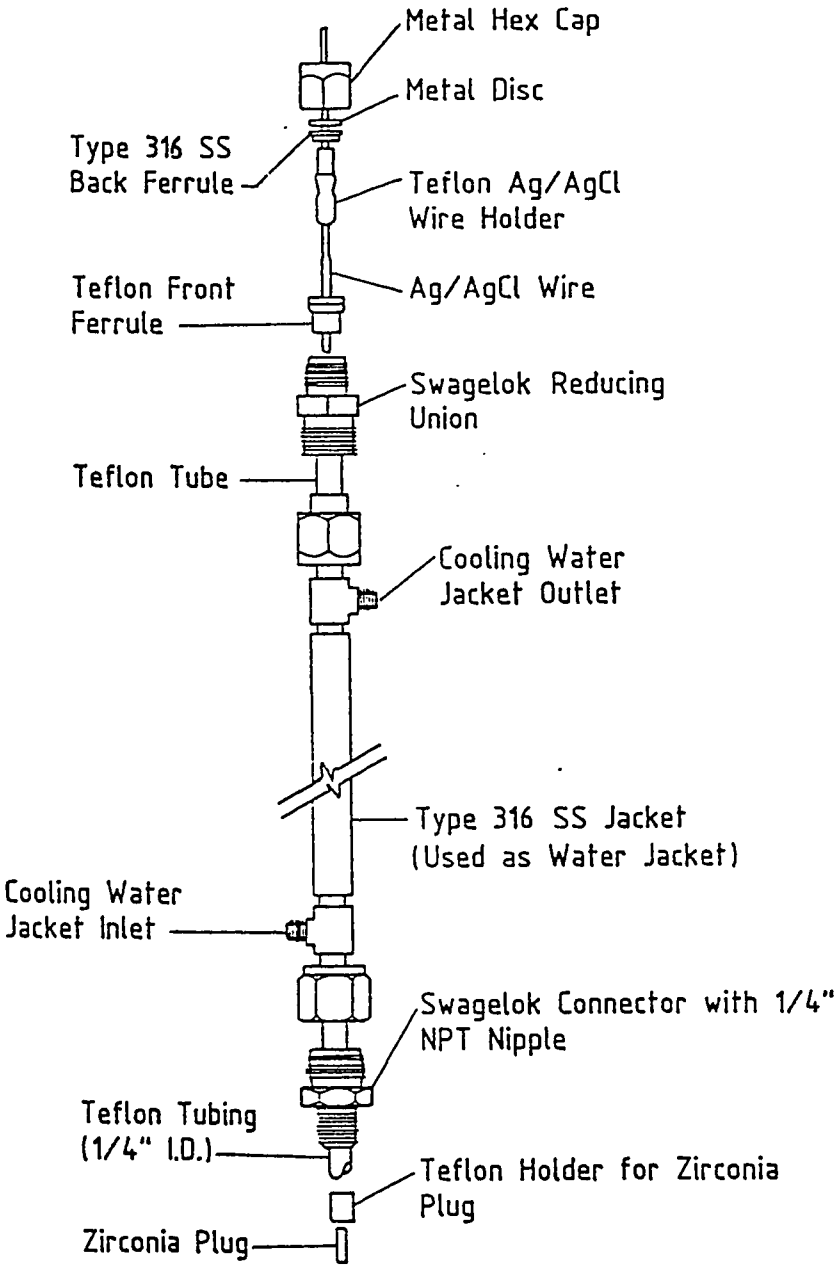

Fig 6.6: Details of high temperature external reference electrode.

6.7 Results and Discussions

The results obtained by potentiodynamic polarization method in deaerated, static and dynamic conditions are summarized in Table 6.1 (a) and 6.1 (b). The electrochemical hysterisis loops obtained are shown in Figs. 6.7, 6.8 and 6.9. The corresponding current vs. time (I-t) and current vs. induction time (I-1/t) diagrams are shown in Figs. 6.10, 6.11, 6.12, 6.13, 6.14 and 6.15.

The difference between the corrosion potential (E_{corr}) and pitting potential (E_p) is given by ΔE. This difference between corrosion potential and pitting potential is taken as the criterion to predict pitting resistance of aluminum. In general the higher values of ΔE suggest a higher pitting resistance and vice versa [57].

The results of investigation under static condition showed the highest value of ΔE, ($\Delta E = E_{corr} - E_p$), (423 mV_{SCE}) for T4-temper of alloy Al6013-20SiC(p), thus suggesting its pitting resistance to be the heighest followed by the alloy composite in as fabricated form (F) (408mV_{SCE}) and O-temper (377mV_{SCE}) in a decreasing order.

From the results under dynamic condition, as shown in Table 6.2, it is evident that increased flow rate has an adverse effect on the pitting resistance of alloy. At a velocity of 0.4 m/s, the value of ΔE for T4-temper was -360 mV_{SCE}. As the velocity was increased to 0.95 m/s, the value of ΔE increased to -395 mV_{SCE}. This increase indicated that the alloy was more susceptible to pitting at higher velocities compared to lower velocities.

The results obtained under dynamic flow conditions at elevated temperatures are shown in Table 6.3, 6.4 and 6.5. Cyclic polarization curves under dynamic conditions are shown in Figs 6.22 to 6.27. The variation of ΔE versus temperature for two velocities is shown in Figs 6.28 to 6.30. The result showed highest value of ΔE for T4-temper, thus suggesting, its highest pitting resistance.

It has been reported by Bhat *et al.* [57], that the presence of secondary phase compounds makes the SiC particles and matrix interface very reactive, which becomes the site for pit initiation. Fig's 6.31 and 6.32, show the pitting of T4-temper of the alloy in 3.5 wt% NaCl solution. It is shown by the micrograph that SiC particles are not attacked and that pits are initiated at the SiC/matrix interface. The high pitting resistance of T4-temper can be attributed to its homogeneous and smoothening of SiC particles by natural age hardening.

To conclude, the pitting resistance of alloy Al6013-20SiC(P) decreases in general with increased temperature in dynamic flow conditions, however, the alloy in T4-temper shows a better resistance than the alloy either in O-temper and F form.

TABLE 6.1: Details of electrochemical parameters (a) under static conditions (b) Dynamic conditions

(a)

Al6013-20sSiC(p)	Ecorr (mVsce)	Ep (mVsce)	ΔE=Ecorr-Ep (mVsce)
O-Temper	-1010	-670	340
F-Temper	-1005	-650	355
T4-Temper	-1025	-660	365

(b)

Al6013-20SiC(P)	Velocity (m/s)	Ecorr (mVsce)	Pitting Pot. Ep (mVsce)	ΔE=Ecorr-Ep (mVsce)
O-Temper	0.4	-940	-620	310
	0.95	-980	-630	350
F-Temper	0.4	-980	-650	330
	0.95	-980	-620	360
T4-Temper	0.4	-970	-610	360
	0.95	-1010	-615	395

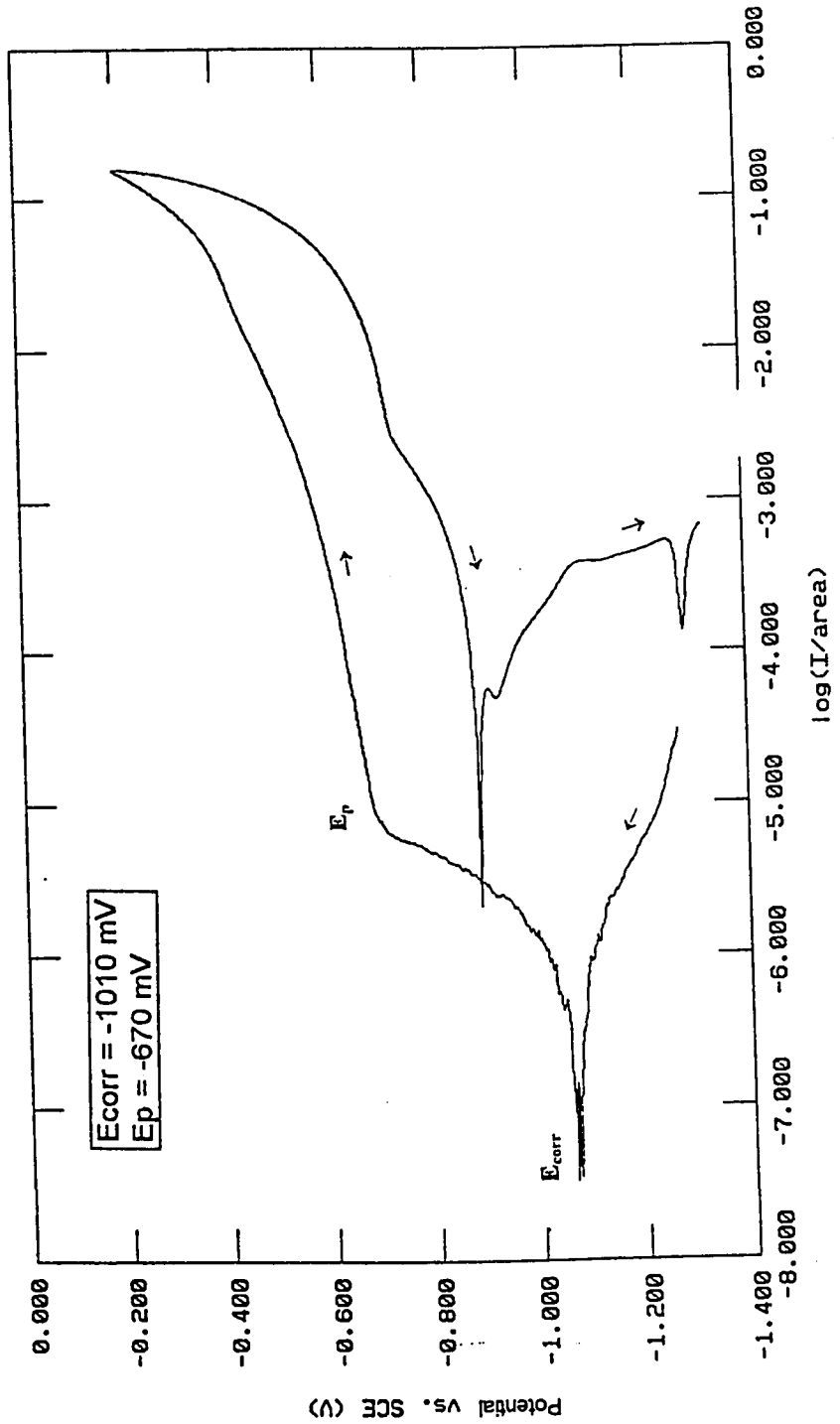

Fig 6.7: Hysteresis loop of Al 6013-20SiC(p) -O.

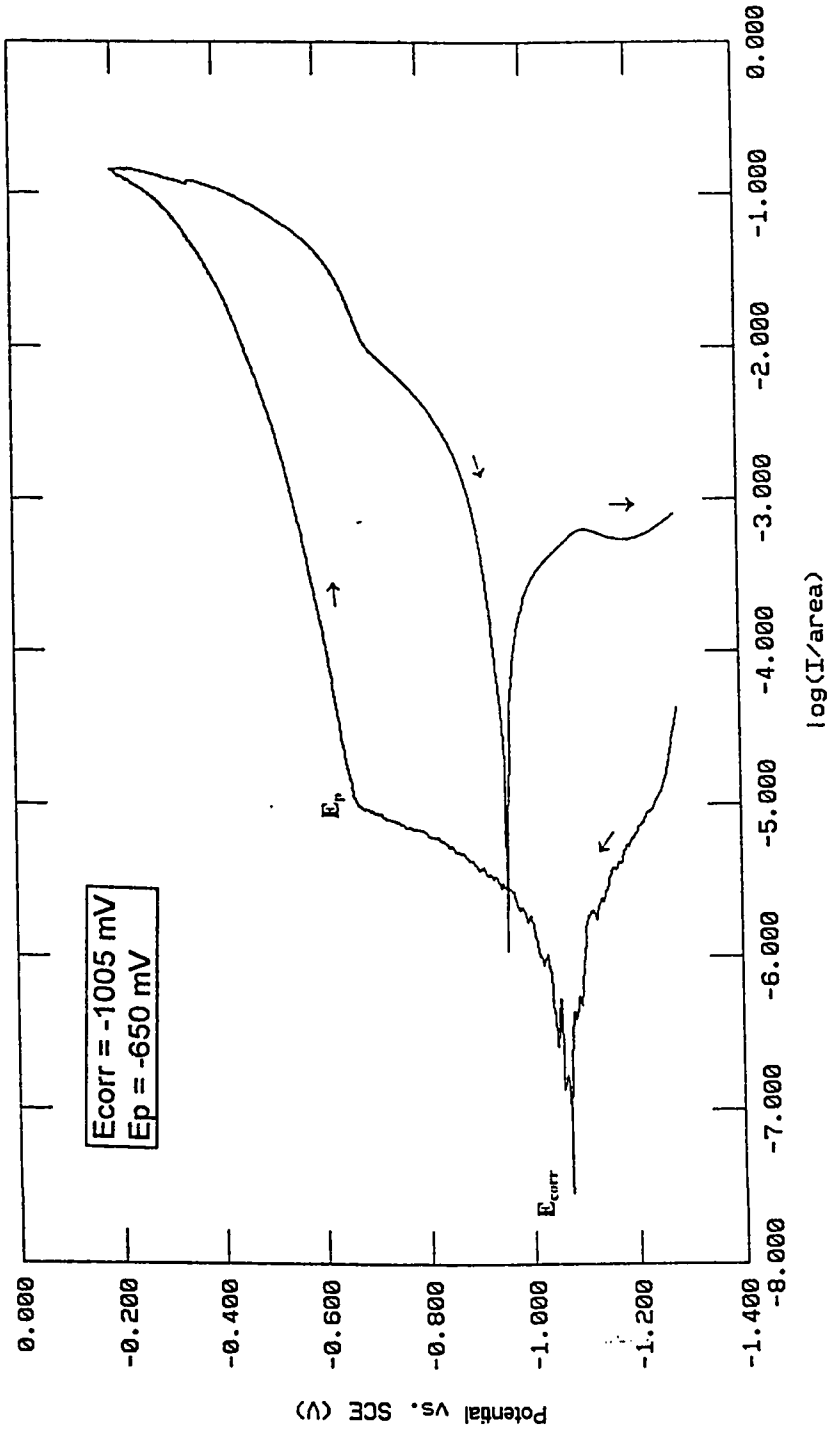

Fig 6.8: Hysteresis loop of Al 6013-20SiC(p) -F.

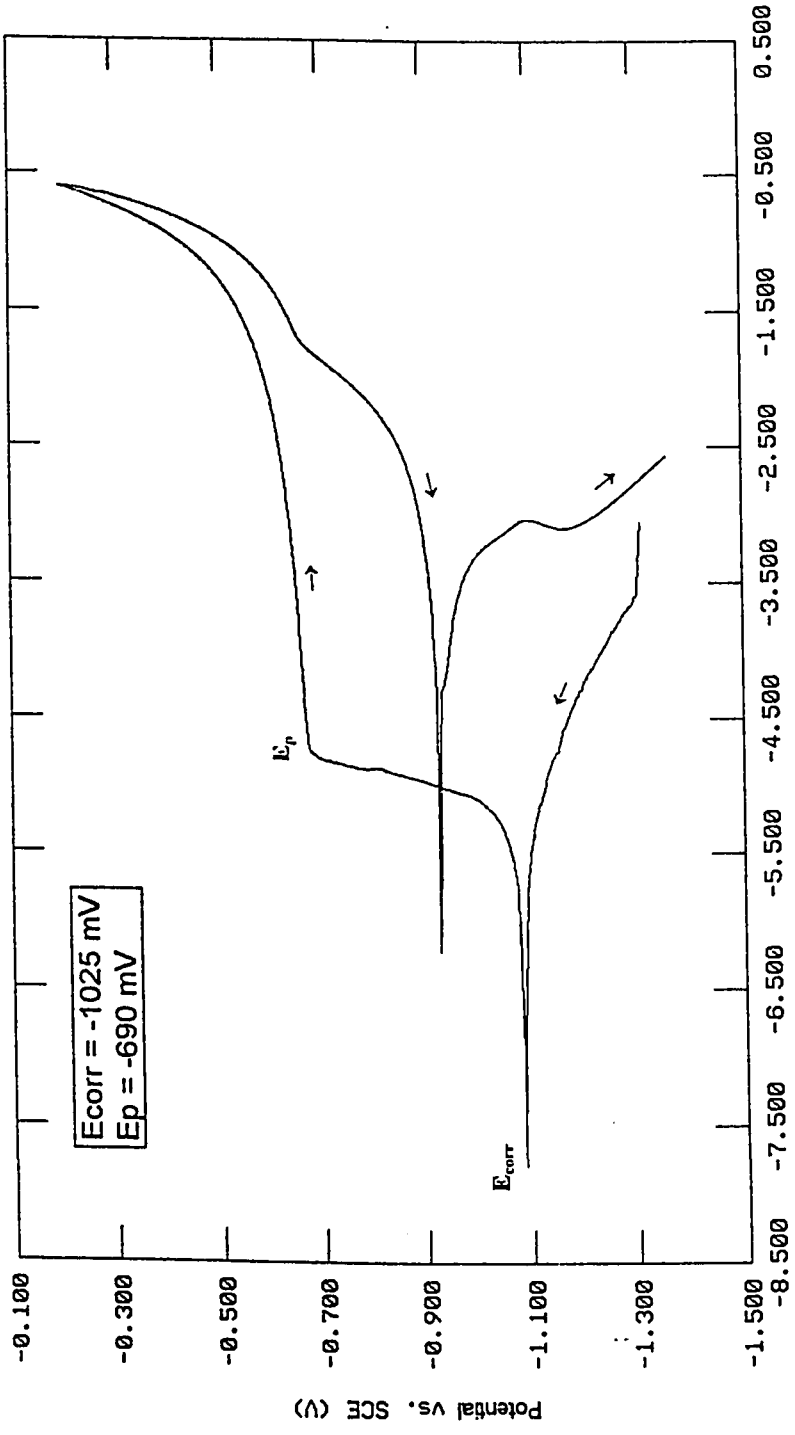

Fig 6.9: Hysteresis loop of Al 6013-20SiC(p) -T4.

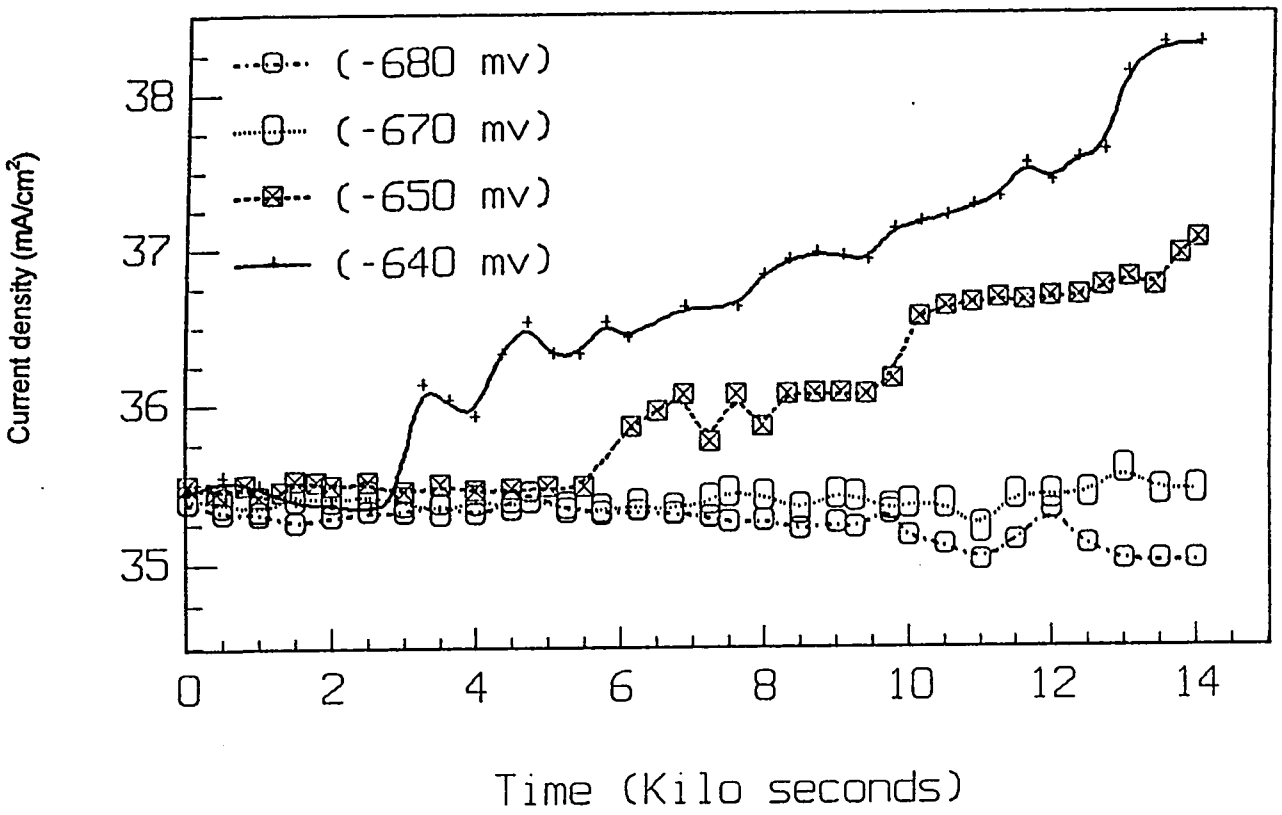

Fig 6.10: I- t Diagram of Al 6013-20SiC(p) -O.

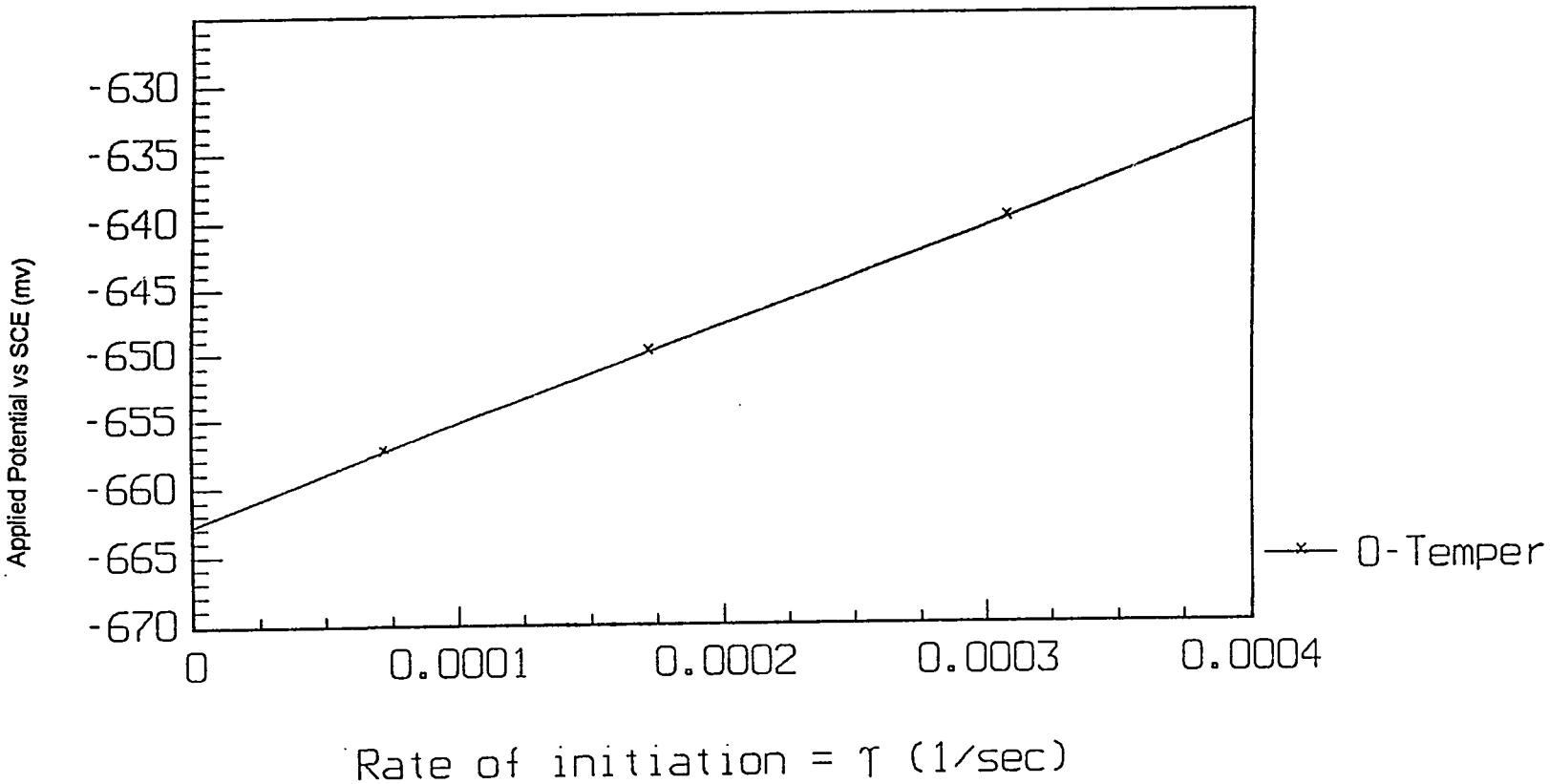

Fig 6.11: Determination of E_P by potentiostatic induction time method for Al 6013-20SiC(p) -O.

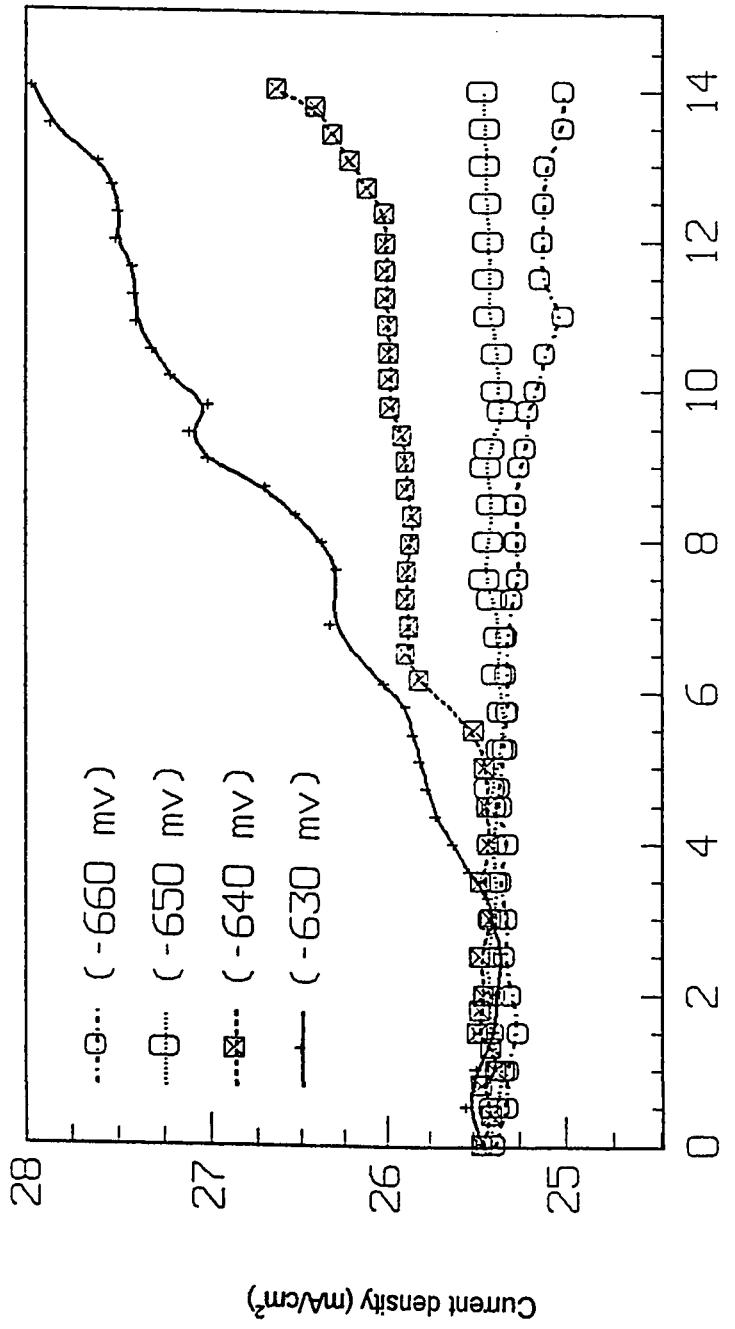

Fig 6.12: I-t Diagram of Al 6013-20SiC(p) -F.

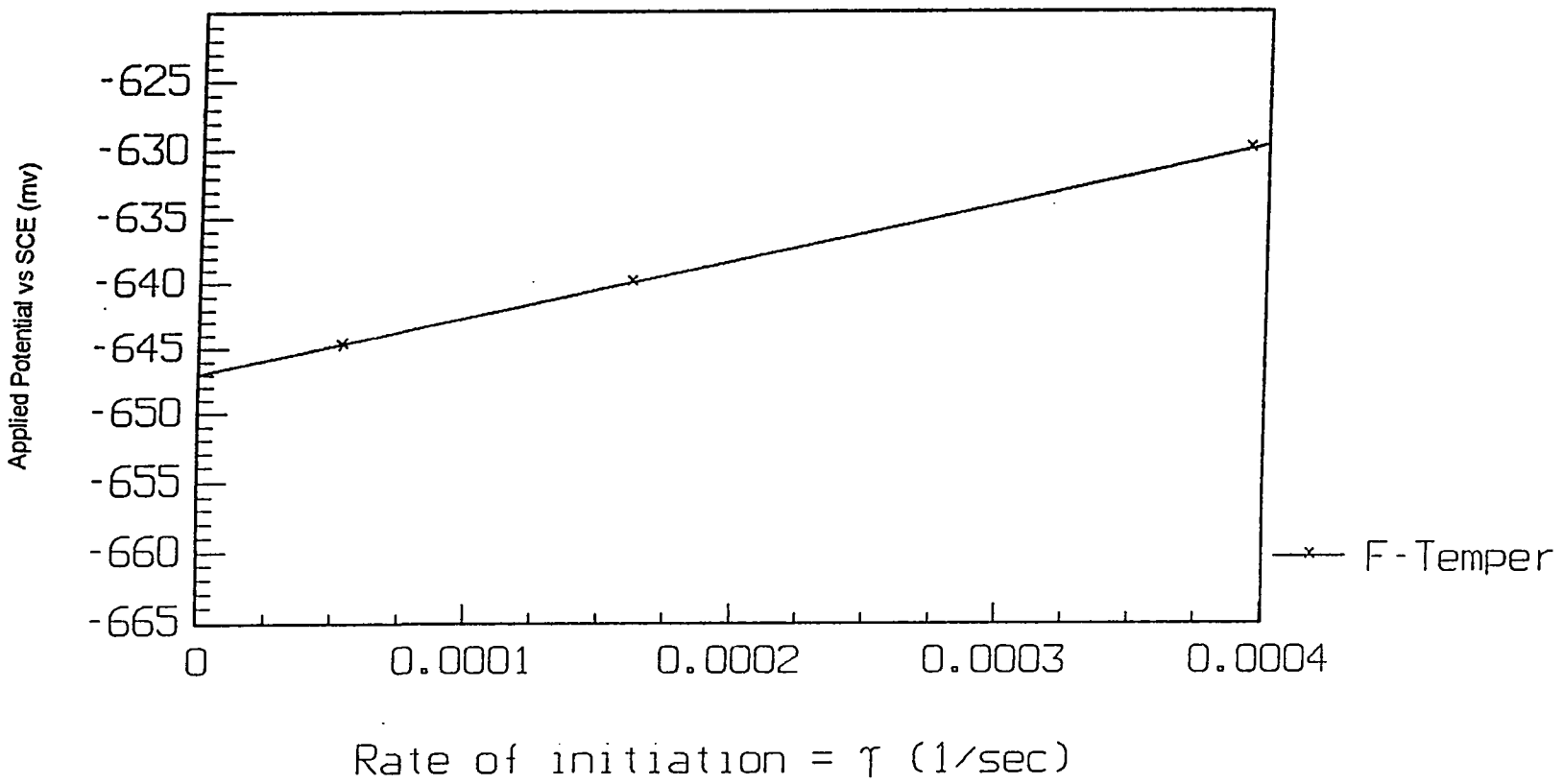

Fig 6.13: Determination of E_p by potentiostatic induction time method for Al 6013-20SiC(p) -F.

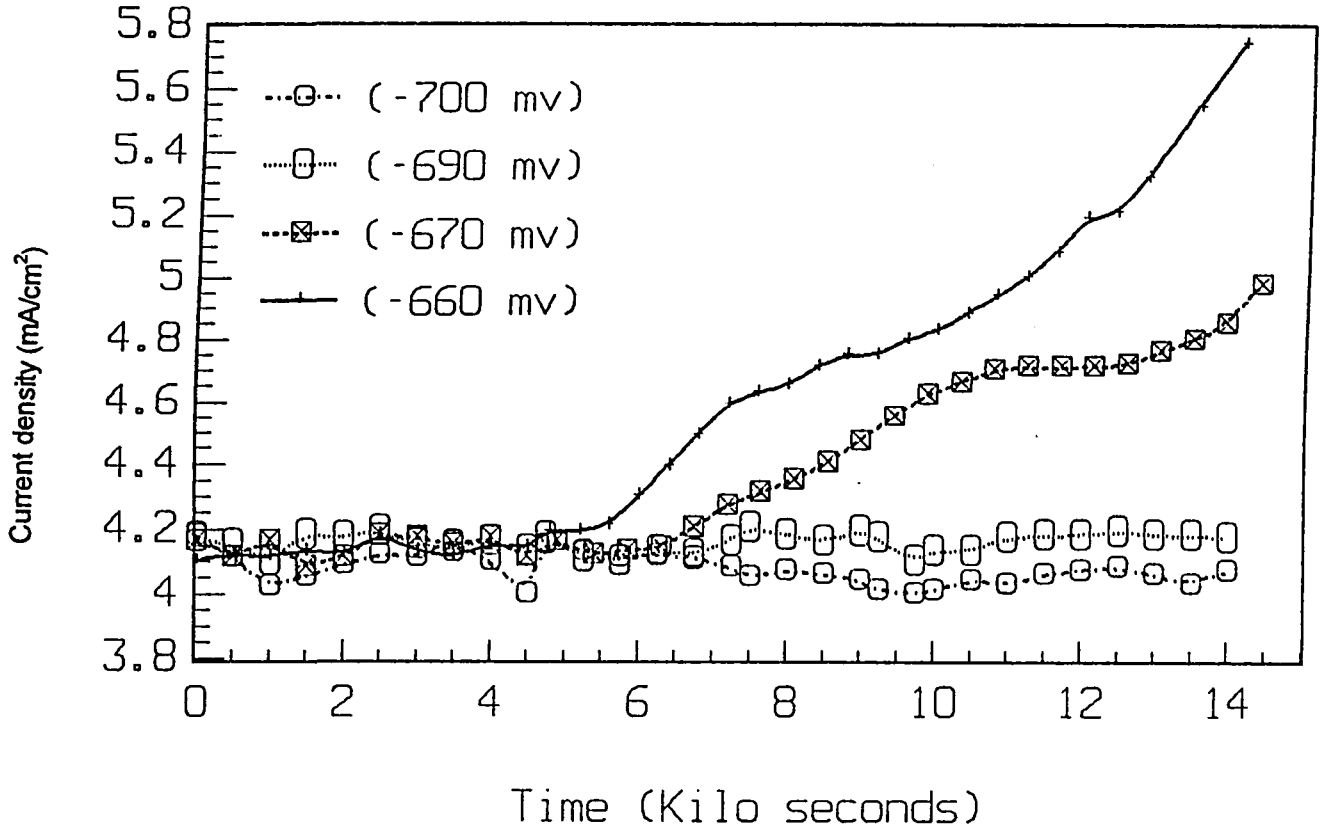

Fig 6.14: I- t Diagram of Al 6013-20SiC(p) -T4.

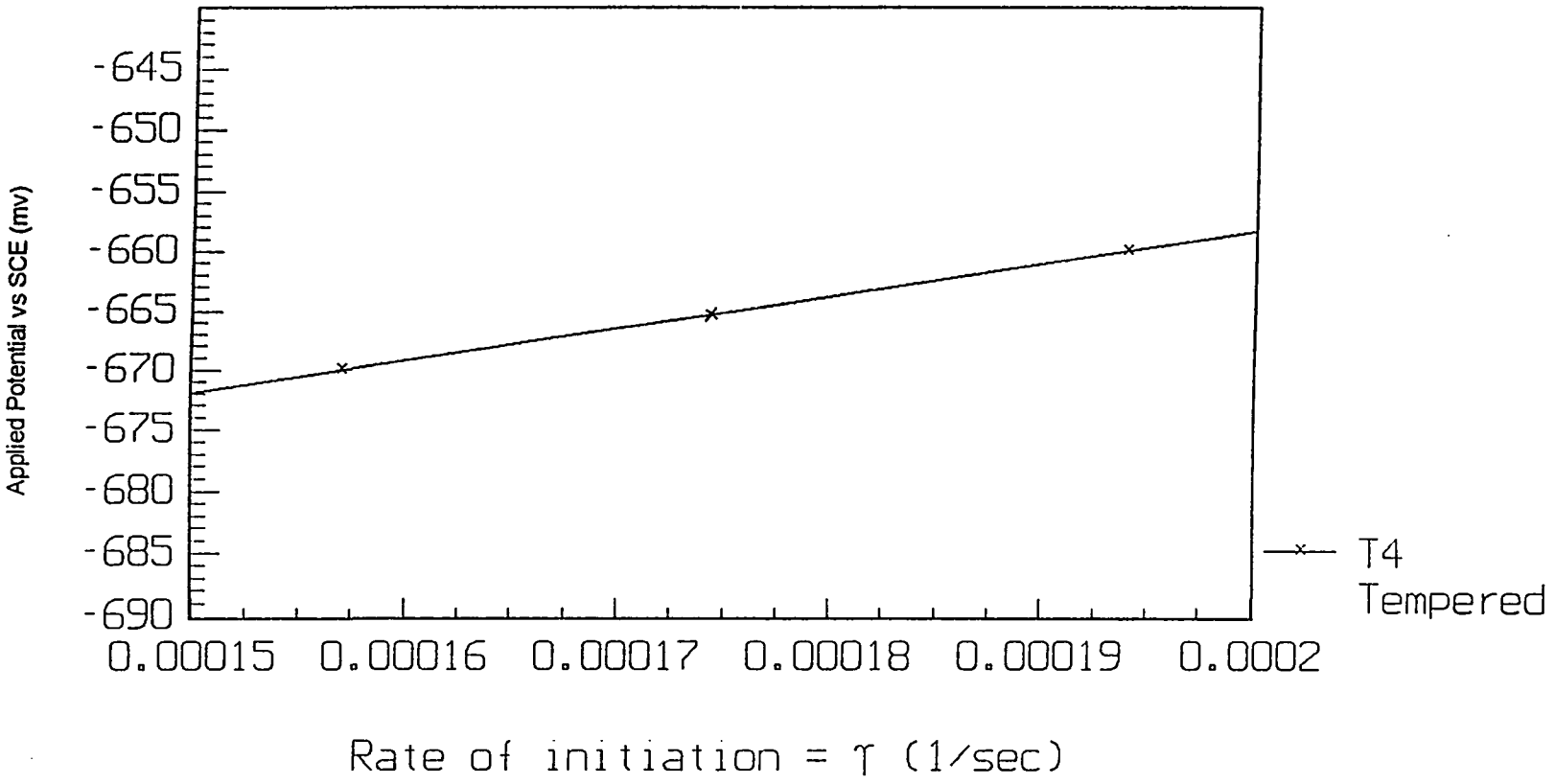

Fig 6.15: Determination of E_p by potentiostatic induction time method for Al 6013-20SiC(p) -T4.

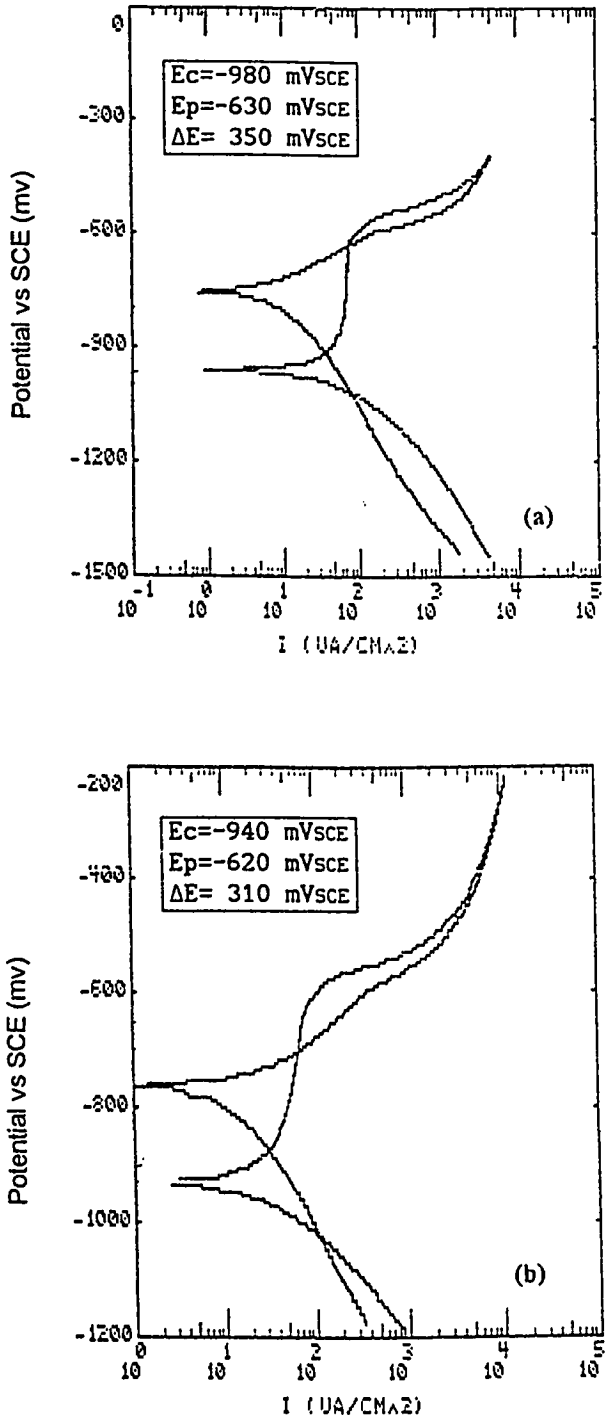

Fig 6.16: Cyclic polarization curves of Al6013-20SiC(P)-O at (a) 0.4 m/s (b) 0.95 m/s.

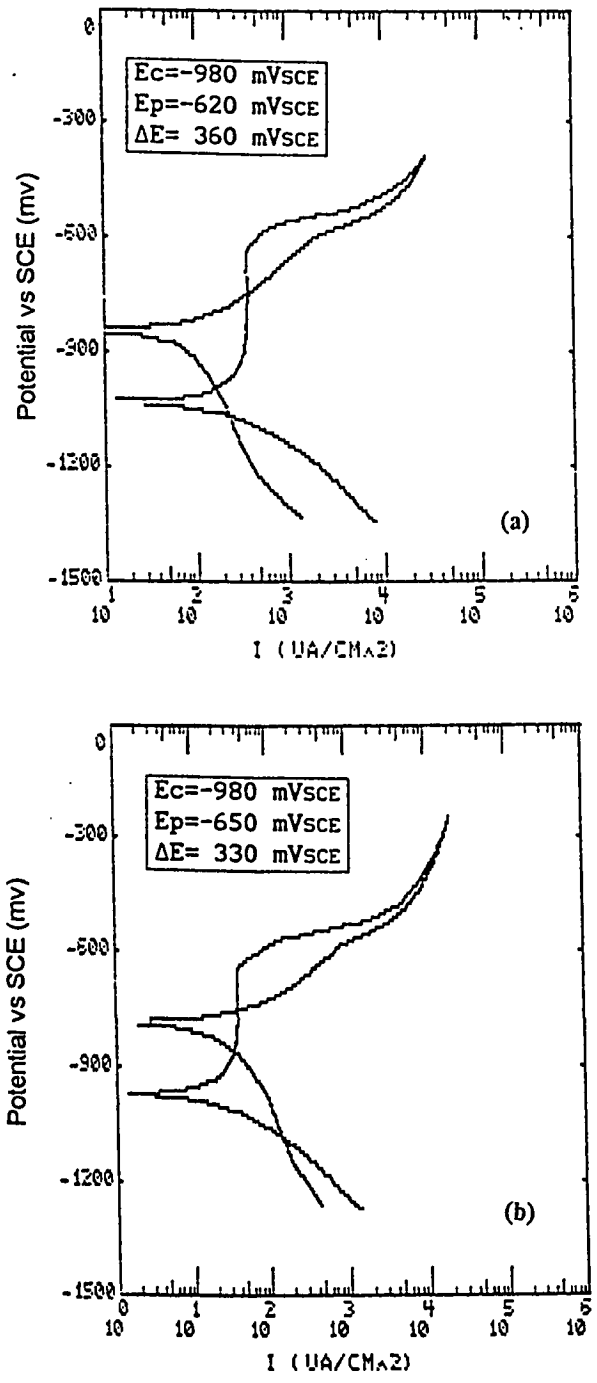

Fig 6.17: Cyclic polarization curves of Al6013-20SiC(P)-F at (a) 0.4 m/s (b) 0.95 m/s.

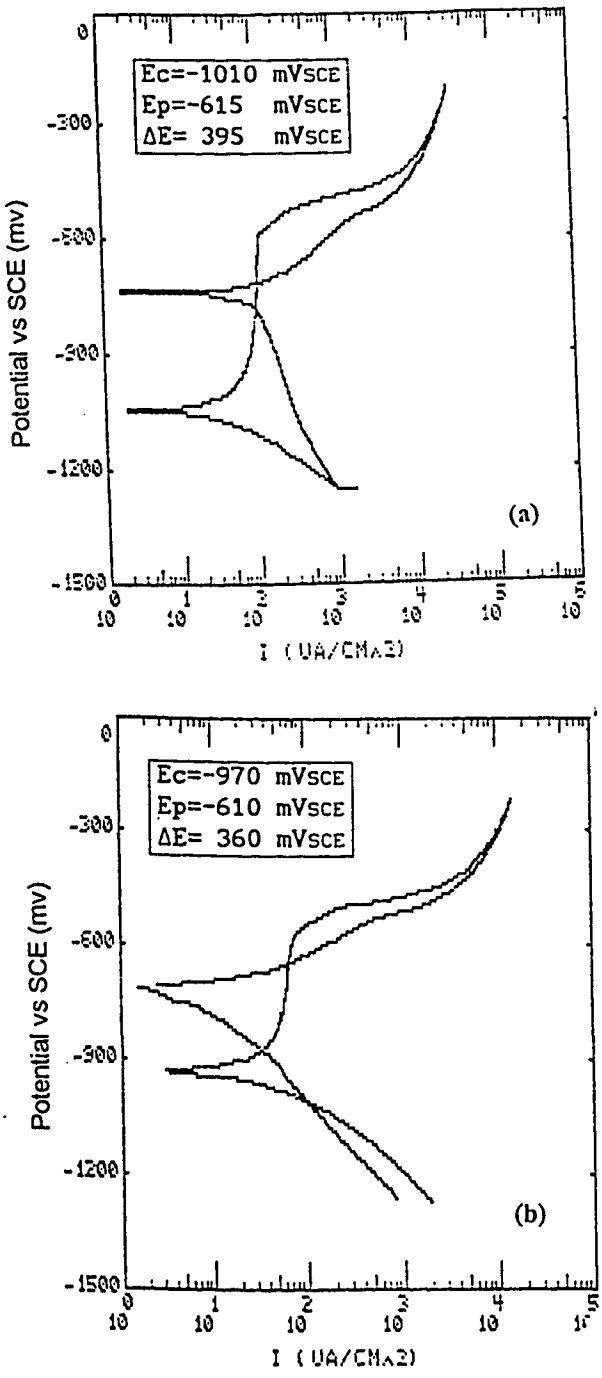

Fig 6.18: Cyclic polarization curves of Al6013-20SiC(P)-T4 at (a) 0.4 m/s (b) 0.95 m/s.

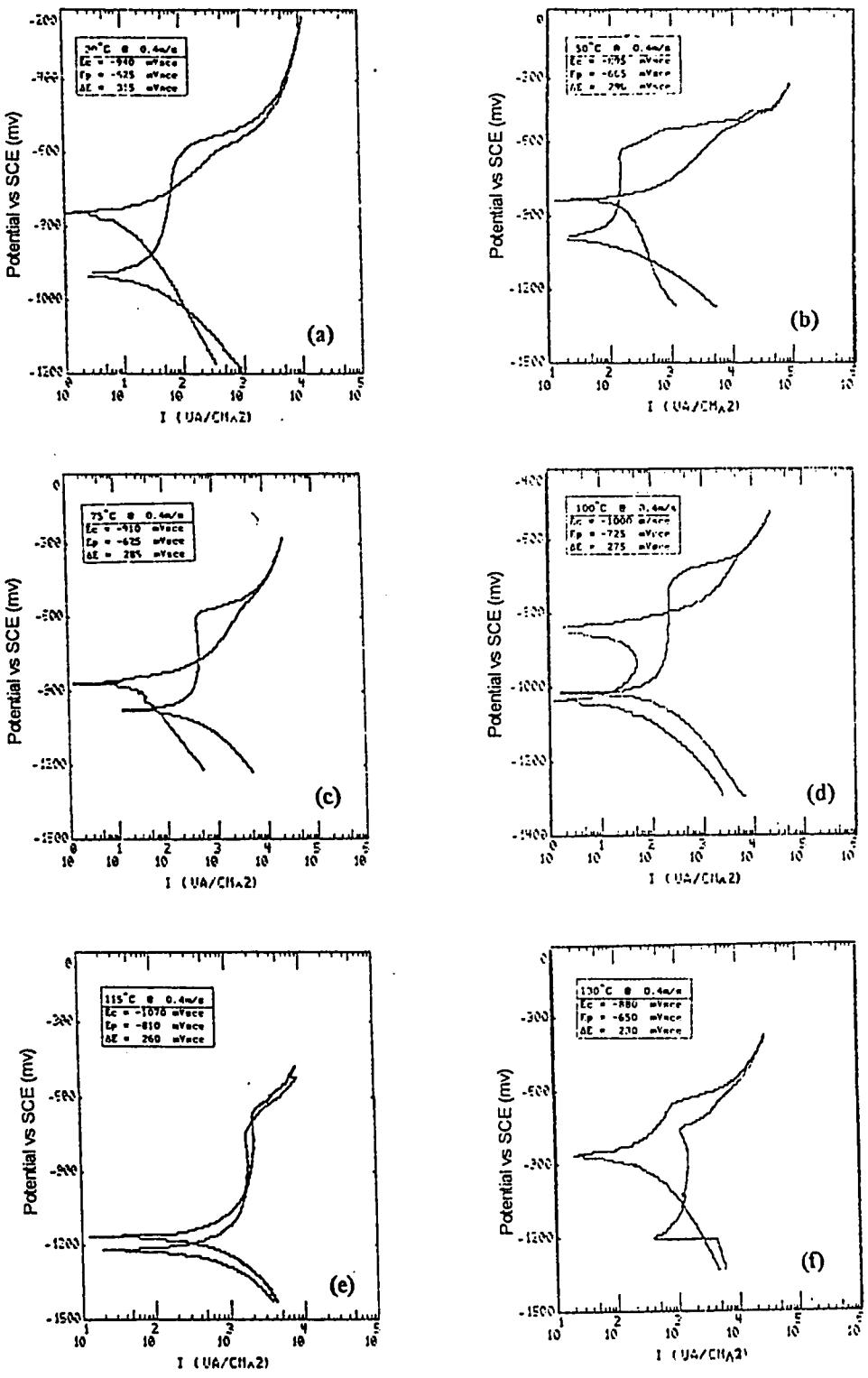

Fig 6.19: Cyclic polarization curves of Al6013-20SiC(P)-O at 0.4 m/s and at (a) 30°C (b) 50°C (c) 75°C (d) 100°C (e) 115°C (f) 130°C

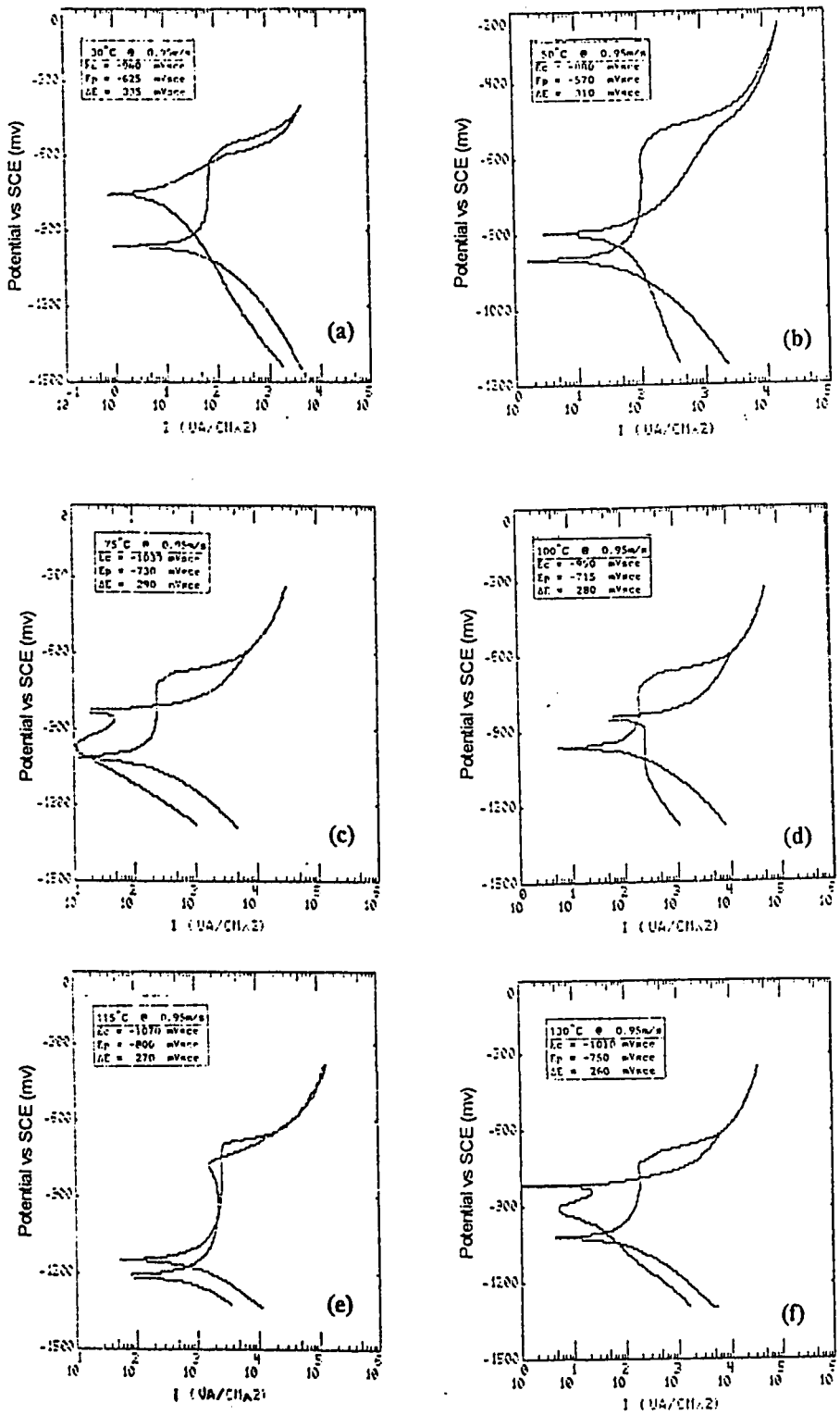

Fig 6.20: Cyclic polarization curves of Al6013-20SiC(P)-O at 0.95 m/s and at (a) 30°C (b) 50°C (c) 75°C (d) 100°C (e) 115°C (f) 130°C

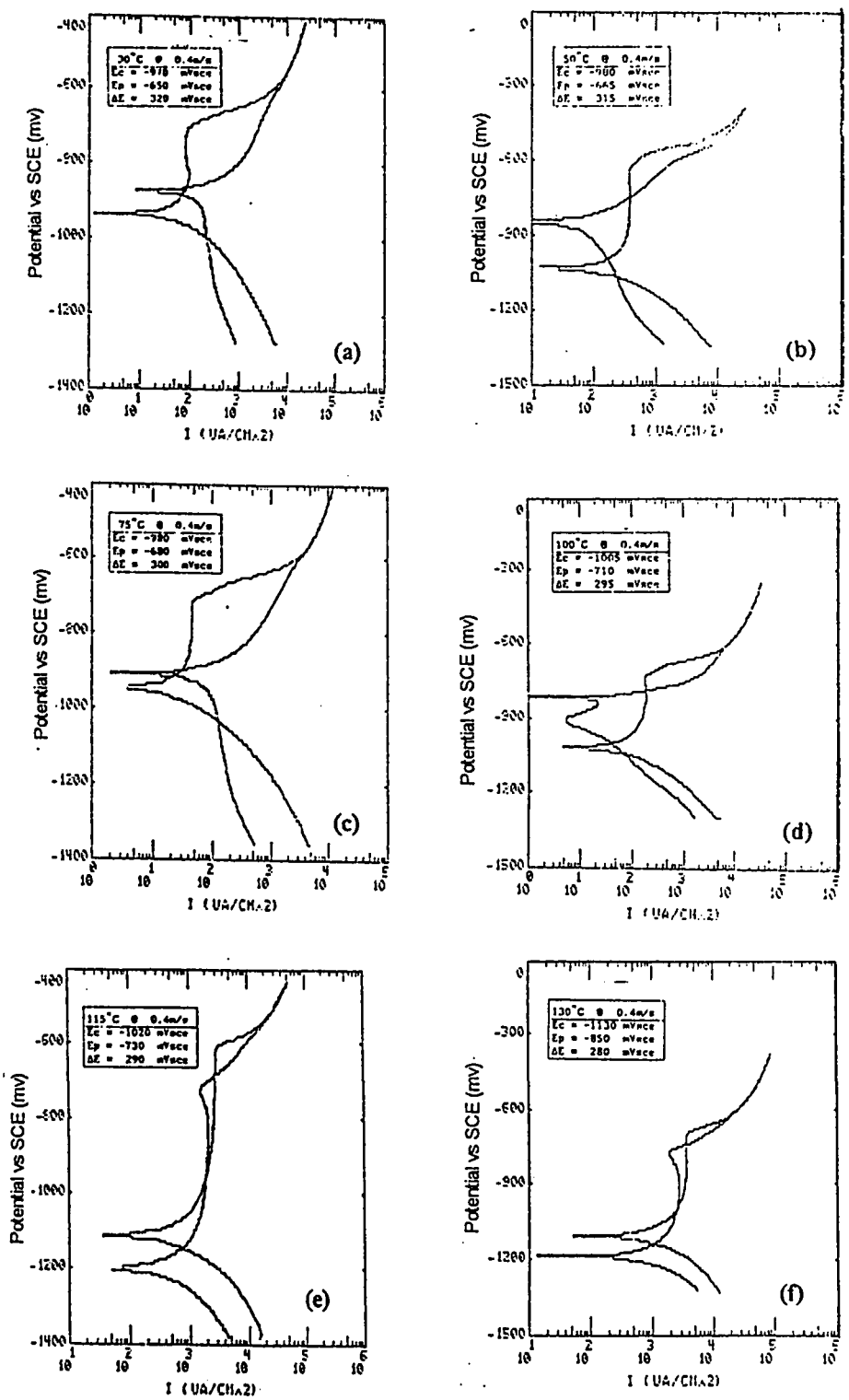

Fig 6.21: Cyclic polarization curves of Al6013-20SiC(P)-F at 0.4 m/s and at (a) 30°C (b) 50°C (c) 75°C (d) 100°C (e) 115°C (f) 130°C

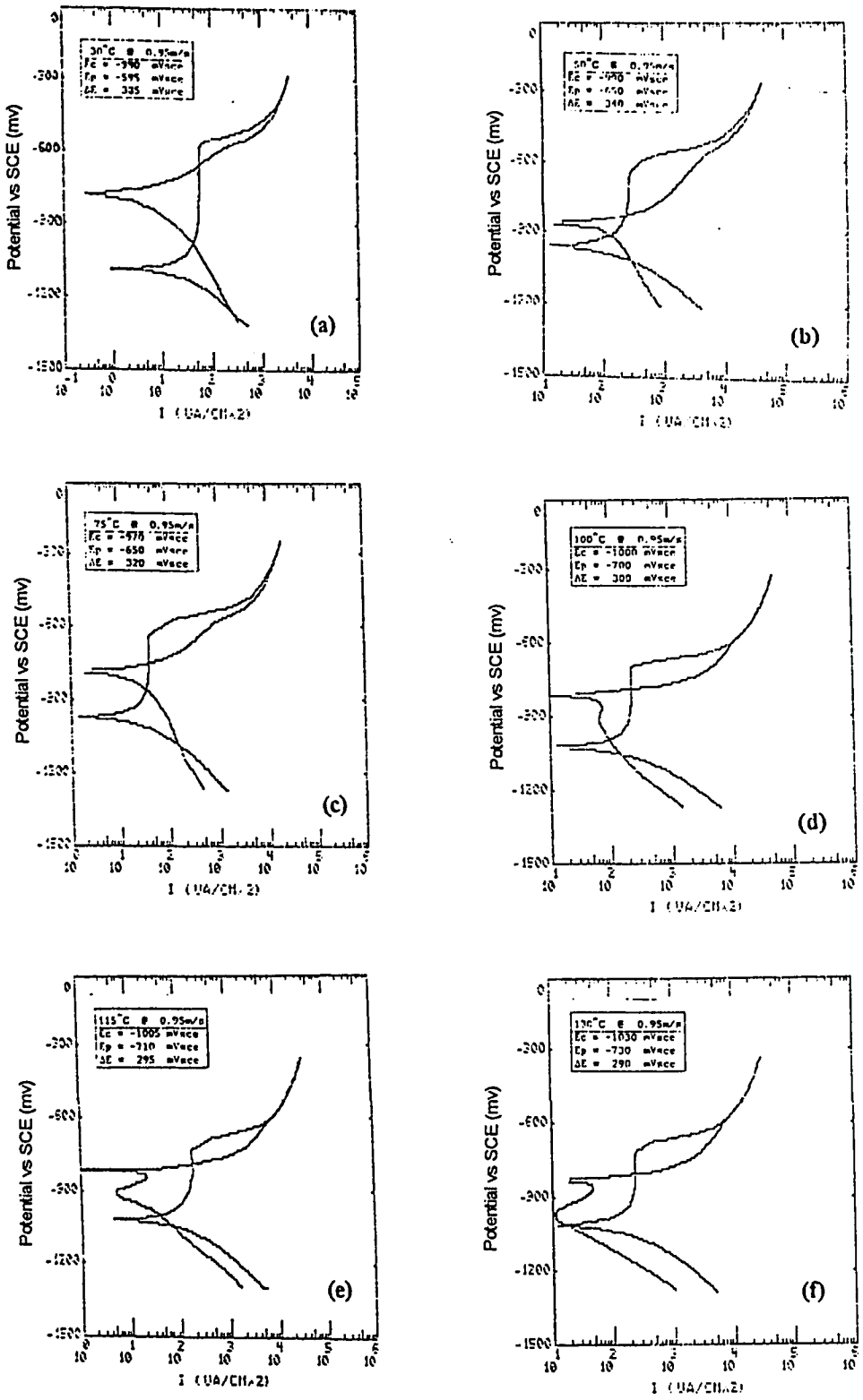

Fig 6.22: Cyclic polarization curves of Al6013-20SiC(P)-F at 0.95 m/s and at (a) 30°C (b) 50°C (c) 75°C (d) 100°C (e) 115°C (f) 130°C

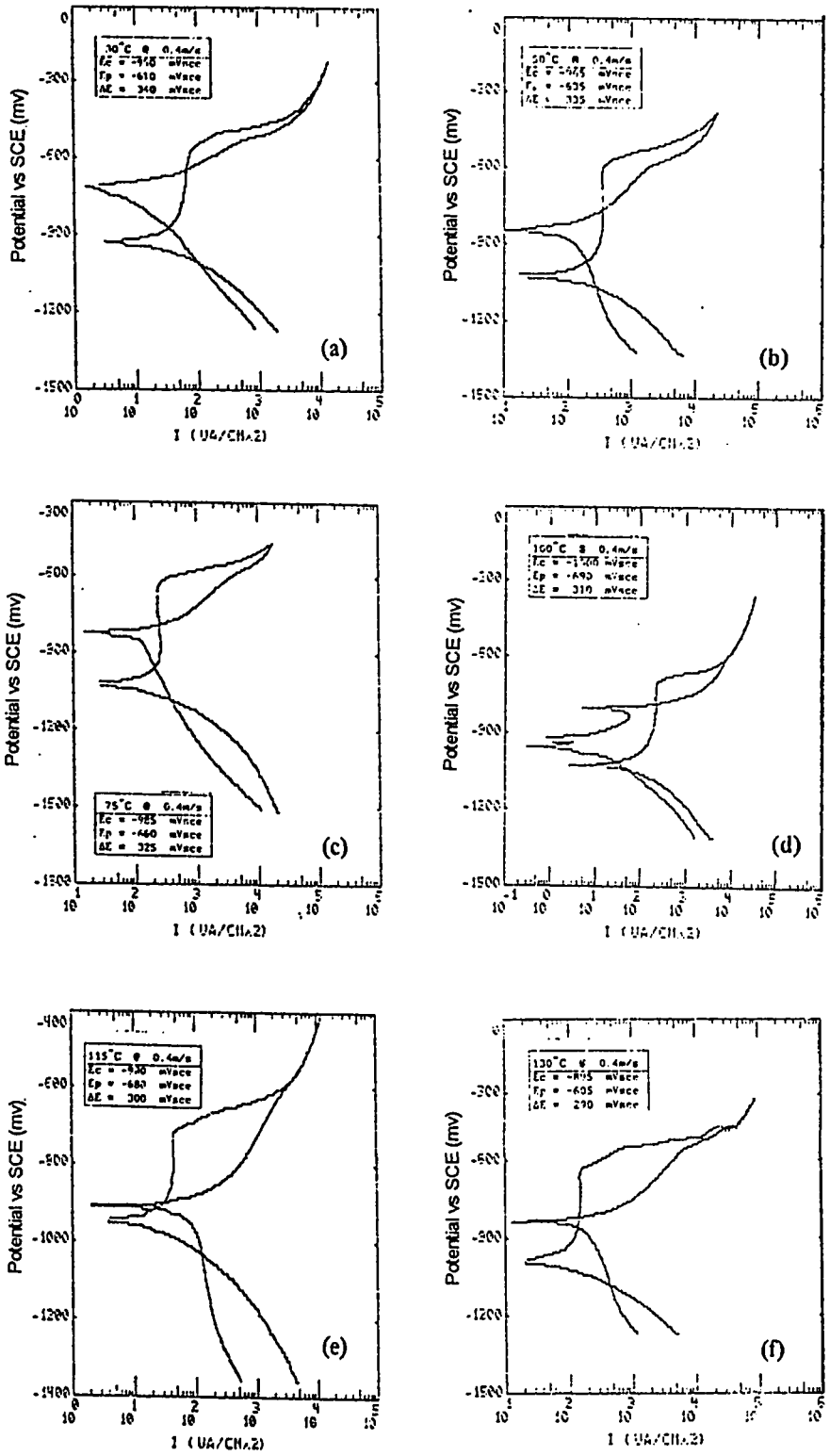

Fig 6.23 Cyclic polarization curves of Al6013-20SiC(P)-T4 at 0.4 m/s and at (a) 30°C (b) 50°C (c) 75°C (d) 100°C (e) 115°C (f) 130°C

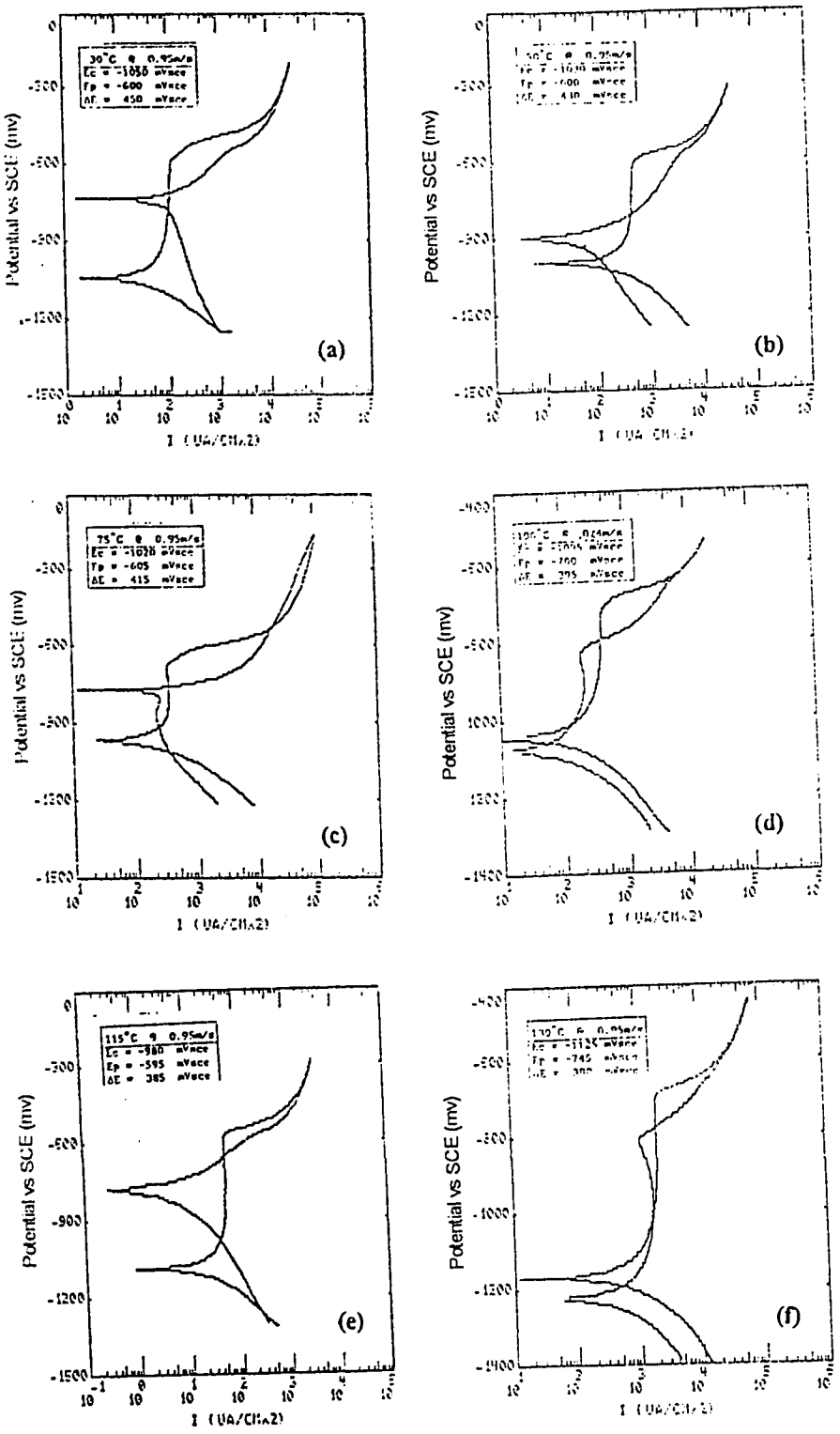

Fig 6.24: Cyclic polarization curves of Al6013-20SiC(P)-T4 at 0.4 m/s and at (a) 30°C (b) 50°C (c) 75°C (d) 100°C (e) 115°C (f) 130°C

TABLE 6.2: Variation of pitting resistance (ΔE) of Al6013-20SiC(P) (a) O-temper (b) F-temper (c) T4-temper

(a)

Temp (°C)	ΔE@0.4 m/s (mV sce)	ΔE@0.95 m/s (mV sce)
30.00	325.00	335.00
50.00	290.00	310.00
75.00	285.00	290.00
100.00	275.00	280.00
115.00	260.00	270.00
130.00	230.00	260.00

(b)

Temp (°C)	ΔE@0.4 m/s (mV sce)	ΔE@0.95 m/s (mV sce)
30.00	320.00	385.00
50.00	315.00	340.00
75.00	300.00	320.00
100.00	295.00	300.00
115.00	290.00	295.00
130.00	280.00	290.00

(c)

Temp (°C)	ΔE@0.4 m/s (mV sce)	ΔE@0.95 m/s (mV sce)
30.00	340.00	450.00
50.00	335.00	430.00
75.00	325.00	415.00
100.00	310.00	395.00
115.00	300.00	385.00
130.00	290.00	380.00

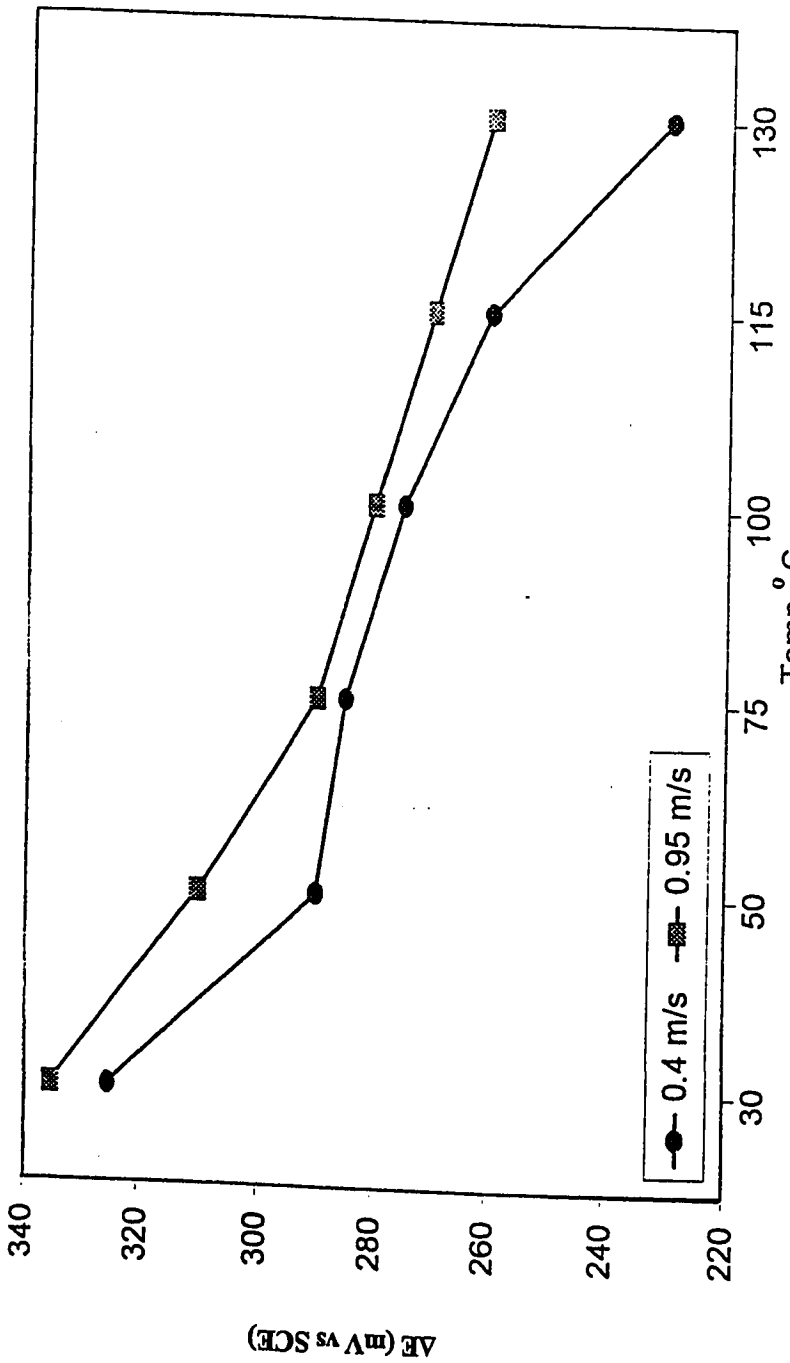

Fig 6.25: Variation of pitting resistance (ΔE) of Al6013-20SiC(P)-O with temperature

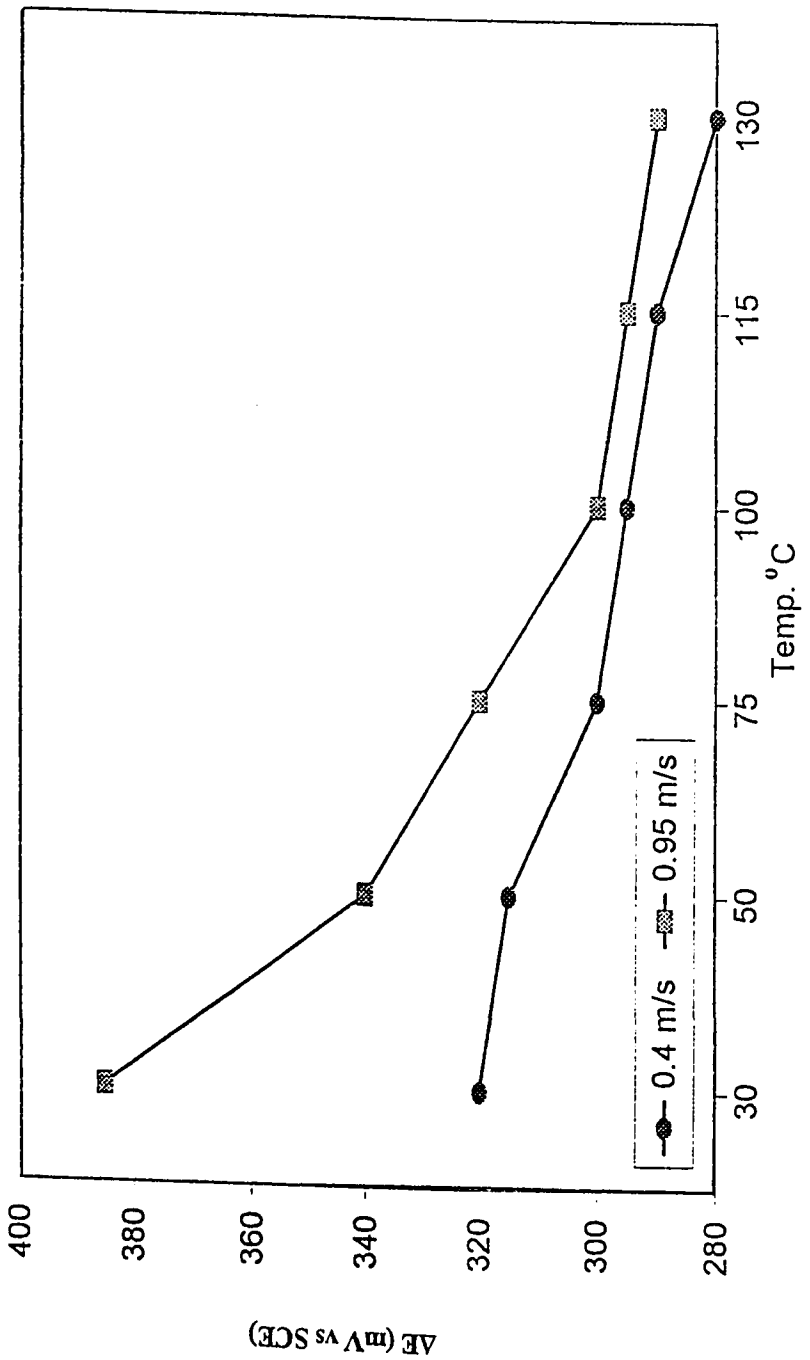

Fig 6.26: Variation of pitting resistance (ΔE) of Al6013-20SiC(P)-F with temperature

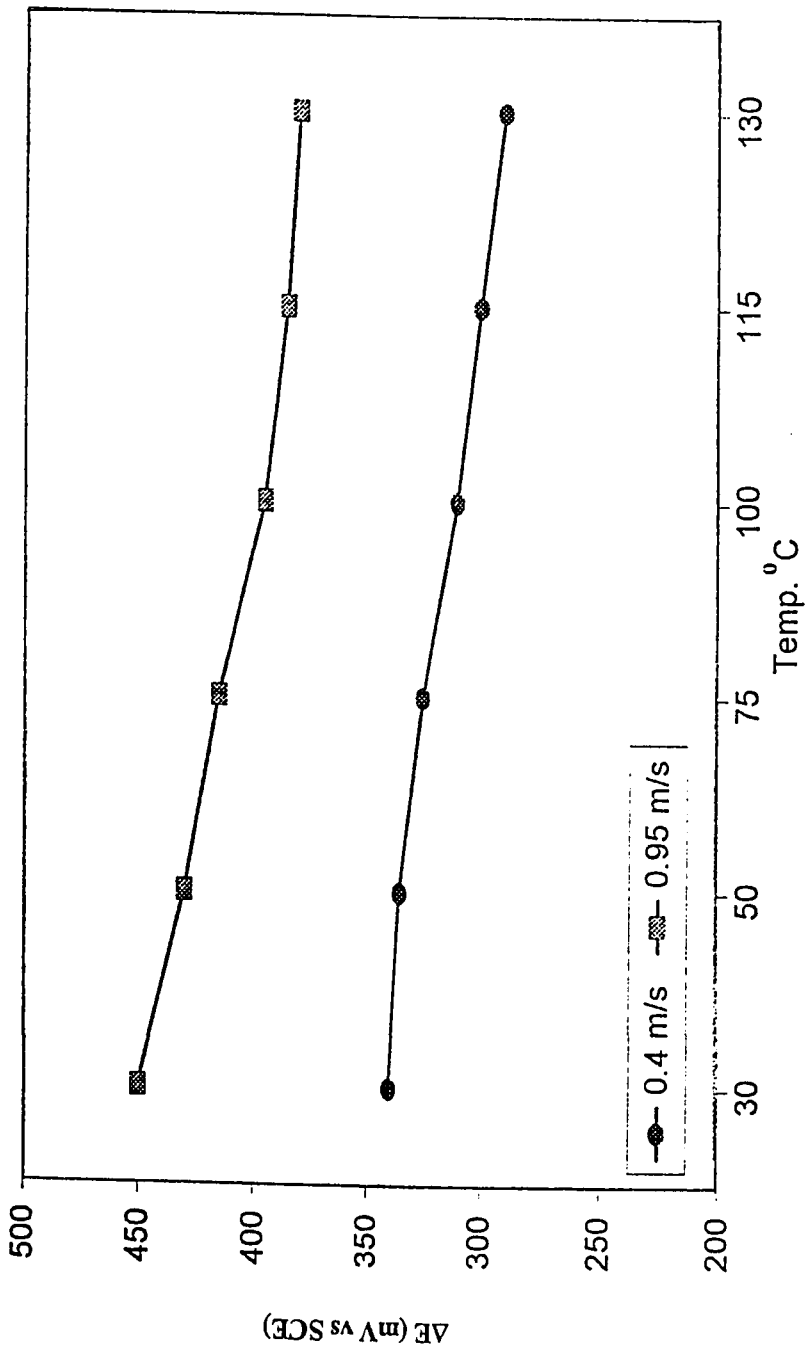

Fig 6.27: Variation of pitting resistance (ΔE) of Al6013-20SiC(P)-T4 with temperature

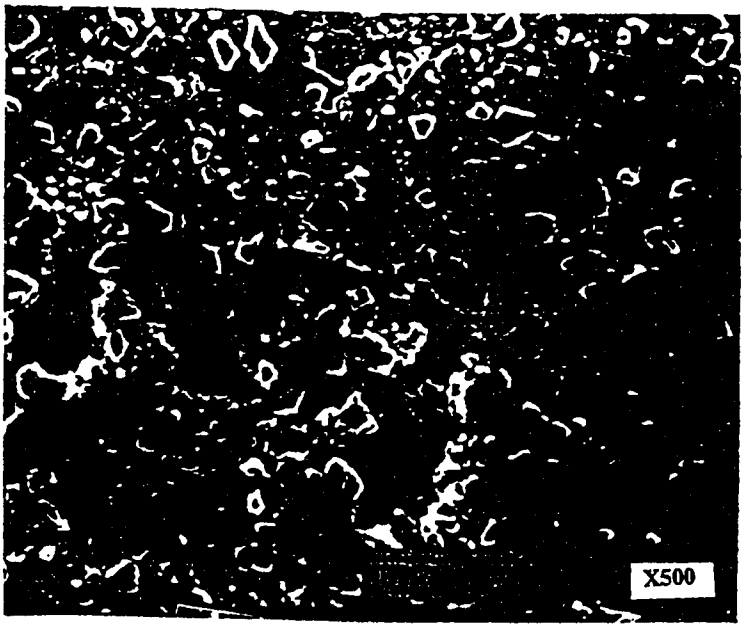

Fig 6.28: Micrograph of pitting in Al6013-20SiC(P)-T4

Fig6.29: Micrograph showing a closer look at the pitting in Al6013-20SiC(P)-T4

Chapter 7

CONCLUSIONS

On the basis of the studies made and the experiments conducted to investigate the effect of heat treatment on the flow induced corrosion of Al/SiC(P) metal matrix composite at elevated temperature, following conclusions can be drawn.

(a) Of the three types of samples studied, O-annealed, F-as fabricated and T4-naturally age hardened of Al6013-20SiC(P) metal matrix composite studied in this investigation, T4-temper showed the lowest corrosion rate in both aerated and deaerated 3.5 wt% NaCl solution, under static and dynamic flow conditions. It was also found that deaeration of corrosive media lowered the corrosion rate of T4-temper by 47.96% in static conditions and 35.42 % in dynamic conditions.

The surface topography revealed that in F-temper the SiC particles were randomly placed and were not uniformly distributed. It was also found that most of the particles had sharp edges. The micro graph of T4-temper showed that age hardening not only increased uniformity in SiC particles but also rounded off the sharp edges.

The most dominant attack found in weight loss technique under static condition was intergranular and pitting corrosion. However in the case of dynamic condition most of the metal was removed by erosion. More efforts are therefore needed to increase the bonding between SiC particles and matrix material.

(b) Results of the open circuit potential vs time studies showed that the potential of naturally age hardened (T4) of alloy Al6013-20SiC(P) metal matrix composite shifted towards more positive direction (-686mV$_{SCE}$ to -680mV$_{SCE}$ in aerated and -687mV$_{SCE}$ to -675mV$_{SCE}$ in dearated conditions) as compared to O-temper and F-form in 3.5 wt% NaCl solution. This shift towards positive direction indicated the tendency for oxide film formation in T4-temper. However the highest corrosion resistance offered by T4-temper can be attributed to its more homogeneous structure, rounding of SiC particles and decreased cathodic to anodic areas ratio.

(c) Results of electrochemical pitting analysis under static condition showed a high value of ΔE ($\Delta E=E_{corr}-E_p$) for T4-temper compared to O and F-tempers. A higher value of ΔE suggests a higher resistance to pitting as shown by experimental evidence on O, F and T4-tempers of the composite.

(d) Results of electrochemical pitting studies under dynamic flow conditions showed that an increase in the temperature from 30°C to 130°C decreased the pitting resistance of O-temper by 29.2 % and 22.38% in 3.5 wt% NaCl solution at velocities of 0.4 m/s and 0.95 m/s respectively. For the F-form the decrease was between 18.63 % and 24.6 %, while for T4-temper the decrease was observed between 14.7 % and 15 %. The least decrease in pitting resistance was shown by alloy 6013-20SiC(P) in (T4)

naturally age hardened condition. Natural age hardening had a beneficial effect on the pitting resistance of the alloy.

The surface topography of the samples showed that most dominant attack was pitting corrosion and no evidence of attack on SiC particles was observed.

7.1 Future Recommendations

In the light of investigations presented, following recommendations are made for future work.

(1) To minimize the corrosion rate of the alloy Al6013-20SiC(P) under dynamic flow conditions and elevated temperature, it is suggested that research be conducted to study the effect of coatings such as Chromate, Cerium sulphate polymer and graphite on the corrosion resistance of alloy Al6013-20SiC(P) and similar composites.

(2) As shown by the studies conducted, the microstructures of the alloy has a significant bearing on the corrosion resistance. It would be therefore of interest to make detailed investigation on the effect of SiC particles distribution and secondary phases on the corrosion resistance.

(3) A life prediction methodology using modeling and experimental techniques is also required to judge the long term performance of the material.

(4) Since the erosion corrosion rate of this composite increases rapidly with velocity, it would be of interest to find new techniques for improved bonding between the matrix and the particles.

(5) The application potential of alloy Al6013-20SiC(P) in various applications needs to be explored.

Appendix

Nominal Composition of Aluminum Alloys

A1: Nominal Composition of Aluminum Alloys

Alloy	Per Cent of Alloying Elements—Aluminum and Normal Impurities Constitute Remainder								
	Silicon	Copper	Manganese	Magnesium	Chromium	Nickel	Zinc	Lead	Bismuth
2EC	0.40	...	...	0.6	...	...	...	...	...
2011	...	5.5	...	...	...	...	...	0.50	0.50
2014	0.8	4.4	0.8	0.40	...	...	...	...	...
2017	...	4.0	0.50	0.50	...	...	...	...	...
2018	...	4.0	...	0.6	...	2.0	...	...	...
2024	...	4.5	0.6	1.5	...	...	...	...	...
2025	0.8	4.5	0.8	...	...	...	...	...	...
2117	...	2.5	...	0.30	...	...	...	...	...
2218	...	4.0	...	1.5	...	2.0	...	...	...
2219①	...	6.3	0.30	...	...	...	...	...	...
2618①	...	2.3	...	1.5	...	1.0	...	...	...
3003	...	...	1.2	...	...	...	...	...	...
3004	...	...	1.2	1.0	...	...	...	...	...
3105	...	...	0.9	0.50	...	...	...	...	...
4032	12.2	0.9	...	1.1	...	0.9	...	...	...
4043	5.0	...	...	...	...	...	...	...	...
5005	...	...	...	0.8	...	...	...	...	...
5050	...	...	...	1.4	...	...	...	...	...
5052	...	...	...	2.5	0.25	...	...	...	...
5056	...	...	0.10	5.2	0.10	...	...	...	...
5083	...	...	0.8	4.45	0.10	...	...	...	...
5086	...	...	0.45	4.0	0.10	...	...	...	...
5154	...	...	...	3.5	0.25	...	...	...	...
5254	...	...	...	3.5	0.25	...	...	...	...
5356①	...	...	0.10	5.0	0.10	...	...	...	...
5357	...	...	0.30	1.0	...	...	...	...	...
5454	...	...	0.8	2.75	0.10	...	...	...	...
5456	...	...	0.8	5.25	0.10	...	...	...	...
5457	...	...	0.30	1.0	...	...	...	...	...
5554①	...	...	0.8	2.8	0.10	...	...	...	...
5556①	...	...	0.8	5.25	0.10	...	...	...	...
5557	...	...	0.25	0.6	...	...	...	...	...
5652	...	...	...	2.5	0.25	...	...	...	...
6053	0.7	...	...	1.3	0.25	...	...	...	...
6061	0.6	0.25	...	1.0	0.25	...	...	...	...
6062	0.6	0.25	...	1.0	0.06	...	...	...	...
6063	0.40	...	...	0.7	...	...	...	...	...

Continued

Nominal Composition of Aluminum Alloys

Alloy	Per Cent of Alloying Elements—Aluminum and Normal Impurities Constitute Remainder								
	Silicon	Copper	Manganese	Magnesium	Chromium	Nickel	Zinc	Lead	Bismuth
6066	1.3	0.9	0.9	1.1	...	...	...	...	...
6151	1.0	...	...	0.6	0.25	...	...	...	...
6262	0.6	0.25	...	1.0	0.09	...	...	0.50	0.50
6463	0.40	...	...	0.7	...	...	...	...	...
6563	0.30	...	...	0.50	...	...	...	...	...
6951	0.30	0.25	...	0.6	...	...	...	...	...
7072	...	...	...	...	...	...	1.0	...	...
7075	...	1.6	...	2.5	0.30	...	5.6	...	...
7079	...	0.6	0.20	3.3	0.20	...	4.3	...	...
7178	...	2.0	...	2.7	0.30	...	6.8	...	...
7277	...	1.25	...	2.0	0.25	...	4.0	...	...

①Nominal Titanium content—0.10 per cent.
②Titanium 0.06; Vanadium 0.10; Zirconium 0.18.
③Iron 1.1; Titanium 0.07.
④Boron 0.02.

REFERENCES

[1] Sir Geoffery Allen, presidential address, **Materials world.** Volume II, Number 6, 1994, pp. 326-330.

[2] Dell Skluzak and Tajima, *"The use of Improved Corrosion resistant Aluminum Alloy 6013 on the Navy's P-7A Aircraft"*, **Society of automotive engineering (SAE) Transactions**, Vol. 1, 1990, pp. 77-92.

[3] *"Aluminum and Aluminum alloys"*, **American society for materials (ASM) specialty handbook, ASM International.** The material information society. Vol 2, 1994.

[4] S.V. Nair, J.K. Tien and R.C. Bates, *"SiC-reinforced Aluminum metal matrix composites"*, **International Metals Reviews**, Vol.30, 1985, pp. 275-290.

[5] D.F. Hasson, C.R. Crowe, J.S. Ahearn and D.C. Cooke, *"Failure mechanisms in high performance materials"*, **Cambridge University** Press, 1985, pp. 147.

[6] M. Kawachi, *"The use of Aluminum in desalination system"*, **Aluminum verlag, 51**, Jahrg, 1975.

[7] American society for materials (ASM) International *"Engineered Materials Hand Book (Composites)"*, Vol I, 1989.

[8] Jacques E. Schoutens, *"Metal Matrix Composite Materials Today"*, **Journal of materials.** June 1985, pp. 43.

[9] K.D.Lore and J.S.Wolf, *"Investigation of the aqueous corrosion of SiC -Al metal matrix composites"*, **Extended abstract, No. 154, Electrochemical society**, Denver, 1981.

[10] R.A.Bonewitz, *"An electrochemical evaluation of aluminum*

alloys 3003, 3004 and 5012 for desalination", **Corrosion**, Vol 3, 1974, pp. 30-41.

[11] B. Agarwal and L.Broutman, **Analysis and performance of fiber composites**, John Wiley and sons, Newyork, N.Y., 1980.

[12] Z.Ahmed, *"Pitting of modified alloys in Arabian Gulf water and the effect of temperature on the kinetic of pitting"*, **Corrosion and Industrial Problems**, Ed., V.Ashworth, Pergamon Press, 1987, pp.315.

[13] J. Tanaka, H. Ichikawa, T. Hayase, K. Okamura and T. Matsuzawa, *"Mechanical properties of SiC fiber reinforced Al. composites"*, **Progress in science and engineering of composites**, Ed., ICCM-IV, Tokyo, 1982.

[14] R.Arone, O. Botstein, B. Shpigler, *"Mechanical Behavior of SiC particulates reinforced Aluminum metal matrix composites"*, **Israel journal of technology**, Vol. 24., 1988, pp. 393-399.

[15] R.S. Kaneko, L.Bakow and E.W. Lee., *"Aluminum Alloy 6013 sheet for new U.S. Navy Aircraft"*., **Journal of Metals**,Vol. 42, 1990, pp. 16-18.

[16] D.Aidun, P.Martin and J.Sun, *"Effect of Heat treatment on the Mechanical Properties of SiCp/6061 Al composite"*, **Journal of Materials Engineering and Performance (JMEPEG)**, Vol. 1(5), 1992, pp. 615-624.

[17] L.Wei and J.C. Huang, *"Influence of Heat Treatment and Hot Working on Fracture toughness of Cast Aluminum Base Composites"*, **Material Science and Technology**, 1993, Vol. 9, pp. 841-849.

[18] P.P. Trzaskoma, E. Mc Cafferty and C.R. Crowe, *"Corrosion Behavior of SiC/Al Metal Matrix Composites"*, **Journal of Electrochem. Soc., Electrochemical Science and Technology**, Vol. 130, 1983, pp. 1804-1808.

[19] J. Chaudhuri, Y.M. Tan, K.Patni and A. Effekhari, *"Comparison of corrosion-fatigue properties of 6013 bare, Alcad*

2024 and 2024 bare Aluminum alloy sheet materials" **Journal of Materials Engineering and Performance (JMEPEG)**, Vol. 1, 1992, pp. 91-96.

[20] Zaki Ahmad, *"Corrosion-Erosion characteristics of Al-SiC composite at elevated temperatures and controlled velocities in marine environment"*, **proposal for King Abdul Aziz city for science and technology (KACST)**, Riyadh, 1994.

[21] Denise M. Aylor and Patrick J. Moran, *"Effect of Reinforcement on the Pitting Behavior of Aluminum-Base Metal Matrix Composites"*, **J. Electrochem. Soc.: Electrochemical Science and Technology**, Vol. 132, 1985, pp. 1277-1281.

[22] R.C.Pacceij and V.S.Agarwala, **Corrosion**, NACE, Vol.44, 1988, pp. 680.

[23] L.W. Shemilt and E.I Shoukry, *"Action of Mass Transfer Analysis in Corrosion System"*, **Heat and Mass Transfer in Metallurgical Systems**, Edited by D.Brian Spalding and N.N Afgan, pp 687-709.

[24] Abdul Aleem B.J., *"The Effect Of Suspended Solids On Flow Dependent Corrosion Of Tube Material For Desalination"*, **M.S. Thesis, Department of Mechanical Engineering**, March 1989.

[25] Barry C. Syrett, *"Erosion-Corrosion Of Copper-Nickel Alloys in Sea water and Other Aqueous Environments- A Literature Review"*, **Corrosion NACE**, Vol. 32, No. 6, 1976.

[26] T.K. Ross, G.C. Wood and I.Mahmud, *"The Anodic Behavior of Iron Carbon Alloys in Moving Acid Media"*, **Journal of Electrochemical Society**,.Vol. 113, 1966, pp. 334.

[27] K.D. South and D.H.Jones, *"Corrosion Inhibition in Moving Media"*, **Journal of Applied Chemistry**, Vol 12, 1962, pp 314-319.

[28] Trung Hung Nguaygen and R.T. Foley, *"On the Mechanism of Pitting of Aluminum"*, **Journal of the Electrochemical Society** Vol. 126, 1979, pp. 1855-1876

[29] E.G. Bohlmann and F.A. Posey, "*Aluminum and Titanium Corrosion in Saline Water at Elevated Temperatures*", **Research offered by the Office of Saline Water, U.S. department of the interior, under Union Carbide Corporation's contract with U.S Atomic Energy Commission** (Oak Ridge National Laboratory), 1971.

[30] Eugene A. Avallone, Theodore Baumeister III., **Mark's Standard Handbook for Mechanical Engineers**. Ninth Edition, McGraw-hill book Company, Vol 2, 1989.

[31] The American Society for testing materials, *:Standard Practice for laboratory Immersion Corrosion Testing of Metals*", Standard G31-72, Annual standard Vol. 01.03, re-approved 1990, pp. 102-109.

[32] The American Society for testing materials, "*Standard Practice for preparing, Cleaning and Evaluating Corrosion Test Specimens*", Annual standard Vol. 01.03 and 03.02, 1990, 35-41.

[33] K. Nisancioglu and H.Holtan, "*Correlation of the open-circuit and electrochemical measurements for the pitting corrosion of aluminum in chloride media*", **Werkstoff und Korrosion**, Vol.30, 1979, pp. 105-113.

[34] R.A. Bonewitz, "*An Electrochemical Evaluation of 3003, 3004 and 5050 Aluminum Alloy for Desalination*", **Corrosion NACE**, Vol 30, 1974, pp 53-59

[35] Poulson, Bryan, "*Electrochemical Measurements in Flowing Solution*", **Corrosion Since**, Vol. 23, No. 4, 1983, pp. 391-430.

[36] K.D. south, "*Electrochemical Measurements in Flowing Inhibited Acid*", **M. Tech. Thesis**, Brunal University, 1969.

[37] R. A. Bonewitz, "*An electrochemical Evaluation of 1100, 5052, 6063 Aluminum Alloys for Desalination*", **Corrosion NACE**, Vol. 29, 1973, pp. 215-318.

[38] C.W. Wranglin, "*Corrosion and Protection of Metals*", **Chapman and Hall**, London 1985.

[39] A.J. Griffiths and Turnbull, *"An Investigation of The Electrochemical Polarization Behavior of 6061 Aluminum Metal Matrix Composites"*, **Corrosion Science**, Vol. 36, 1994, pp. 23-35.

[40] Szlarska-Smialawska Z. and Janik-Czachor M. *"The analysis of electrochemical methods for the determination of characteristics potential of pitting corrosion"*, **Corrosion Science**, Vol 11, 1971, pp.901-906

[41] A. Turnbull., *"Review of Corrosion studies on Aluminum Metal Matrix Composites"*., **National physical laboratory (NPL) Report DMM(A) 15**, 1990.

[42] Paiye, H., and Ketcham, S., *"Effect of Titanium in Galvanic Corrosion"*, **Corrosion, NACE**, Vol 8, 1952, pp. 413-417.

[43] T.S. Srivatsan, J.Mattingly, *"Influence of heat treatment on the tensile properties and fracture behavior of an aluminum alloy-ceramic particle composite"*, **Journal of Materials Science** Vol 28, 1993, pp.661-620.

[44] Shadman Jawad Rashidi, *"Corrosion Resistance and Potential Suitability of Recent Developed Aluminum Alloys for Desalination Application"*, **M.S. Thesis**, Department of Mechanical Engineering, 1983.

[45] D.A. Davis, M.G. Vassilaros and J.P. Gudas, *"Corrosion fatigue Stress Corrosion Characteristics of Metal Matrix Composites in Sea Water"*, **Material Performance**, Vol 22, 1982, pp. 38-42.

[46] Zaki Ahmad, *"The Effect of Velocity on the Open Circuit Potential and corrosion rate of Aluminum alloys"*, **Editions Metaux**, Vol 32, 1985,.

[47] Trung hung Ngaygen and R.T. Foley, *"On the Mechanism of pitting of Aluminum"*, **Journal of Electrochemical Society**, Vol. 126, 1979, pp.1855

[48] W.Neil C. Garrard, *"The Corrosion Behavior of*

Aluminum-Silicon Carbide Composites in Aerated 3.5% Sodium Chloride", **Corrosion Science**, Vol 36, No. 5, 1994, pp. 837-851.

[49] D.J. Lloyd, *"Particle Reinforced Aluminum and Magnesium Matrix Composites"*, **International Materials Reviews**, Vol 29, No. 1,1994, pp. 1-22

[50] Alan L. Geiger and J. Andrew Walker *"The Processing and Properties of Discontinously Reinforced Aluminum Composites"*, **The journal of the materials, Metals & Materials Society**, Vol. 43, No. 8, 1991, pp. 8-15.

[51] Franck A. Girot, J.M. Quenisset and R. Naslain, *"Discontinuously-Reinforced Aluminum Matrix Composites"*, **Composites Science and technology**, Vol 30, 1987, pp. 155-184.

[52] S. Kohara, N. Muto, *fabrication of SiC Fiber-Aluminum Composite Materials"*, **Progress in Science and Engineering of Composites**, Ed., ICCM-IV, Tokyo, 1982.

[53] S. Lin, H. Shih and F. Mansfeld, *"Corrosion Protection of Aluminum Alloys and Metal Matrix Composites By polymer Coatings"*, **Corrosion Science**, Vol. 33, 1992, pp. 1331-1349.

[54] Y. Waku, T. Yamamoto, M. Suzuki, M. Tokuse, T.Nagasawa and T. Nishi, *"Mechanical Properties of Aluminum Alloy Composites Reinforced with New Continuous SI-Ti-C-O Fibers"*, **34th International SAMPE Symposium and Exhibition**, 1989, pp.2278-2288.

[55] L.H. Hihara and R.M. Latanision, *"Suppressing Galvanic Corrosion in Graphite/Aluminum Metal Matrix Composites"*, **Corrosion Science**, Vol. 34, No. 4, 1993, pp.655-665.

[56] Ahmad Zaki, *"The effect of velocity on the Corrosion Behavior of Aluminum 3Mg in North Sea Water"*, **METAUX Corrosion Industries**, West Germany, Vol. LVII No. 677, 1982, pp. 1-8.

[57] M.S.N. Bhat, M.K. Surappa and H.V. Sudheker, **Journal of Material Science**, Vol. 26, 1991, pp. 4991.

[58] J.B. Cotton and B.P. Dowing, *"Corrosion resistance of Titanium to Sea Water"*, transaction of Institute of Marine Engineering, Vol. 1, 1957, pp. 311-319.

[59] A. Broli and H. Holtan, *"Determination of characteristics pitting potentials for aluminum bu use of the potentiostatic methods"*, **Corrosion Science**, Vol. 17, 1977, pp. 28-34.

Vitae

- Aleem Aman Khokhar
- Born on July 6th 1966 in Karachi, Pakistan
- Received Bachelor of Engineering (B.E) degree in Mechanical Engineering from NED University of Engineering and Technology, Karachi, Pakistan in 1991
- Joined the Department of Mechanical Engineering at King Fahd University of Petroleum and Minerals (KFUPM), Dhahran, Saudi Arabia as a Research in September 1992
- Received Master of Science (M.S) degree in Mechanical Engineering from KFUPM, Saudi Arabia in July 1995